Institute of Molecular Virology
Prof. Dr. Frank Kirchhoff

Identification of potential HIV restriction factors by combining evolutionary signatures with functional analyses

Dissertation

to obtain the Doctoral Degree of Human Biology (Dr. biol. hum.)
at the Faculty of Medicine, University of Ulm

presented by
Ali Gawanbacht-Ramhormose
Shiraz

2014

Present Dean: Prof. Dr. Thomas Wirth

1st reviewer: Prof. Dr. Frank Kirchhoff
2nd reviewer: Prof. Dr. Barbara Spellerberg

Date of graduation: 11/28/2014

Contents

List of Abbreviations V
1 Introduction 1
1.1 HIV replication cycle 1
1.2 Hallmarks of restriction factors 3
1.3 Criteria for the selection of candidate genes 5
1.3.1 Interferon stimulated genes 5
1.3.2 Upregulated genes in HIV-1 infected individuals 6
1.3.3 Interaction between cellular and HIV-1 proteins 6
1.3.4 Positive selection 7
1.4 Generation of a short list of candidate genes 7
1.5 Scientific aims 8
2 Material and Methods 11
2.1 Material 11
2.1.1 Cell lines 11
2.1.2 Human primary cells 11
2.1.3 Bacteria 11
2.1.4 Nucleic acids 12
2.1.5 Enzymes 16
2.1.6 Media 16
2.1.7 Reagents and utilities 17
2.1.8 Kits 19
2.1.9 Buffers and solutions 19
2.1.10 Antibodies 20
2.1.11 Equipment 21
2.1.12 Software 21
2.2 Methods 22
2.2.1 Preparation of competent bacterial cells 22
2.2.2 DNA methods 22
2.2.3 Eukaryotic cell culture and transfection 25
2.2.4 Virological methods 27
2.2.5 Biochemical methods 28
2.2.6 Flow cytometric analysis 31

2.2.7 RNA methods 32
2.2.8 Statistical analysis 33
3. Results 34
3.1 Generation and functionality of expression vectors 34
3.2 Cell viability upon transfection of candidate genes 35
3.3 Establishment of HEK293T cell-based functional assays 36
3.3.1 Cotransfection setup targeting *late steps* of HIV-1 replication 36
3.3.1.2 Some candidate factors inhibit HIV-1 virion production in a dose-dependent manner 39
3.3.2 Transduction setup targeting *early steps* of HIV-1 replication 45
3.4 Impact of candidates on promoter activities 47
3.4.1 A high proportion of candidates reduces HIV-1 LTR activity 47
3.4.2 Several candidate genes inhibit diverse viral promoters 48
3.4.3 FAS and TNFRSF10A are potent NF-κB activators 49
3.5 Effects of candidate genes on late viral gene expression & protein processing 50
3.5.1 Western blot confirmed the impact of several candidates on late viral gene products 51
3.5.2 CD164, CD1A, CD3G and SPN affect viral Env processing 52
3.6 Expression of candidate genes in HIV-1 target cells 53
3.6.1 Detection of candidate genes in primary cells by Western blot 53
3.6.2 Detection of CD164 and OAS1 in primary blood cells 54
3.7 IL-1A does not increase HIV-1 infection of human primary cells 55
3.8 IFI16 restricts the production of infectious HIV-1 57
3.8.1 IFI16 impairs HIV-1 LTR promoter activity and Gag processing 57
3.8.2 IFI16 inhibits different HIV strains and its antiviral effect is evolutionarily conserved 60
3.8.3 The antiviral effect of IFI16 is antagonized by HIV-1 Vpr 60
4. Discussion 61
5. Summary 70
References 72

List of Abbreviations

A	Alanine
α	Alpha
ADP	Adenosine diphosphate
AGM	African Green Monkey
AIDS	Acquired Immunodeficiency Syndrome
AMP	Adenosine monophosphate
APC	Allophycocyanin
APOBEC3G	Apolipoprotein B mRNA-editing enzyme-catalytic polypeptide-like 3G
APOL	Apolipoprotein L
ATCC	American Type Culture Collection
β	Beta
BFP	Blue Fluorescent Protein
BSA	Bovine serum albumin
BST2	Bone marrow stromal cell antigen 2
$CaCl_2$	Calcium chloride
CCR5	C-C chemokine receptor 5
CD	Cluster of Differentiation
cDNA	Complementary DNA
cGAS	Cyclic GMP-AMP synthase
CMV	Cytomegalovirus
CO_2	Carbon dioxide
CP	Cytoplasma
CPZ	Chimpanzee
C_T	Cycle threshold
CXCR4	C-X-C chemokine receptor 4
D	Aspartic acid
°C	Degree Celsius
Δ	Delta
δ	Delta
DMEM	Dulbecco's Modified Eagle's Medium
d_N	Numbers of nonsynonymous mutations
DNA	Deoxyribonucleic acid
DNase	Deoxyribonuclease
dNTP	Deoxyribonucleotide
d_S	Numbers of silent mutations
DTT	Dithiotreitol
ε	Epsilon
EBV	Epstein-Barr Virus
E. coli	Escherichia coli
e.g.	Exempli gratia

EDTA	Ethylenediaminetetraacetic acid
eGFP	Enhanced Green Fluorescent Protein
ELISA	Enzyme-linked immunosorbent assay
Env	Envelope
et al.	Et alteri
FACS	Fluorescence-activated cell sorting
Fc	Fragment constant part
FCGR3A	Low affinity immunoglobulin gamma Fc region receptor III-A
FCS	Fetal calf serum
FITC	Fluorescein isothiocyanate
γ	Gamma
g	Gram
Gag	Group-specific antigen
GAPDH	Glyceraldehyde 3-phosphate dehydrogenase
GBP5	Guanylate binding protein 5
gp	Glycoprotein
GMP	Guanosine monophosphate
GTP	Guanosine triphosphate
h	hour
HAART	High active antiretroviral therapy
HBS	Hepes buffered saline
HCl	Hydrochloric acid
HEK	Human Embryonic Kidney
HeLa	Henrietta Lacks
HEPES	4-(2-hydroxyethyl)-1-piperazineethanesulfonic acid
HIV	Human Immunodeficiency Virus
HPLC	High-performance liquid chromato-graphy
HRP	Horse Radish Peroxidase
HSV	herpes simplex virus
ICP0	Infected cell polypeptide 0
ID	Identification
IE	Immediate early
IFI	Interferon-inducible protein
IFITM	Interferon-induced transmembrane protein
IFN	Interferon
IKK-β	Inhibitor of nuclear factor kappa-B kinase subunit beta
IL	Interleukin
Inc.	Incorporation
IRES	Internal ribosome entry site
ISG	Interferon stimulated gene
κ	Kappa
KCl	Potassium chloride
kDa	Kilo-Dalton

KH_2PO_4	Potassium dihydrogen phosphate
L	Ligand; Liter
LB	Luria-Bertani
LTR	Long terminal repeat
M	Meter; Molar
m	Mili
µ	Micro
MAC	Rhesus Macaque
M-CSF	Macrophage colony-stimulating factor
MDM	Monocyte-derived macrophage
MFI	Mean fluorescence intensity
$MgCl_2$	Magnesium chloride
min	Minute
MOI	Multiplicity of infection
M-PER	Mammalian Protein Extraction Reagent
mRNA	Messenger RNA
MT	Metallothionein
MTT	3-(4,5-dimethylthiazol-2-yl)-2,5-diphenyltetrazolium bromide
Mx	Myxovirus resistance protein
n	Nano
Na_2HPO_4	Disodium phosphate
NaCl	Sodium chloride
NaOH	Sodium hydroxide
v	Nu
NC	Nucleus
NCBI	National Center for Biotechnology Information
Nef	Negative factor
NF-κB	Nuclear factor kappa-light-chain-enhancer of activated B cells
NIAID	National Institute of Allergy and Infectious Diseases
NIH	National Institutes of Health
OAS	2-5-oligoadenylate synthetase
ω	Omega
OD	Optical density
P	Proline
PAGE	Polyacrylamide gel electrophoresis
PARP	Poly (ADP-ribose) polymerase
PBMC	Peripheral blood mononuclear cells
PBS	Phosphate-buffered saline
PCR	Polymerase chain reaction
PerCP	Peridinin chlorophyll
PFA	Paraformaldehyde
pH	Potentia hydrogenii
PI	Protease inhibitor

PIC	Pre-integration complex
PIP	Prolactin-induced protein
PKR	Protein kinase R
Pol	Polymerase
PSMD13	26S proteasome non-ATPase regulatory subunit 13
PVDF	Polyvinylidene fluoride
PVDV	Polyvinylidene difluoride
qPCR	Quantitative real time PCR
rcf	Relative centrifugal force
Rev	Regulator of expression of virion proteins
RLU/s	Relative light units per second
RNA	Ribonucleic acid
RNase	Ribonuclease
rpm	Revolutions per minute
RPMI	Roswell Park Memorial Institute
s	second
SAMHD1	SAM domain and HD domain-containing protein 1
SDS	Sodium dodecyl sulfate
SGOL2	Shugoshin-like 2
SIV	Simian immunodeficiency virus
SIVagm	SIV isolated from african green monkey
SIVcpz	SIV isolated from chimpanzee
SIVmac	SIV isolated from rhesus macaque
SOC	Super optimal broth with catabolite repression
Sp1	Specificity protein 1
SPAG5	Sperm associated antigen 5
SPN	Sialophorin
STING	Stimulator of interferon genes
SV40	Simian Virus 40
τ	Tau
TAE	Tris-based, acetic acid, EDTA
Tat	Transactivator of transcription
TK	Thymidine kinase
TMB	3,3',5,5'-Tetramethylbenzidine
TNFRSF	Tumor necrosis factor receptor superfamily
TRIM	Tripartite motif-containing protein
Tris	Trishydroxymethylaminomethane
U	Unit
USA	United States of America
UV	Ultraviolet
V	Valine; Volt
v/v	Volume per volume
Vif	Viral infectivity factor

Vpr	Viral protein R
VPRBP	Vpr binding protein
Vpu	Viral protein U
VSVg	Vesicular Stomatitis Virus glycoprotein
w/v	Weight per volume
WHO	World Health Organization
www	World wide web
Y	Tyrosine
ζ	Zeta
ZWINT	ZW10 interacting kinetochore protein

1 Introduction

Despite 30 years of intense research [3, 16, 39, 83], the human immunodeficiency virus (HIV) still represents a global health problem with an estimated 35.3 million HIV infected people worldwide in 2012 [97]. To date, there is no cure or vaccine [40], but available highly active antiretroviral therapy can slow down and control viral disease progression [10]. Over the last decade, research focused on identifying cellular encoded candidate genes with direct antiviral potential. These so called restriction factors interfere with multiple steps of the HIV replication cycle [56]. Several factors with direct antiviral capacity have been described so far, including apolipoprotein B mRNA-editing enzyme-catalytic polypeptide-like 3G (APOBEC3G) [5], tripartite-motif-containing protein 5α (TRIM5α) [94], as well as SAM domain and HD domain-containing protein 1 (SAMHD1) [34, 48], which inhibit early processes like uncoating or reverse transcription. Additionally, Tetherin/bone marrow stromal cell antigen 2 (BST2)/CD317 is known to cause retention of HIV virions at the cell surface occurring late in the viral replication cycle [67, 99]. All these cellular factors share common characteristics of known restriction factors as they interact with viral proteins, are upregulated during HIV-1 infection or by Interferons (IFNs), and display features of codon-specific positive selection. Using a combined evolutionary genomics and transcriptomics approach, our lab has identified thirty genes that share these common characteristics of known restriction factors, and I tested their ability to inhibit HIV-1. The identification of novel HIV restriction factors will increase our understanding of the complex interplay between HIV and the immune system. Furthermore, the detailed characterization of the underlying antiviral mechanisms, also in the context of viral evasion strategies to counteract the restriction, may provide new therapeutic interventions to control HIV pathogenesis and spread.

1.1 HIV replication cycle

$CD4^+$ T helper cells and macrophages are the main HIV target cells (Figure 1). The virus binds to CD4 via its trimeric gp120 glycoproteins [8] and a co-receptor (CCR5 or

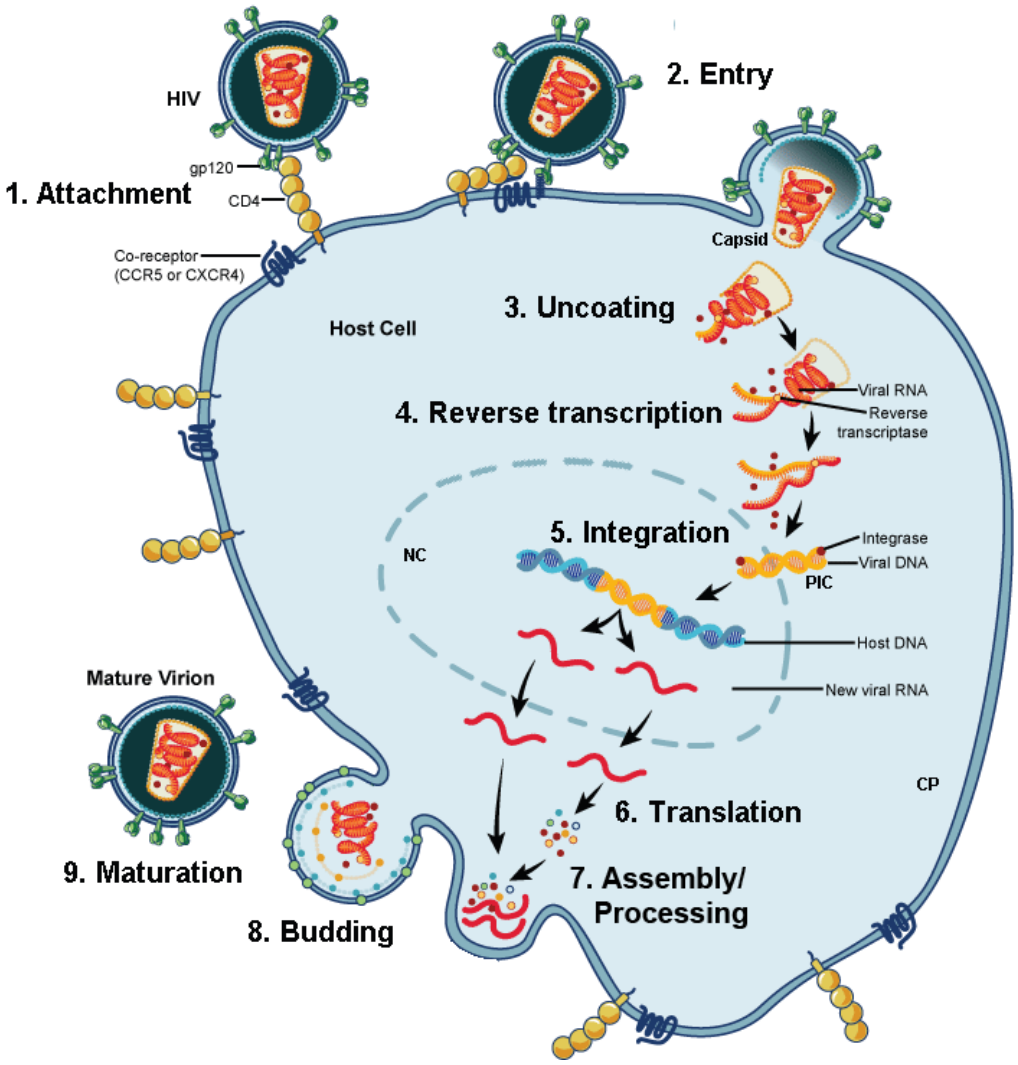


Figure 1: HIV replication cycle: Schematic presentation of individual steps during HIV replication occurring in the cytoplasm (CP) or nucleus (NC). PIC=preintegration complex, modified from NIAID (06/24/14) [66].

CXCR4), resulting in a conformational change in the transmembrane gp41 subunits [104]. This allows direct fusion with the plasma membrane [41, 63], and thereby, the capsid containing two viral RNA copies is released into the cytoplasm. Already during the process of uncoating [1], error-prone reverse transcription takes place generating viral DNA. Together with delivered viral proteins, the HIV coding DNA forms the pre-integration complex (PIC) that is transported into the nucleus [60]. Viral DNA is randomly integrated into the host euchromatin, and the cellular transcription as well as splicing machinery are hijacked to generate different viral mRNA versions [57]. Viral mRNA transcripts are transported into the cytoplasm and translated into early HIV gene

products like Rev, Tat and Nef, followed by the expression of additional late viral proteins (Gag and Pol polyprotein, as well as gp160, Vif, Vpr and Vpu). For assembly of new virions, full-length genomic mRNA together with processed viral proteins are translocated to the cell membrane where immature particles are formed [62]. After budding and proteolytic maturation, infectious virions are released from the host cell and can maintain virus propagation.

1.2 Hallmarks of restriction factors

Restriction factors are usually characterized by four distinct properties [29, 56]: The key feature is the direct and dominant inhibition of virus replication by intervening with one or several specific steps of the viral replication cycle. Secondly, the pathogen has frequently evolved counteraction strategies to reduce the extent of restriction. Thirdly, genes encoding for restriction factors are frequently under positive selection pressure, reflecting the rapid co-evolution between the host and invading pathogen [9]. Finally, restriction factors are part of the first line of defense against virus infection since their expression is typically inducible by type I Interferons (IFNs). In case of HIV, several factors with direct antiviral capacity have been described, including APOBEC3G, Tetherin/BST2/CD317, TRIM5α, and SAMHD1. Recently, the interferon-inducible myxovirus resistance protein B (MxB), and the glycoprotein named 90K have been shown to inhibit HIV replication (Figure 2). By comparing the transcriptomes of restrictive cells to susceptible cells, APOBEC3G was the first identified restriction factor against HIV [92]. This cytidine deaminase is packaged into assembling HIV virions [5]. It inhibits reverse transcription and introduces lethal hypermutations in the viral genome in the absence of the viral protein Vif [28, 58]. Comparable approaches revealed Tetherin as a potent restriction factor against different enveloped viruses [67, 99]. This type I IFN inducible protein causes retention of viral particles on the infected cell's surface, and its antiviral activity is counteracted by the HIV-1 viral protein U (Vpu) [87]. Trim5α was identified by a screening method based on monkey cDNA selection of restrictive cells within a susceptible cell population [94]. It interferes with the viral uncoating process thereby blocking viral cDNA synthesis. In general, Trim5α proteins are poor inhibitors of viruses that are naturally found in the same host species due to

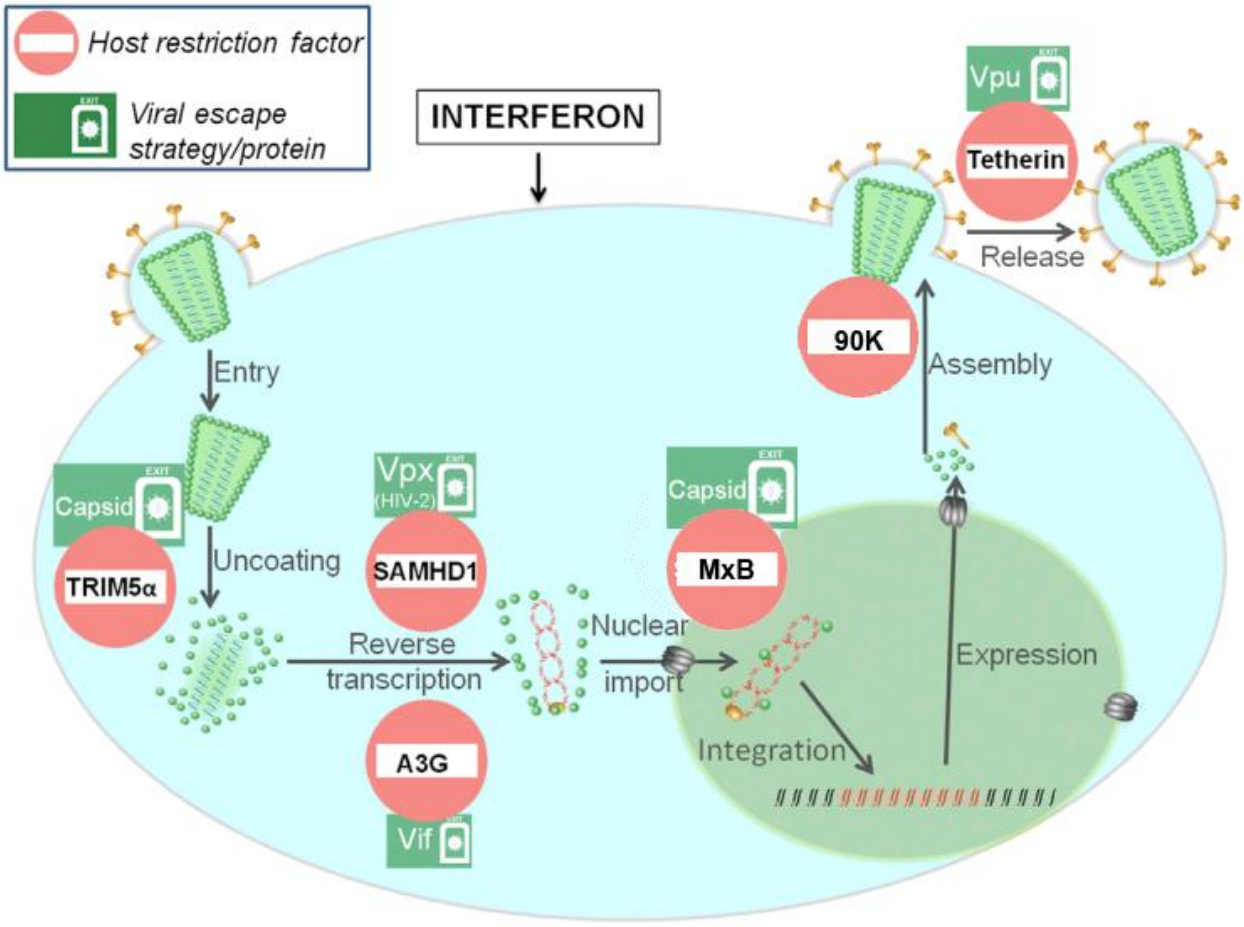


Figure 2: Known HIV restriction factors: Schematic diagram showing HIV restriction factors (red circles) known to restrict different steps in the HIV replication cycle. Viral escape strategies counteracting restriction factors (e.g., viral antagonists or resistance mutations in the viral capsid) are depicted by green exit squares. A3G=APOBEC3G, modified from Haller, 2013, 371–373 [26].

mutations in the viral capsid protein leading to evasion, but are often active against retroviruses of other species, reflecting a powerful barrier for cross-species-transmissions of primate lentiviruses [30]. SAMHD1 was identified by proteomic approaches using affinity purification followed by mass spectrometry [34, 48]. As already demonstrated in 1993, increasing dNTP levels in resting peripheral blood cells can enhance HIV replication [18], and exactly this is where SAMHD1 executes its antiviral function in non-dividing myeloid cells. As a dNTPase, SAMHD1 reduces the intracellular levels of available nucleotides thereby resulting in an early restriction during the process of reverse transcription [23, 76]. Almost all primate Vpx proteins that are found in simian immunodeficiency viruses (SIVs), and many Vpr proteins counteract SAMHD1 in a species-specific manner by inducing the proteosomal degradation of SAMHD1 [52, 108]. The type I IFN-inducible MxB protein was former

often used as a negative control for MxA, which is a well described potent effector against diverse DNA and RNA viruses [26]. In 2013, two independent groups identified MxB as an HIV restriction factor by examining the transcriptome of HIV-1 restrictive cell lines upon type I IFN treatment [24, 38, 54]. It is thought that MxB targets the viral capsid protein and blocks nuclear transfer of the PIC [24, 38], or inhibits viral integration [54]. In 2013, Lodermeyer *et al.* demonstrated that the IFN-stimulated gene 90K decreases the infectivity of HIV-1 particles [55]. 90K interferes with the proteolytic processing of HIV-1 Env proteins resulting in imperfect incorporation of the glycoproteins into HIV virions.

1.3 Criteria for the selection of candidate genes

Several high throughput-screening approaches have been performed to identify novel HIV restriction factors. All attempts were either based on genome-wide screens in combination with RNAi technologies [53, 109], on a subset of human genes that are upregulated upon IFN treatment [91], or encoding for proteins that directly interact with HIV proteins [42]. In this work, the available information based on different datasets were collected to narrow down the number of human genes with antiviral potential against HIV-1. First, I assembled the number of human genes that are known to interact with HIV-1 proteins, and/or are upregulated during HIV-1 infection or by IFNs. Further, our collaborators determined which of these genes show significant evidence for local positive selection at one or more amino acid sites to generate a shortlist of candidate genes for functional validation concerning their impact on HIV.

1.3.1 Interferon stimulated genes

The IFN family of cytokines is one of the key components of antiviral innate immunity and has been first described in 1957 [35]. Upon viral infection, IFNs provide the first line of defense against virus replication and spread. IFNs have been classified into three classes according to the cellular receptor complex they signal through [79]. Type I IFNs consist of 13 IFN-α subtypes, and a single isoform of IFN-β, IFN-δ, IFN-ε, IFN-ζ, IFN-κ, IFN-ν, IFN-τ and IFN-ω, respectively. Upon viral infection, type I IFNs are

produced within hours and bind to their receptor complex, which is expressed on all nucleated cells. Thereby, multiple signaling pathways are induced [2], resulting in the expression of many IFN stimulated genes (ISGs). Prominent examples are the Mx proteins [27], the protein kinase R (PKR) [19], and the 2-5-oligoadenylate synthetase (OAS)/RNaseL system [33] which are known to exhibit antiviral activity. All ISG expression datasets are collected on the steadily growing Interferome open access database [85]. For this approach, 1714 human ISGs published both in the first version of this platform [86], and in the open source InnateDB database [7] were included.

1.3.2 Upregulated genes in HIV-1 infected individuals

Another useful option to identify potential host restriction factors is the investigation of increased mRNA expression levels during HIV-1 infection. Therefore, I took advantage of published transcriptome data generated from HIV-1 infected patients in comparison to healthy individuals. 180 cellular genes are included in this approach as they have significantly elevated expression levels in $CD4^+$ and $CD8^+$ T cells of untreated HIV-1 infected patients compared to healthy controls [81, 82]. Additionally, 360 genes are included based on a report on altered gene expression in lymphatic tissue during HIV-1 infection [51].

1.3.3 Interaction between cellular and HIV-1 proteins

Direct protein interactions with cellular proteins are essential for HIV-1 to complete its replication cycle. These so-called ´dependency factors` are collected in the NCBI HIV-1 protein interaction database [14, 73, 77]. As mentioned above, direct protein interplay and viral antagonism are also hallmarks of restriction factors. Therefore, adding 1251 human genes described in the NCBI HIV-1 protein interaction database extended this approach. Moreover, 350 additional cellular genes are included in this study as they have been shown to directly interact with HIV-1 proteins in human HEK293T and Jurkat cells by affinity tagging and purification mass spectrometry [36].

1.3.4 Positive selection

Genomic evolution occurs when spontaneous mutations arise in individual organisms within a population and, through vertical transmission, gradually become fixed in the population. The bulk of occurring mutations is undirected and fixed by the stochastic process of neutral drift without affecting the species fitness [69, 105]. In contrast, some mutations result in a selective advantage that enhances their fixation rate within the genome. In turn, genes that display the property of positive (or diversifying) selection tend to evolve more rapidly and contribute to the divergence of species. Positively selected genes are enriched for roles in sensory perception, immunity, tumor suppression, apoptosis and reproduction [45, 69, 70, 105]. Importantly, genes under positive pressure are often involved in the continually occurring dynamic ´arms races` between the host and invading pathogens, reflecting the rapid co-evolution. Host adaptations rapidly counteract upcoming viral adaptations and *vice versa*, setting up repeated adaptive steps by both host and pathogen. The availability of several complete genome sequences of different primate species allows to combine comparative analysis methods and phylogenetic approaches with improved statistical power [44, 107].The positive selection of certain alleles can be elucidated by the ratio (d_N/d_S) of the numbers of nonsynonymous (d_N) to silent mutations (d_S) per coding site compared to the genome-wide median [43, 65]. Only when the amino acid change offers a selective advantage, it is fixed at a higher rate than a silent mutation. Therefore, a d_N/d_S value greater or equal to one is a convincing indicator for positive gene selection.

1.4 Generation of a short list of candidate genes

Based on the above, our collaborators from Lausanne (Prof. Amalio Telenti; Institute of Microbiology Lausanne) evaluated in detail the frequency of genes under positive selection within the human genome. First, genome-wide codon alignments of orthologous genes for up to nine primate species (human, chimpanzee, gorilla, orangutan, macaque, marmoset, tarsier, bushbaby, and mouse lemur) were collected from Ensembl v57. One-to-one primate gene trees were generated [101], and used for the rest of the analyses. To avoid false positive events due to sequencing errors [90],

d_N/d_S estimates were generated using both Ensembl Compara's protein-based alignments, and DNA-based alignments of primate sequences generated from genomic DNA alignments (Table 1). Telenti and colleagues found that 3.9% of all human genes (841 of 21,389) show evidence for global positive selection (Figure 3). Under consideration of the above-described databases, among these genes, 27 encode for proteins that are known to directly interact with HIV-1 proteins, an additional 21 genes are known to be upregulated during HIV-1 infection, whereas eight human genes fulfill both criteria. Overall, thirty candidate genes show significant evidence for local positive selection at one or more amino acid sites (Table 1), and were therefore selected for functional studies. As a proof-of-principle, TRIM5α and APOBEC3G were also identified as positively selected genes, whereas Tetherin, SAMHD1, MxB and 90K showed global d_N/d_S ratios below the selection threshold, although they all displayed features of codon-specific positive selection.

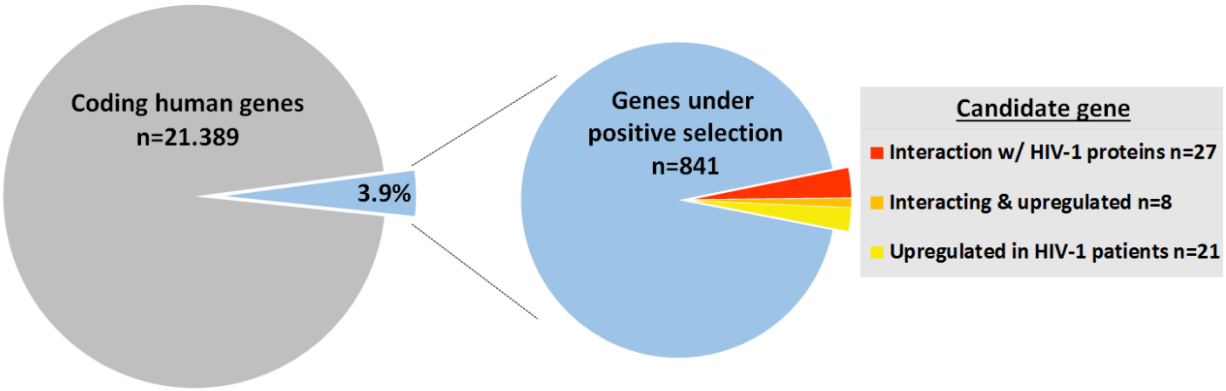


Figure 3: Human genes under positive selection pressure: In orthogonal screens, 841 human genes were identified to be under positive selection, of which 27 are known to interact with HIV-1 proteins, 21 are upregulated during HIV-1 infection, and eight that fulfill both criteria.

1.5 Scientific aims

By combining evolutionary genomics and transcriptomics approaches, thirty human genes have been identified that share common characteristics of known anti-HIV-1 restriction factors like APOBEC3G or Tetherin. Theses candidate genes interact with HIV-1 proteins, and/or are upregulated during HIV-1 infection or by IFNs. Additionally, they show significant evidence for local positive selection at one or more amino acid sites. The objective of the present study was to amplify these thirty candidate genes

from human cDNA and clone them into expression vectors to examine their antiviral activity in different cell-based assays. First, I monitored possible cytotoxic effects when candidate genes are overexpressed in HEK293T cells. Cotransfection of cells with the candidate gene and HIV-1 proviral constructs, or transfection of cells followed by transduction with VSVg-pseudotyped HIV-1 allowed determining their impact on HIV-1 early and/or late gene expression, virion production and infectivity, as well as viral protein processing. To identify possible antagonistic effects of the viral accessory proteins Vpr, Vpu, and Nef, the experiments were performed with an HIV-1 triple-mutant, bearing premature stop codons within these three viral genes, in parallel to the wild type construct. Furthermore, I investigated the influence of candidate genes on various promoter activities to monitor specificity, and their expression and induction in relevant HIV-1 primary target cells. This approach may allow the identification of novel anti-HIV-1 restriction factors and represents the first steps to understand the underlying mechanisms, uncovering new insights into the interplay between host and invading virus. Thereby, this may reveal new targets for antiretroviral therapy to control HIV-1 replication, pathogenesis and spread.

Table 1: Candidate genes selected on the basis of evolutionary history in primates, expression during HIV-1 infection *in vivo,* or issued from the HIV-1 interaction database: d_N/d_S estimates were calculated using both Ensembl Compara's protein-based alignments (columns c_m0 and c_m), and DNA-based alignments of primate sequences generated from genomic DNA alignments (column g_m0). The "m0" columns (c_m0 and g_m0) show gene-wide d_N/d_S values estimated using the SLR software under a one-ratio model (i.e. one d_N/d_S value per gene), while the "m" column (c_m) shows the mean across the gene of all codon-specific d_N/d_S estimates using SLR's sidewise model [59]. SLR-based analysis was confirmed by generating similar gene-wide d_N/d_S estimates using the M0 codon model as implemented by PAML(column paml_dnds). The raw and adjusted p-values for sidewise positive selection, measured using the so-called 'site' test for positive selection [106] are also included (column paml_pval, and Benjamini-Hochberg FDR-adjusted: paml_adj_pval). E=differentially expressed during HIV-1 infection *in vivo*; I= included in the NCBI HIV-1 interaction database.

		SLR dN/dS estimates: c_m0, c_m: amino-acid alignments			PAML dN/dS Estimates	PAML M7/M8 test For positive selection		
Ensembl_Gene_ID	Gene_Name	c_m0	c_m	g_m0	paml_dnds	paml_pval	paml_adj_pval	Association
ENSG00000100342	APOL1	1.27	1.31	NA	1.22	<0.001	<0.001	E
ENSG00000128284	APOL3	1	0	1.04	0.93	<0.001	<0.001	E
ENSG00000221963	APOL6	0.88	1.02	1.96	0.59	0.001	0.002	E
ENSG00000135535	CD164	0.9	1.03	0.84	0.72	<0.001	0.001	E
ENSG00000158477	CD1A	0.85	0.74	1.21	0.94	<0.001	<0.001	I
ENSG00000198851	CD3E	0.89	0.81	1.05	0.78	<0.001	<0.001	I
ENSG00000196352	CD55	0.85	0.93	1.08	0.86	<0.001	<0.001	I
ENSG00000026103	FAS	0.62	1.09	1.07	0.67	<0.001	<0.001	I
ENSG00000203747	FCGR3A	NA	0.78	1.41	0.75	<0.001	<0.001	I
ENSG00000154451	GBP5	0.6	0.84	1.38	0.58	0.002	0.004	E
ENSG00000163565	IFI16	1.06	1.07	0.99	0.97	<0.001	<0.001	I
ENSG00000137965	IFI44	0.8	1.03	1.05	0.79	<0.001	<0.001	I,E
ENSG00000137959	IFI44L	0.73	0.85	1.25	0.77	<0.001	0.001	E
ENSG00000142089	IFITM3	NA	1.32	0.57	0.1	0.013	0.024	E
ENSG00000115008	IL1A	0.94	1	0.56	0.89	<0.001	<0.001	I
ENSG00000164399	IL3	1.48	1.59	1.11	0.43	0.006	0.012	I
ENSG00000205358	MT1H	1.01	3.08	0.74	0.27	0.002	0.004	I,E
ENSG00000205364	MT1M	1.39	2.15	3.37	0.34	0.008	0.016	I
ENSG00000187193	MT1X	2.01	1.68	1.67	0.23	0.007	0.016	I,E
ENSG00000089127	OAS1	0.67	0.61	1.22	0.62	<0.001	<0.001	I,E
ENSG00000138496	PARP9	0.85	0.95	1.04	0.85	<0.001	<0.001	E
ENSG00000159763	PIP	1.96	1	2.36	1.09	<0.001	<0.001	I
ENSG00000185627	PSMD13	0.15	0.09	1.07	0.05	<0.001	<0.001	I
ENSG00000163535	SGOL2	0.63	1.08	0.64	0.66	0.001	0.002	E
ENSG00000135899	SP110	0.89	1.17	0.99	0.82	0.001	0.003	I,E
ENSG00000076382	SPAG5	0.75	0.86	1.09	0.64	0.008	0.016	E
ENSG00000197471	SPN	0.76	1.12	NA	0.72	<0.001	<0.001	I
ENSG00000104689	TNFRSF10A	0.98	1.17	1.84	0.74	0.001	0.002	I
ENSG00000173530	TNFRSF10D	1.19	1.41	2.8	0.9	0.002	0.004	I
ENSG00000122952	ZWINT	0.54	1.02	0.44	0.46	0.01	0.019	E

2 Material and Methods

2.1 Material

2.1.1 Cell lines

HEK293T: Human embryonic kidney (HEK) derived cell line expressing the large T antigen of simian virus 40 [25]. Obtained from ATCC™.

TZM-bl: HeLa cell-derived cell line stably transfected with CD4 and CCR5 expressing endogenous levels of CXCR4. Tat-driven luciferase and β-galactosidase genes are expressed under the control of the HIV LTR-promoter [75]. Obtained from Drs. Kappes and Wu and Tranzyme Inc. through the NIH AIDS Reagents Program.

2.1.2 Human primary cells

PBMCs: Human peripheral blood mononuclear cells (PBMCs) were collected from the buffy coat of blood samples after density gradient centrifugation using lymphocyte Biocoll separation solution.

$CD4^+$ T cells: Human $CD4^+$ T cells were isolated from buffy coat by negative selection.

MDMs: Monocytes were separated from PBMCs by plastic adherence and differentiated into monocyte-derived macrophages (MDMs) in the presence of 10% (v/v) AB-positive human serum and 15 ng/mL macrophage colony-stimulating factor.

2.1.3 Bacteria

***Escherichia coli* XL-2 blue™:** endA1 supE44 thi-1 recA1 gyrA96 relA1 lac [F' proAB lacIqZΔM15 Tn10 (Tetr) Amy Camr] (Stratagene)

2.1.4 Nucleic acids

2.1.4.1 Synthetic oligonucleotides

Oligonucleotides were purchased from Biomers (Ulm) and are listed in table 2.

Table 2: Synthetic oligonucleotide pairs for amplification of human and non-human primate transcripts.

Target gene	Primer ID	Sequence 5'-3'
APOL1	CK31	CGTCTAGACCATGAGATTCAAAAGCCACACTGTG
	CK32	CTACGCGTTCACAGTTCTTGGTCCGCCTG
APOL3	DS654	CGTCTAGACCATGGGACTGGGCCAAGGGTG
	DS655	CTACGCGTTCAGTGGGTATGGCATGGATTC
APOL6	DS638	CGTCTAGACCATGGACAACCAGGCGGAG
	DS639	CTACGCGTTCATGTAAACTGTACATACACACAGACACAC
CD164	DS636	CGTCTAGACCATGTCGCGGCTCTCCCGCTC
	DS637	CTACGCGTTTACAGAGTGTGGTAATTTCGTTCTTTAG
CD1A	DS648	CGTCTAGACCATGCTGTTTTTGCTACTTCCATTG
	DS649	CTACGCGTTTAACAGAAACAGCGTTTCCTGAAC
CD3E	DS652	CGTCTAGACCATGCAGTCGGGCACTCAC
	DS653	CTACGCGTTCAGATGCGTCTCTGATTCAGGCCAG
CD55	CK27	CGTCTAGACCATGACCGTCGCGCG
	CK28	CTACGCGTCTAAGAAACTAGGAACAGTCTGTATACTTGTGTG
FAS	CK33	CGTCTAGACCATGCTGGGCATCTGGACCCT
	CK34	CTACGCGTCTAGACCAAGCTTTGGATTTCATTTCTGAAG
FCGR3A	DS660	CGTCTAGACCATGGGTGGAGGGGCTG
	DS661	CTACGCGTTCATTTGTCTTGAGGGTCCTTTC
GBP5	DS646	CGTCTAGACCATGGCTTTAGAGATCCACATGTCAG
	DS647	CTACGCGTTTAGAGTAAAACACATGGATCATCGTTATTAAC
IFI16	CK25	CGTCTAGACCATGGGAAAAAAATACAAGAACATTGTTC
	CK26	CTACGCGTTTAGAAGAAAAAGTCTGGTGAAGTTTCCATAC
IFI44	DS650	CGTCTAGACCATGGCAGTGACAACTCGTTTG
	DS651	CTACGCGTCTATTTTTTTCCTTGTGCACAGTTG
IFI44L	DS634	CGTCTAGACCATGGTTGAAAGATGCAGCCGTC
	DS635	CTACGCGTTCAAATGCAGGGCTGTAACG
IFITM3	JH92	CGTCTAGACCATGAATCACACTGTCCAAACCTTC
	JH93	CTACGCGTCTATCCATAGGCCTGGAAGATCAGC
IL1A	DS656	CGTCTAGACCATGGCCAAAGTTCCAGACATG
	DS657	CTACGCGTCTACGCCTGGTTTTCCAGTATCTG

IL3	JH88	CGTCTAGACCATGAGCCGCCTGCCC
	JH89	CTACGCGTTCAAAAGATCGCGAGGCTC
MT1H	JH84	CGTCTAGACCATGGACCCCAACTGCTCC
	JH85	CTACGCGTTCAGGCACAGCAGCTGC
MT1M	NG75	CTAGTTCTTCTGCCTCCTCTTCTGTCAC
	NG76	GTGACAGAAGAGGAGGCAGAAGAACTAG
MT1X	JH84	CGTCTAGACCATGGACCCCAACTGCTCC
	JH96	CTACGCGTGCAGCTGCTGTGCCTGA
OAS1	CK23	CGTCTAGACCATGATGGATCTCAGAAATACCCCAG
	CK24	CTACGCGTTCAGGAGACCTGGGTTCTGTC
PIP	CK29	CGTCTAGACCATGCGCTTGCTCCAGCTC
	CK30	CTACGCGTTTATTCTACCTTTAGGATTTCAATAGTATAAAACC
PSMD13	JH94	CGTCTAGACCATGAAGGACGTACCGGGC
	JH95	CTACGCGTCTAGGTGAGGATGTCATGGGCC
SP110	DS644	CGTCTAGACCATGTTCACCATGACAAGAGCCATG
	DS645	CTACGCGTTCAAGGAAGAGTCCAGAAACCGCCGTC
SPN	DS658	CG TCTAGA CC ATGGCCACGCTTCTCCTTC
	DS659	CTACGCGTTTAAGGGGCAGCCCCGTC
TNFRSF10A	DS642	CTACGCGTTCACTCCAAGGACACGGCAG
	DS643	CGTCTAGACCATGTTCACCATGACAAGAGCCATG
TNFRSF10D	JH86	CGTCTAGACCATGGGACTTTGGGGACAAAGC
	JH87	CTACGCGTTCACAGGCAGGACGTAGCAGAG
ZWINT	NG77	CGTCTAGACCATGGAGGCAGCGGAGACA
	NG78	CTACGCGTTCATGGCAAATTTACATCTCCAG
agm_IFI16	CK101	GCRGTTCCGTTTCTGGGAACTTTACTGATTTATCTC
	CK128	CTACGCGTTTAGAAAAAAAAGTCTGGTGAAGTTTCCATAC
cpz_IFI16	CK127	CGTCTAGACCATGGAAAAAAAATACAAGAACATTGTTC
	CK82	CGTGCGGCCGCGAAGAAAAAGTCTGGTGAAGTTTCCATAC
mac_IFI16	CK83	CGTCTAGAGCCACCATGGAAAAAAAATACAAGAACATTGTTC
	CK129	CTACGCGTTTAGAAAAAAAAGCCTGGTGAAGTTTCCATAC

2.1.4.2 Expression vectors and plasmids

All used plasmids contain an ampicillin or kanamycin resistance gene for selection in bacteria.

pBR_NL4-3_IRES_eGFP: Proviral construct encoding the clone of HIV-1 M NL4-3 and containing a functional *nef* gene followed by an internal ribosomal entry site (IRES) and the *eGFP* gene [88].

pBR_NL4-3_IRES_eGFP_Δ3: HIV-1 M NL4-3 based proviral construct bearing premature stop codons within the *nef*, *vpu* and *vpr* genes [103].

pBR_NL4-3_IRES_eGFP_Δnef: HIV-1 M NL4-3 based proviral construct bearing a premature stop codon within the *nef* gene [88].

pBR_NL4-3_IRES_eGFP_Δvpu: HIV-1 M NL4-3 based proviral construct bearing a premature stop codon within the *vpu* gene [87].

pBR_NL4-3_IRES_eGFP_Δvpr: HIV-1 M NL4-3 based proviral construct bearing a premature stop codon within the *vpr* gene [78].

pBR_NL4-3_Δ3_ΔSp1_IRES_eGFP: HIV-1 M NL4-3 based proviral eGFP-reporter construct bearing premature stop codons within the *nef*, *vpu* and *vpr* genes, with mutated Sp1 binding sites in the 5' LTR promoter [6].

p_HIV-1_CH293: Plasmid encoding the proviral clone of chronic HIV-1 M subtype C isolate [72].

pXL-TOPO_CH198: Plasmid encoding the proviral clone of transmitted founder HIV-1 M subtype C isolate [72].

pBluescript_HIV-1_O_pCMO2.5: Proviral construct coding for HIV-1 O pCMO2.5 clone [96].

pBR_HIV-2_7312AJK_IRES_eGFP: Proviral construct coding for HIV-2 7312AJK clone containing a functional *nef* gene followed by an IRES and the *eGFP* gene [17].

XL-TOPO_SIVagm_Sab92018: Full-length clone of SIVagmSab transmitted founder virus [22].

pCR-XL_TOPO_SIVcpzPtt_MB897.2: Proviral construct coding for full-length SIVcpzPtt clone [4].

pBR_SIVmac239: Plasmid encoding the proviral clone of SIVmac239 [12].

pHIT-G_VSVg: Vector expressing Vesicular Stomatitis Virus glycoprotein (VSVg).

pCG_NL4-3_nef*_IRES_BFP: Bicistronic expression vector containing a nonfunctional HIV-1 *nef* gene under the control of the CMV immediate early promoter and coexpressing BFP via an IRES [88].

pGL3_enhancer_NL4-3 LTR: Expression vector for Firefly luciferase under the control of the HIV-1 LTR promoter. The 3'-LTR of HIV-1 NL4-3 was inserted into the pGL3 enhancer vector from Promega via XhoI/MluI.

pCG_NL4-3_tat: Vector expressing HIV-1 Tat protein under the control of the CMV immediate early promoter.

pTK_Red_Firelfly_Luciferase: Vector expressing Firefly luciferase under the control of the herpes simplex virus thymidine kinase promoter purchased from Thermo Scientific.

pCMV_Red_Firelfly_Luciferase: Vector expressing Firefly luciferase controlled by the human cytomegalovirus immediate early promoter purchased from Thermo Scientific.

pNF-κB_Firefly_Luciferase: Vector expressing Firefly luciferase under the control of a promoter with three NF-κB binding sites.

pTAL-Gaussia Luciferase: Vector expressing Gaussia luciferase under the control of a minimal promoter purchased from Clontech.

pIKK-β_ca_mutant: Plasmid expressing a constitutively active mutant of IKK-β.

pIFNb_Firefly_Luciferase: Vector expressing Firefly luciferase controlled by human Interferon-β (IFN-β) core promoter [31].

2.1.4.3 Molecular weight size marker

1kb Plus DNA Ladder was purchased from Life Technologies.

2.1.4.4 Synthetic nucleotides

dNTPs for Polymerase Chain Reaction were purchased from Life Technologies.

2.1.4.5 TaqMan™ probes

Gene Expression Assay for human OAS1 (#4331182, Hs00973637_m1) and human GAPDH (#4331182, Hs03929097_g1) were purchased from Life Technologies.

2.1.5 Enzymes

Restriction endonucleases were purchased from New England BioLabs.

EDTA-Trypsin was purchased from Life Technologies.

Alkaline phosphatase was purchased from Roche.

2.1.6 Media

DMEM: Dulbecco's Modified Eagle Medium (DMEM) was complemented with L-glutamine (350 mg/mL), streptomycin (120 mg/mL), penicillin (120 mg/mL) and 10% (v/v) heat inactivated fetal calf serum (FCS).

RPMI: Roswell Park Memorial Institute (RPMI) 1640 medium was complemented with L-glutamine (350 mg/mL), streptomycin (120 mg/mL), penicillin (120 mg/mL) and 10% (v/v) heat inactivated FCS.

Luria-Bertani (LB) medium: Bacto Tryptone (10 g/l), Bacto Yeast Extract (5 g/l), NaCl (8g/l), glucose (1 g/l), ampicillin or kanamycin (100 mg/l)

LB agar: LB medium complemented with 1.5% (w/v) Bacto Agar.

2.1.7 Reagents and utilities

Table 3: Reagents and utilities used in this work including their distributors.

AB-positive human serum	Sigma-Aldrich
Agarose	Difco
Ampicillin	Bayer
Annexin V binding buffer	BD Biosciences
Bacto tryptone	BD Biosciences
β-mercaptoethanol	Sigma-Aldrich
BSA 10%	KPL
Buffers for restriction digestion	New England BioLabs
Calciumchloride	Sigma-Aldrich
Cell culture flasks	Sarstedt
Cell culture well plates	Greiner
Cell scraper	Sarstedt
Complete ultra™ Tablets, Mini, EDTA free	Roche
Cryo tubes	Sarstedt
Dimethylsulfoxid	Fluka
Disodium hydrogen dehydrate phosphate	AppliChem
Dithiotreitol	Life Technologies
Dulbecco's Modified Eagle Medium	Gibco
Ethanol	Sigma-Aldrich
Ethidium bromide	Sigma-Aldrich
Ethylenediaminetetraacetic acid	Biochrom
FACS clean solution	BD Biosciences
FACS flow solution	BD Biosciences
FACS shutdown solution	BD Biosciences
FACS tubes	BD Biosciences
Falcon tubes	Sarstedt
Fetal calf serum	Life Technologies
Ficoll separation solution	Biochrom
Filtered tips	Sarstedt
Gal-screen™ substrate	Applied Biosystems
Gloves	VWR
L-Glutamine	Life Technologies
HPLC water	VWR
Hydrochloric acid	VWR
Hydrogen peroxide	VWR
Immobilon-FL™ Transfer Membrane	Millipore
Incidin foam	EcoLab
Interferon-α A/D	Sigma-Aldrich
Interferon-γ	Sigma-Aldrich

Interleukin-2	Sigma-Aldrich
Isopropanol	Merck
Isopropyl β-D-1-thiogalactopyranoside	Roche
Magnesium chloride	Sigma-Aldrich
M-CSF	R&D Systems
Methanol	Sigma-Aldrich
Microwell plates (white)	Nunc
Milk powder	Merck
M-PER™ Mammalian Protein Extraction Reagent	Thermo Scientific
MTT Thiazolyl Blue Tetrazolium Bromide	Sigma-Aldrich
NuPAGE™ Antioxidant	Life Technologies
NuPAGE™ MES SDS Running Buffer	Life Technologies
NuPAGE™ Novex 4-12% Bis-Tris Gel 1.0 mm	Life Technologies
Paraformaldehyde	Merck
PCR tubes	Biozym
Penicillin	Gibco
Phosphat buffered saline	Gibco
Phytohaemagglutinin	Murex
Pipette tips	Sarstedt
Potassium chloride molecular biology grade	Applichem
Potassium dihydrogen phosphate BioChemica	Applichem
Poly-L-Lysine	Sigma-Aldrich
Precision Plus™ Protein Kaleidoskop Standard	Bio-Rad
Protein Loading Buffer	LI-COR
Reaction tubes	Eppendorf
Reagent reservoirs	VWR
Roswell Park Memorial Institute medium	Gibco
Serological pipettes	Sarstedt
SOC medium	Gibco
Sodium chloride	Sigma-Aldrich
Sodium hydroxide	VWR
Sodiumdodecylsulfate	Sigma-Aldrich
Stericup Filter Unit 0.45 µm	Millipore
Syringe	BD Biosciences
Tris	VWR
Tryptone	Sigma-Aldrich
Trypsin	Gibco
Triton X-100	Sigma-Aldrich
Tween 20	Roth
Whatman™ paper	Bio-Rad
Wipes	Kimberly-Clark
Yeast extract	BD Biosciences
X-gal	Roth

2.1.8 Kits

Table 4: Commercial kits used in this work including their distributors.

Annexin V detection Kit	BD Biosciences
DNA Ligation Kit Ver.2.1	Takara Bio Inc.
Gal-Screen™ System	Applied Biosytsems
Gaussia luciferase System	P.J.K.
Human $CD4^+$ T cell Rosette Sep™	STEMCELL Technologies
Luciferase Assay System	Promega
Miniprep Kit	Qiagen
NucleoBond™ Xtra Midi EF	Macherey & Nagel
Phire™ Hot Start DNA polymerase Kit	Thermo Scientific
Phusion™ HF PCR Kit	Biozym
Qiashredder™	Qiagen
Rneasy™ Mini Kit	Qiagen
SuperScript™ III Reverse Transcriptase Kit	Life Technologies
TaqMan™ Fast Universal Master Mix	Applied Biosystems
Topo™ vektor Cloning Kit	Life Technologies
UltraClean™ 15 DNA purification Kit	MoBio Laboratories Inc.
Wizard™ Plus Midiprep Kit	Promega
Zero Blunt TOPO™ PCR Cloning Kit	Invitrogen

2.1.9 Buffers and solutions

1x PBS: 140mM NaCl, 8.1mM Na_2HPO_4, 2.7mM KCl, 1.5mM KH_2PO_4, adjust pH to 7

FACS buffer: PBS complemented with 1% FCS (v/v)

Fixation buffer for flow cytometry: PBS with 1% FCS (v/v) and 2% PFA (w/v)

Antibody buffer for Western blot: 0.2% Tween 20 in PBS with 1% milk powder (w/v)

Blocking buffer for Western blot: 0.2% Tween 20 in PBS with 5% milk powder (w/v)

Transfer buffer for Western blot: 47.9mM Tris, 38.6mM glycine, 1.3mM SDS and 20% methanol (v/v) in distilled water, adjust pH to 8.3

ELISA/Western blot wash buffer: 0.05% Tween 20 in PBS

Lysis solution for ELISA: 10% Triton X-100 in distilled water

Blocking solution for ELISA: PBS with 10% FCS (v/v)

Stop solution for ELISA: 1N HCl

10x HBS: 8.18% NaCl (w/v), 5.94% HEPES (w/v) and 0.25% Na_2HPO_2 x $2H_2O$ (w/v) in distilled water. For 2x HBS preparation, the 10x stock solution was diluted with distilled water (final pH 7.12) and sterilized by filtration.

Calcium chloride for transfection: 2M $CaCl_2$ in distilled water

50x TAE buffer: 2M Tris-HCl, 1M acetic acid, 0.1M EDTA, adjust pH to 8.3

Agarose gel loading buffer: 0.25% (w/v) bromophenol blue, 0.25% (w/v) xylene cyanol, 30% (v/v) glycerol

Gaussia substrate dilution buffer: 0.1M Tris, 0.3M sodium ascorbate, adjust pH to 7.4

2.1.10 Antibodies

Table 5: Antibodies used in this work including their distributors.

Anti-p24 ab9071	Abcam
Anti-Annexin V APC	BD Biosciences
Anti-APOL6	Abcam
Anti-CD11c FITC	BD Biosciences
Anti-CD14 APC	BD Biosciences
Anti-CD164	BioLegend
Anti-CD4 PerCP	BD Biosciences
Anti-Env	Kindly provided by V. Bosch
Anti-GBP5	Santa Cruz
Anti-IFI16 1G7	Santa Cruz
Anti-mouse 800CW	LI-COR
Anti-mouse IgG1 APC	BioLegend
Anti-mouse IRDye 680	LI-COR
Anti-p24	Eurogentec
Anti-rabbit 680	LI-COR
Anti-rabbit IgG, Fc-HRP	Dianova
Anti-rabbit IRDye 800CW	LI-COR
Anti-SP110	Santa Cruz
Dynabeads™ CD3/CD28	Life Technologies
Isotype control mouse IgG2b APC	BD Biosciences
Anti-β-actin	Abcam

2.1.11 Equipment

Table 6: Equipment used in this work including their distributors.

Axiovert® 40 CFL	Zeiss
Belly Dancer®	IBI Scientific
Cell culture incubator STERI-CULT®	Thermo Scientific
Centrifuge 5417R	Eppendorf
Centrifuge 5810R	Eppendorf
Certomat® IS incubator shakers	Satorius
Compartment dryer	Binder
FACS Canto II®	BD Biosciences
Geldoc® XR	Bio-Rad
Nanodrop® 2000 spectrophotometer	Thermo Scientific
Odyssey® Infrared Imaging System	LI-COR
Orion® II Microplate Luminometer	Berthold
PAGE apparatus	Life Technologies
pH meter FiveEasy®	Mettler Toledo
Pump	Welch
Safety cabinet	Thermo Scientific
StepOnePlus® qPCR System	Life Technologies
Table centrifuge	Bio-Rad
Thermomax® microplate reader	Molecular devices
Thermomixer	Eppendorf
Trans-Blot® SD Semi-Dry electrophoretic Transfer Cell	Bio-Rad
UV transilluminator, 366nm	Syngene
Veriti® Thermal Cycler	Life Technologies
Voltage PowerPAC Basic Power Supply	Bio-Rad
Vortex-Genie 2®	USA Scientific

2.1.12 Software

Table 7: Software used in this work including their distributors.

CorelDRAW™ X4	Corel Corporation
FACSDiva™ 6	BD Bioschiences
FlowJo™ 7	Treestar
Illustrator™ CS2	Adobe
Image Studio™ Lite	LI-COR
Office™ Professional Plus 2013	Microsoft
Photoshop™ CS5.1	Adobe
Prism™ 5	GraphPad
Odyssey™ Infrared Imaging	LI-COR
Quantity One™	Bio-Rad

Simplicity™	Simplicity Software Technologies Inc
Softmax Pro™	Molecular Devices
StepOnePlus™ Software v2.3	Life Technologies
Windows™ 7	Microsoft
Windows™ XP	Microsoft

2.2 Methods

2.2.1 Preparation of competent bacterial cells

A volume of 50mL LB medium was inoculated with 500µL of an E.coli overnight culture and incubated at 37°C and 200rpm on a Certomat® IS incubator shaker (Satorius) until the OD600 reached 0.5-0.6. The bacteria were pelleted by 10min centrifugation at 4,000rpm and 4°C. The supernatant was discarded and the pellet was resuspended in 10mL ice cold 100mM $MgCl_2$. Bacteria were incubated on ice for 20min and pelleted for 10min at 4,000rpm and 4°C. The supernatant was discarded and the pellet was resuspended in 1mL of ice cold 100mM $CaCl_2$ supplemented with 15% glycerol. Aliquots of 100µL were stored at -80°C.

2.2.2 DNA methods

2.2.2.1 Plasmid DNA preparation

5mL (mini preparation) or 150mL (midi preparation) LB medium supplemented with ampicillin/kanamycin (100µg/mL) was inoculated and incubated at 37°C with vigorous shaking on a Certomat® IS incubator shaker (Sartorius) for 12-16h. For propagation of proviral constructs, cultures were kept at 30°C to avoid recombinative events. Overnight cultures were used for plasmid DNA purification carried out as described in the general protocol for high-copy plasmids supplied with the Kit by the manufacturers. Plasmid DNA for cloning procedures was prepared using the Plasmid DNA Mini Prep Kit (Qiagen). For higher amounts, plasmid DNA was prepared utilizing the Wizard™ Plus Midiprep purification Kit (Promega) or NucleoBond™ Xtra Midi EF (Macherey &

Nagel). DNA quality and concentrations were determined using the Nanodrop® 2000 spectrophotometer (Thermo Scientific).

2.2.2.2 Restriction digestion

1µg of plasmid DNA was digested by restriction endonucleases in supplied buffers (New England BioLabs) according to the manufacturer's instructions in a final volume of 20µL. Digestions were performed at 37 °C for at least two hours using a thermomixer (Eppendorf).

2.2.2.3 Agarose gel electrophoresis

Gel electrophoresis of DNA was performed in 0.6-2% (w/v) agarose gels in 1xTAE buffer containing 0.2µg/mL ethidium bromide. DNA samples were mixed with 5x loading dye and agarose gel electrophoresis was carried out in 1xTAE at 140V for 30min using Voltage PowerPAC Basic Power Supply (Bio-Rad). Imaging was performed using the high-resolution Geldoc® XR system and Quantity One™ software (Bio-Rad). Visualization at 366nm on a UV transilluminator (Syngene) allowed DNA band isolation using a scalpel. The DNA fragments were purified via the UltraClean™ 15 DNA Purification Kit (MoBio Laboratories Inc.) according to the manufacturer's protocol.

2.2.2.4 DNA ligation

Vector and insert DNA were mixed in a ratio of 1:2 and ligated using a DNA Ligation Kit Ver2.1 (TaKaRa) according to the manufacturer's protocol. Ligation was performed at 16°C for at least four hours.

2.2.2.5 Transformation of competent bacteria

DNA was incubated on ice with 12-15µL of competent *E. coli* XL2 Blue cells for 20min in order to allow DNA uptake. After the cells were heat-shocked for 30s at 42°C, cells were incubated on ice for 2.5min followed by the addition of 200µl SOC medium. The transformed cells were incubated at 37°C on a shaker (Eppendorf) for 40min and

spread on LB agar plates containing respective antibiotics (100µg/mL). The plates were kept at 37°C in a compartment dryer (Binder) for up to 16h to allow the formation of single bacterial colonies. In case of proviral constructs, the temperature was reduced to 30°C to avoid recombinative events.

2.2.2.6 Polymerase chain reaction (PCR)

All PCR reactions were performed with either Phire™ Hot Start DNA polymerase Kit (Thermo Scientific) or Phusion™ HF PCR Kit (Biozym) in a Veriti® Thermal Cycler (Life Technologies) in a total volume of 20µL. dNTPs were purchased from Life Technologies and the following PCR conditions were used:

(1) Initial denaturation: 98°C, 1min

(2) Denaturation: 98°C, 5s

(3) Annealing: Tm-5°C, 5s

(4) Extension: 72°C (20s/kb)

35 cycles

(5) Final extension: 72°C, 1 min.

2.2.2.8 Generation of expression vectors

Human transcripts were amplified from human cDNA generated from primary blood cells by a standard PCR reaction using primers (Table 2) introducing XbaI and MluI restriction sites flanking the transcript's open reading frame. For non-human primate orthologue transcripts, the original stop codon was removed to introduce a C-terminal HA-tag (YPYDVPDYA). Orthologous transcripts were cloned via XbaI and NotI restriction sites. Digested PCR products were purified from agarose gels and inserted into the pCG_NL4-3_nef*_IRES_BFP expression vector by replacing the nonfunctional *nef* gene using standard cloning techniques. All PCR-derived inserts were sequenced to confirm their accuracy, silent mutations were accepted.

2.2.2.7 DNA sequencing

DNA sequencing was performed by Eurofins/MWG (Ebersberg). Sequences were analyzed using the Multalin online tool (http://multalin.toulouse.inra.fr/multalin/), sequence reverse complementor (http://bioinformatics.org/sms/rev_comp.html), and DNA/amino acid translation program (http://www.expasy.org/tools/dna.html).

2.2.3 Eukaryotic cell culture and transfection

2.2.3.1 Adherent cell culture

HEK293T and TZM-bl cells were maintained in supplemented DMEM culture medium (see 2.1.6). Cells were kept in T75 (15mL) or T175 (50mL) cell culture flasks (Sarstedt) suitable for adherent cell culture and incubated at 37°C, 90% humidity, and 5% CO_2 in a cell culture incubator STERI-CULT® (Thermo Scientific). According to cellular growth, cells were passaged two to three times per week. Adherent cells were detached from the culture vessel using 0.05% Trypsin/EDTA. After detachment, cells were resuspended in culture medium and passaged 1:5 or 1:10.

2.2.3.2 Transfection of HEK293T cells

HEK293T cells were transiently transfected using the calcium chloride precipitation method. For this purpose, HEK293T cells were seeded in 6-well plates and cultured overnight to obtain a cell density of 60-80% at the day of transfection. Prior to transfection, medium was replaced with 2mL of fresh complete DMEM per well. For transfection, 2.5 to 6µg of plasmid DNA was diluted in 13µL 2M $CaCl_2$ and filled up with sterile water to a final volume of 100µL. The solution was mixed dropwise with an equal volume of 2x HBS followed by rigorous pipetting. The transfection cocktail was added dropwise to the cells. Medium was changed routinely after 6 to 16h, and 2ml fresh complete DMEM was added to the cells.

2.2.3.3 Isolation of human primary blood cells

Human blood concentrates derived from 400 or 500mL whole blood and obtained from the blood bank (Ulm Medical Center), were diluted 1:3 with PBS. Biocoll separating solution (Biochrom) was overlaid with the diluted blood and centrifuged at 1200rcf for 20min without brakes at room temperature. The white interphase layer formed by PBMCs was transferred into a fresh tube and washed twice with PBS. After washing cells were cultured in supplemented RPMI-1640 medium (see 2.1.6). For viral infection, human PBMCs were prestimulated with 1µg/mL PHA and 10ng/mL IL-2 for three days.

2.2.3.4 Isolation and stimulation of human $CD4^+$ T cells

Human $CD4^+$ T cells were isolated from buffy coat by negative selection using the RosetteSep™ Kit (STEMCELL Technologies). Buffy coat was diluted with PBS in 2:3 ratio, and an enrichment antibody cocktail was added according to the manufacturer's instructions. $CD4^+$ T cells were isolated using lymphocyte separation medium as described for PBMCs (see 2.2.3.3), and purity was checked by flow cytometric analysis (see 2.2.6.1). Enriched T cells were cultivated in RPMI-1640 medium supplemented with 10% FCS, and stimulated via CD3/CD28 Dynabeads® (Life Technologies) in a ratio of 1:1 (cell to bead) in the presence of IL-2 (10ng/mL), IFN-α (500U/mL), or IFN-γ (200U/mL) for two days prior to analysis or infection (see 2.2.4.2).

2.2.3.5 Differentiation of human macrophages

$6x10^6$ PBMCs were cultivated in complete RMPI-1640 medium supplemented with 10% (v/v) AB-positive human serum (Sigma-Aldrich) and 15ng/mL macrophage colony-stimulating factor (R&D Systems) in 3mL per 6-well. Monocytes were allowed to differentiate into human monocyte-derived macrophages (MDMs) for seven days. Medium was replaced routinely after three days and differentiation was controlled by flow cytometry (see 2.2.6.1). MDMs were treated with IFN-α (500U/mL), or IFN-γ (200U/mL) for two days prior to analysis or transduction (see 2.2.4.3).

2.2.4 Virological methods

2.2.4.1 Production of virus stocks

HEK293T cells were transiently transfected using the calcium chloride precipitation method as described in section 2.2.3.2. 5µg of proviral DNA was delivered to the cells. For generation of VSVg-pseudotyped particles, 1µg of pHIT-G_VSVg expression vector was included. Medium was changed routinely after 6 to 16h, and fresh DMEM supplemented with 2.5% (v/v) FCS was added to the cells. Infectious supernatants were harvested 30 to 36h post transfection. To remove cellular debris, virus stocks were centrifuged at 2000rpm for 5min and stored at 4°C up to 2 weeks or at -80°C for long-term storage.

2.2.4.2 Infection of human PBMCs and $CD4^+$ T cells

10^6 stimulated primary cells in FACS tubes were washed with PBS and incubated with 400µL of virus stock for 6h at 37°C. Cells were washed twice with PBS, and resuspended in 3mL complete RPMI-1640 medium supplemented with IL-2 (10ng/mL) for three days at 37°C.

2.2.4.3 Transduction of human macrophages

Differentiated MDMs were washed rigorously with PBS and incubated with 600µL VSVg-pseudotyped virus stock for 6h at 37°C. Cells were washed twice with PBS, and kept in 2mL complete RPMI-1640 medium for three days at 37°C.

2.2.4.4 Infectivity assay on TZM-bl reporter cell line

The yield of infectious HIV-1 was determined by an infection assay using TZM-bl indicator cells. One day prior infection, 6000 cells were seeded in flat bottom 96-well dishes in a volume of 100µL complete DMEM. Infection was performed in triplicates with 10 or 100µL of infectious supernatant, unless indicated otherwise. Three days later infection was determined by measuring Tat-driven LTR-dependent β-

galactosidase expression using the Gal-screen Kit from Applied Bioscience as recommended by the manufacturer. Cell lysates were transferred into white microwell plates (Nunc), and β-galactosidase activities were quantified as relative light units per second (RLU/s) using an Orion® II Microplate Luminometer (Berthold).

2.2.4.5 Transduction of transfected HEK293T cells

$4x10^6$ cells were seeded per 6-well in 2mL complete DMEM and transfected on the following day with 2.5µg of pCG vectors expressing individual candidate genes as described in section 2.2.3.2. 30h post transfection, supernatants were removed and cells were incubated with 600µL virus stocks for 6h. Viral inoculum was replaced by 2mL fresh complete DMEM and cells were analyzed two days later by flow cytometry (see 2.2.6.2).

2.2.5 Biochemical methods

2.2.5.1 SDS polyacrylamide gel electrophoresis

Transiently transfected HEK293T cells or primary cells were washed with PBS and lysed in M-PER™ Mammalian Protein Extraction Reagent (Thermo Scientific). The protein amount was normalized by measuring protein concentrations with the Nanodrop® 2000 spectrophotometer (Thermo Scientific). Cell free viral particles were pelleted by centrifugation at 14000rpm for 90min at 4°C before lysis. Lysates were mixed with 4x protein loading buffer (LI-COR) supplemented with 10% β-mercaptoethanol and heated for 5 min at 95°C. 5µL of Precision Plus™ Protein Kaleidoskop Standard (Bio-Rad) and samples were loaded on NuPAGE™ Novex 4-12% Bis-Tris gels (Life Technologies) and run at 150V for 90min using a Voltage PowerPAC Basic Power Supply (Bio-Rad).

2.2.5.2 Western blot

Separated proteins were blotted onto a methanol-activated polyvinylidene difluoride (PVDF) Immobilon-FL™ Transfer Membrane (Millipore) at 0.75mA/cm^2 for two hours in Western blot transfer buffer. Membranes were blocked in PBS containing 5% non-fat dry milk for 30min at room temperature and then incubated overnight with primary antibodies (Table 5) diluted in PBS containing 1% non-fat dry milk at 4°C according to the manufacturers' instructions. Unbound antibodies were removed by three washing steps with 0.05% Tween in PBS. Then, membranes were incubated with fluorophore-conjugated secondary antibodies (Table 5) diluted 1:20,000 in 1% non-fat dry milk in PBS for 20min at room temperature. Membranes were washed three times with 0.05% Tween in PBS. Fluorescence signals were detected with the Odyssey® Infrared Imaging System (LI-COR) and signal intensities were quantified by Image Studio™ Lite (LI-COR) using β-actin for normalization.

2.2.5.3 HIV-1 p24 antigen ELISA

HIV-1 p24 capsid protein content was quantified using a homemade anti-p24 ELISA system. Infectious supernatants or cells were lysed overnight with 1% Triton X-100 at 4°C. Different dilutions of the lysed samples were transferred in p24-antibody coated and blocked Maxisorb flat bottom 96-well plates (Nunc). After overnight incubation in wet chambers at room temperature, unbound capsid proteins were removed by several washing steps. For the quantification of bound p24 antigen the "sandwich"-ELISA method was used. First, a rabbit anti-HIV-1 p24 antibody was added for one hour at 37°C, followed by incubation with a goat anti-rabbit antibody conjugated to horseradish peroxidase (HRP) for two hours at 37°C. TMB peroxidase substrate was added and the reaction was stopped with 1N HCl. The color intensity which is proportional to the amount of p24 capsid antigen was measured at 450nm and 650nm with the Thermomax® microplate reader (Molecular devices). Between each step, wells were washed three times with 0.05% Tween 20 in PBS.

2.2.5.4 Luciferase based promoter reporter assays

To determine the modulation of viral promoter activity, 20,000 HEK293T cells were seeded in flat bottom 96-well plates in 100µL complete DMEM. The next day, cells were cotransfected with 2.5µg of firefly luciferase reporter vectors controlled by the HIV-1 long terminal repeat (LTR), HSV thymidine kinase (Thermo Scientific), CMV immediate early (Thermo Scientific), human IFN-β core promoter, or by an artificial promoter containing three NF-κB binding sites, together with equal amounts of vectors coexpressing the individual candidate genes and BFP, unless indicated otherwise. The HIV-1 LTR promoter was activated by additional transfection of 0.5µg of a plasmid expressing HIV-1 NL4-3 Tat if indicated. In this instance, the amount of cotransfected LTR-reporter vector and plasmids coding for candidates was reduced to 2µg. The NF-κB experiment was also performed in the presence of 1.5µg Δ3 HIV-1 construct. The IKK-β constitutively active mutant was used as a positive control for NF-κB activation. To determine the modulation of HIV-1 LTR activity by IFI16, HEK293T cells were cotransfected with 2µg of pGL3-LTR reporter construct and different amounts of a pCG vector expressing IFI16. The LTR was activated by additional transfection of 0.8µg of an NL4-3 Tat expression vector or a Δ3 HIV-1 NL4-3 proviral clone. Empty vector was used to achieve equal DNA levels in all transfections. 40h post transfection, cells were lysed in Luciferase Cell Culture Lysis Reagent (Promega) and firefly luciferase activity was determined using the Promega Luciferase Assay System according to the manufacturer's protocol. Cell lysates were transferred into white microwell plates (Nunc), and luciferase activities were quantified as relative light units per second (RLU/s) using an Orion® II Microplate Luminometer (Berthold).

2.2.5.5 MTT assay

20,000 HEK293T cells were seeded in flat bottom 96-well plates, and transfected the next day with 0.375µg of vectors expressing candidate genes. After two days, 10µL of MTT 3-(4,5-dimethylthiazole-2-yl)-2,5-diphenyl tetrazolium bromide (Sigma-Aldrich) solution (5mg/mL) was added and incubated for three hours at 37°C. Thereafter, cell free supernatant was discarded, formazan crystals were solubilized in 100µL DMSO-

Ethanol (1:1) and optical density was analyzed at 490/650nm with the Thermomax® microplate reader (Molecular devices) to evaluate metabolic activity of transfected cells.

2.2.6 Flow cytometric analysis

2.2.6.1 Staining of $CD4^+$ T cells and macrophages

10^6 human $CD4^+$ T cells were washed with 1mL cold FACS buffer in FACS tubes and stained with fluorochrome labeled antibodies (Table 5) in 100µL FACS buffer for one hour at 4°C. In case of unlabeled detection antibody, cells were incubated with an APC-conjugated secondary antibody in 100µL FACS buffer for 30min at 4°C under inclusion of the respective isotype control. Cells were washed with 1mL cold FACS buffer and fixed in 300µL fixation buffer. Adherent MDMs were washed with cold PBS, incubated with 0.05% Trypsin/EDTA and carefully detached using a cell scraper (Sarstedt) prior to surface staining in FACS tubes. Flow cytometric analysis was performed with a FACS CANTO® II (BD Biosciences). Purity of negatively isolated $CD4^+$ T cells was routinely checked by surface staining of CD4 and counterstaining for CD11c. The differentiation of MDMs was monitored by staining of CD14 surface expression including an unspecific APC-labeled mouse IgG2b antibody as isotype control.

2.2.6.2 Detection of eGFP and BFP in HEK293T and primary cells

Flow cytometric analysis of intracellular eGFP and BFP reporter expression in transfected/transduced HEK293T cells or infected/transduced primary cells was performed on a FACS CANTO® II (BD Biosciences). Cells were washed with 1mL cold FACS buffer in FACS tubes and fixed in 300µL fixation buffer for at least 20min at 4°C prior to analysis. For analysis of HEK293T cells cotransfected with 2.5µg vector expressing individual candidate genes and BFP, together with 2.5µg of proviral HIV-1 IRES eGFP constructs or transduced by VSVg-eGFP reporter HIV-1, the percentage of $eGFP^+$ cells within the BFP^+ population was determined in relation to $eGFP^+$ cell numbers within the BFP^- population. In addition, the mean fluorescence intensity of

eGFP within the BFP^+ population was determined to monitor the impact on early viral gene transcription.

2.2.6.3 Annexin V staining of transfected HEK293T cells

HEK293T cells were seeded in 6-well plates and transfected the next day with 2.5µg of vectors expressing candidate genes. 40h post transfection, apoptotic cells were monitored by the Annexin V detection Kit (BD Biosciences) according to the manufacturer's instructions. APC signals were measured by a FACS CANTO® II (BD Biosciences).

2.2.7 RNA methods

2.2.7.1 RNA extraction from primary cells

Extraction of total cellular mRNA from primary cells was performed using the RNeasy™ Mini Kit (Qiagen) according to the manufacturer's instructions. Cells were lysed in 350µL of the provided lysis buffer including β-mercaptoethanol. Contaminating DNA was removed by a recombinant DNase solution which was directly applied onto the silica membrane during the preparation. RNA was eluted in 60µL RNase-free water. RNA concentrations were determined by the Nanodrop® 2000 spectrophotometer (Thermo Scientific) and RNA was stored at -80°C if not used immediately.

2.2.7.2 cDNA synthesis

1µg of total mRNA was used for cDNA synthesis via the SuperScript™ III Reverse Transcriptase Kit (Life Technologies) according to the manufacturer's instructions. Initial denaturation was performed for 5min at 65°C using a thermomixer (Eppendorf). cDNA synthesis was carried out via provided Oligo $(dT)_{20}$ (50 pmoles/reaction) for 50min at 50°C and reverse transcription was stopped by heat inactivation for 5min at 85°C. cDNA was used for amplification of human transcripts (see 2.2.2.8) or applied in quantitative real time PCR.

2.2.7.3 Quantitative real time PCR

QPCR for OAS1 mRNA levels in $CD4^+$ T cells and MDMs was performed according to the "two-step" method: Template cDNA was analyzed by TaqMan™ Fast Universal Master Mix (Applied Biosystems) according to the manufacturer's instructions. Validated TaqMan™ Gene Expression Assay for human OAS1 (Life Technologies) and TaqMan™ endogenous GAPDH control (Life Technologies) were applied to determine OAS1 mRNA levels in primary cells upon stimulation. Reactions were set up in a final volume of 20µL as described below:

- 2 x TaqMan™ Fast Universal PCR Master Mix 10µL
- 20x TaqMan™ Gene Expression Assay Mix,
  containing: • Forward PCR primer (18µM)
  • Reverse PCR primer (18µM)
  • TaqMan™ probe (5µM) 1µL
- Template cDNA 0.5µL
- RNase-free water 8.5µL

For multiple mix samples, a master mix was prepared containing all but the cDNA template. The complete reaction was then placed in the StepOnePlus® qPCR System (Life Technologies). The standard thermal cycling profile included initial denaturation at 95°C for 20sec, followed by melting at 95°C for 3sec and annealing/extension at 60°C for 30sec for 38 cycles in total. Gene expression analysis was performed using the comparative ($2^{-\Delta\Delta C_T}$) C_T (cycle threshold) method [89]. Values were normalized to the human GAPDH mRNA signals.

2.2.8 Statistical analysis

Statistical analyses were performed with PRISM™ 5 (GraphPad) using the two-tailed unpaired Student´s t-test. Pearson´s correlation was used to examine the relationship between two groups of variables.

3. Results

Human genes encoding antiviral proteins are commonly under positive selection, upregulated in infected patients, and frequently interacting with viral proteins. 56 human genes sharing these characteristics were identified by combining evolutionary genomics, transcriptomics, and available protein interaction data. These candidate genes may encode previously uncharacterized restriction factors of the human immunodeficiency virus-1 (HIV-1), and thirty of these candidate genes showing significant evidence for local positive selection at one or more amino acid sites, were cloned into expression vectors for functional characterization.

3.1 Generation and functionality of expression vectors

With three exceptions (*PARP9*, *SGOL2*, and *SPAG5)*, all thirty candidate genes showing significant evidence for local positive selection at one or more amino acid sites (Table 1) were amplified from human cDNA and cloned into bicistronic pCG-based vectors coexpressing the blue fluorescent protein (BFP) via an internal ribosomal entry site (IRES) (Figure 4A). To investigate their functionality, these

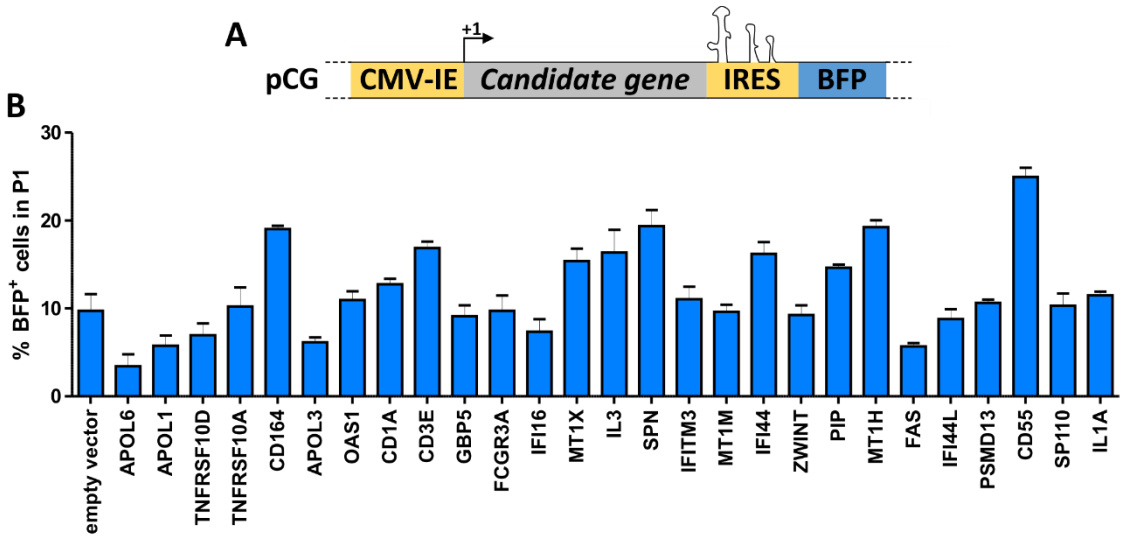


Figure 4: A) Schematic depiction of bicistronic expression vectors: Candidate genes were cloned into a pCG-based vector under the control of the cytomegalovirus immediate early promoter (CMV-IE) followed by an IRES-BFP cassette. **B) BFP expression in HEK293T cells:** Cells were transfected with 2.5µg of the indicated plasmids, and functionality of constructs was determined by flow cytometry after two days (n=3 ± SD).

expression vectors were transfected into HEK293T cells, and transfection rates were determined by flow cytometry. As shown in figure 4B, BFP$^+$ cells were detectable for each construct expressing individual candidate genes. The generation of expression vectors provided a first step towards the establishment of HEK293T cell-based functional assays to investigate possible antiviral effects exerted by the selected candidate factors.

3.2 Cell viability upon transfection of candidate genes

Before investigating the antiviral capacity of the candidate genes, I was interested in possible cytotoxic effects caused by these factors when overexpressed in HEK293T

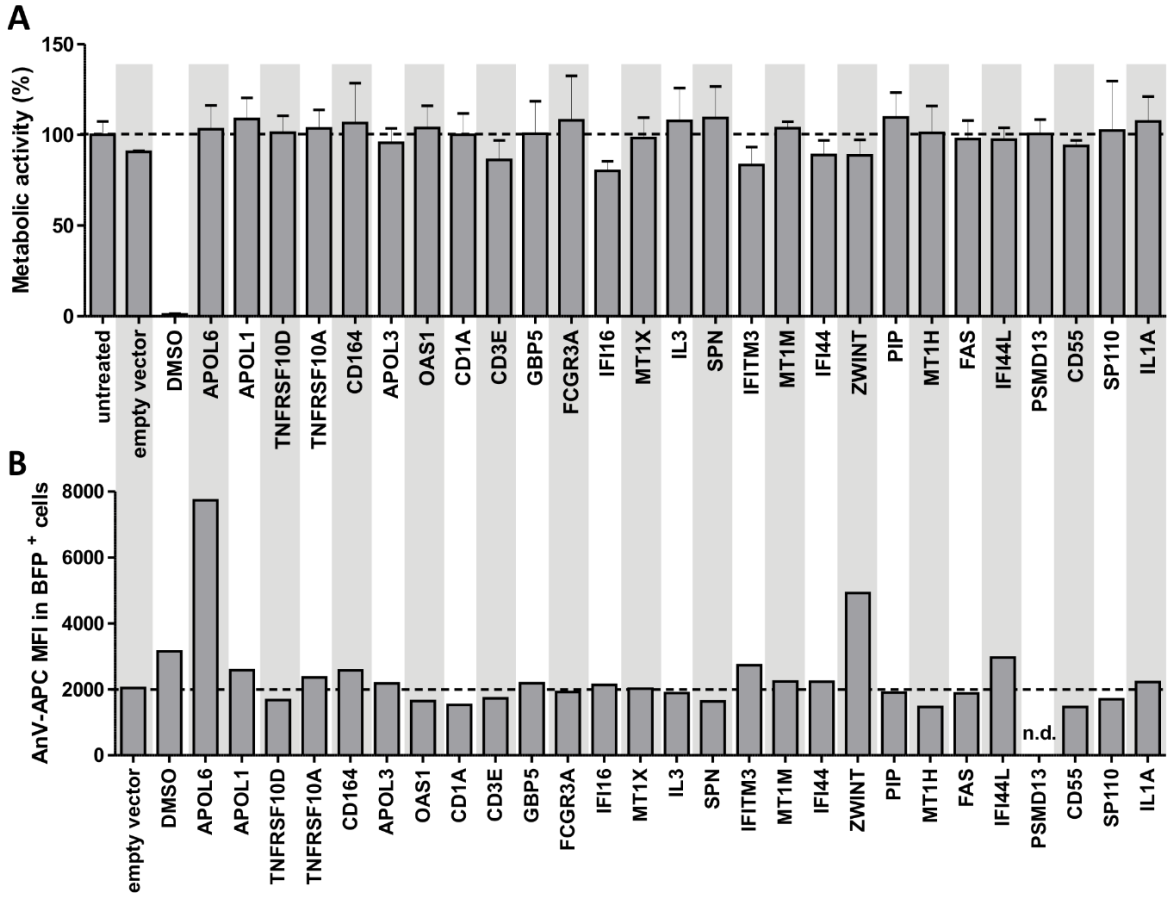


Figure 5: Cell viability in the presence of candidate genes: A) HEK293T cells were transfected with 2.5µg of plasmids coding for the indicated candidate gene, and metabolic activity was examined two days later by a MTT assay. All values were normalized to the BFP only (empty vector) control construct, and DMSO treatment served as a positive control (n=3 ± SD). **B)** Annexin V levels on BFP$^+$ HEK293T cells two days post transfection with 2.5µg DNA. Cells were fixed and the mean fluorescence intensity (MFI) in BFP$^+$ cells was determined by flow cytometry (n=1).

cells. Therefore, a MTT assay, determining cellular enzymatic activity, was performed upon transfection (Figure 5A). None of the candidates significantly reduced the metabolic activity of HEK293T cells when overexpressed. The more sensitive Annexin V staining on HEK293T cells, measuring early apoptotic alterations in plasma membrane structures on single-cell-level, largely confirmed the results. As shown in figure 5B, only two candidates (APOL6 and ZWINT) induced cell death, whereas all other factors did not markedly affect the cell viability.

3.3 Establishment of HEK293T cell-based functional assays

After examination of possible cytotoxic effects induced by the candidate factors in HEK293T cells, I focused on the establishment of functional assays to determine their potential effects against HIV-1. Looking at the HIV-1 replication cycle (Figure 6A), I decided to set up two distinct HEK293T cell-based assays that differed in the time point when the candidate genes were expressed: The first setup involved cotransfection of the candidate gene and proviral DNA, thereby focusing on the late stages of viral replication starting with episomal viral expression. In the second setup, HEK293T cells were transduced with VSVg-pseudotyped viral particles 36h post transfection with the candidate genes. Although this experimental setup altered the usual HIV-1 entry process, it allowed monitoring potential inhibitory effects during the early steps of HIV-1 replication prior to integration.

3.3.1 Cotransfection setup targeting *late steps* of HIV-1 replication

First, candidate genes were cotransfected with a full-length HIV-1 group M NL4-3 based proviral eGFP-reporter construct (Figure 6C). To identify possible antagonistic effects of the viral accessory proteins Vpr, Vpu, and Nef, the experiments were also performed with a triple-mutant (Δ3), bearing premature stop codons within these three genes, in parallel to the wild type (wt) construct. As illustrated in figure 6B, two days after cotransfection both cells and supernatants were harvested to determine the impact of each candidate factor on early and late HIV-1 gene expression, virus

production, and virion release as well as infectivity using flow cytometry, Western blot, p24 capsid ELISA and TZM-bl reporter cell assay, respectively.

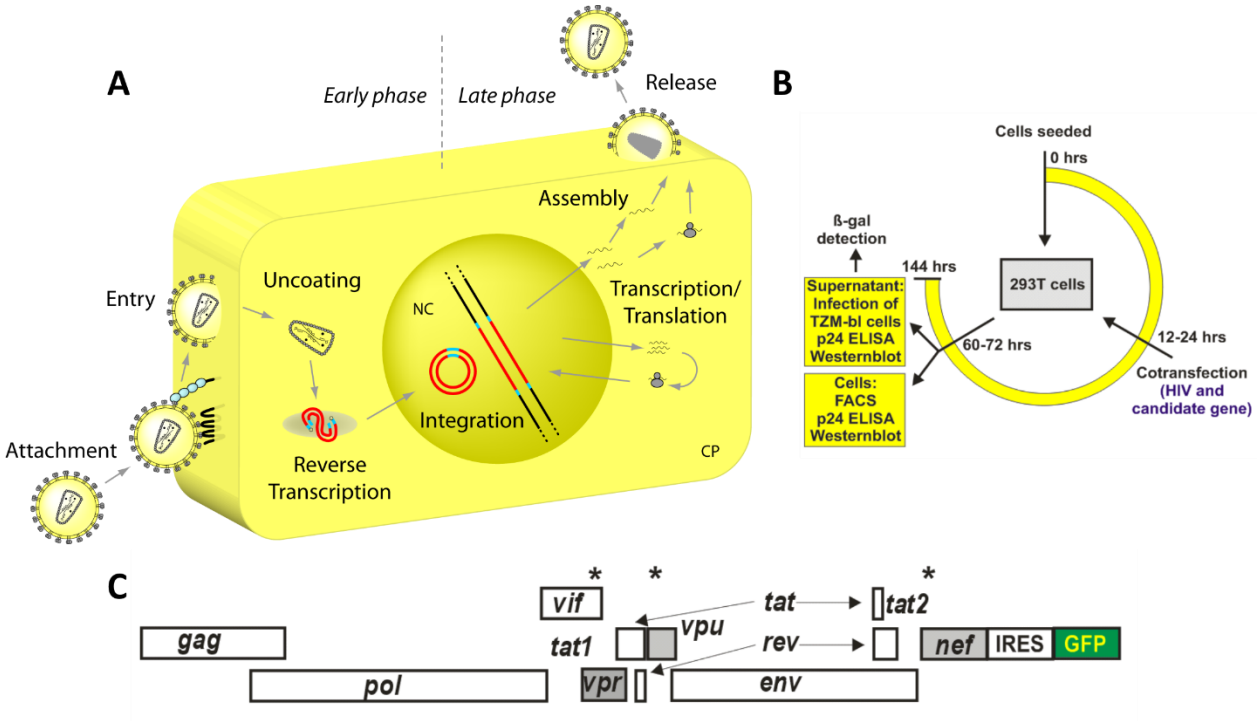


Figure 6: A) Schematic presentation of the HIV-1 replication cycle divided into *early* & *late phase*: The viral replication cycle up to the stage of integration represents the *early* phase, which is followed by the *late* phase. **B) Overview on the work flow in the *late* cotransfection setup,** and **C) Full-length HIV-1 NL4-3 based proviral IRES-eGFP reporter construct:** Positions of premature stop codons in the *vpr*, *vpu* and *nef* genes of the Δ3 derivative are indicated by stars. The eGFP reporter is coexpressed via an IRES from the bicistronic early viral mRNA coding for Nef.

3.3.1.1 The majority of candidates strongly reduces the production of infectious HIV-1

I started testing the supernatants of cotransfected HEK293T cells on TZM-bl reporter cells to determine virus production in the presence of individual candidate genes (Figure 7A). Unexpectedly, overexpression of 15 cellular factors reduced the production of wt virions by more than 75% compared to the sample, in which the wt provirus was cotransfected with a control vector only expressing BFP. For five candidates (APOL1, APOL6, TNFRSF10A, TNFRSF10D and CD164) the inhibitory effect against wt HIV-1 reached more than 90%. In contrast, IL-1A enhanced the production of infectious wt HIV-1 by nearly two fold.

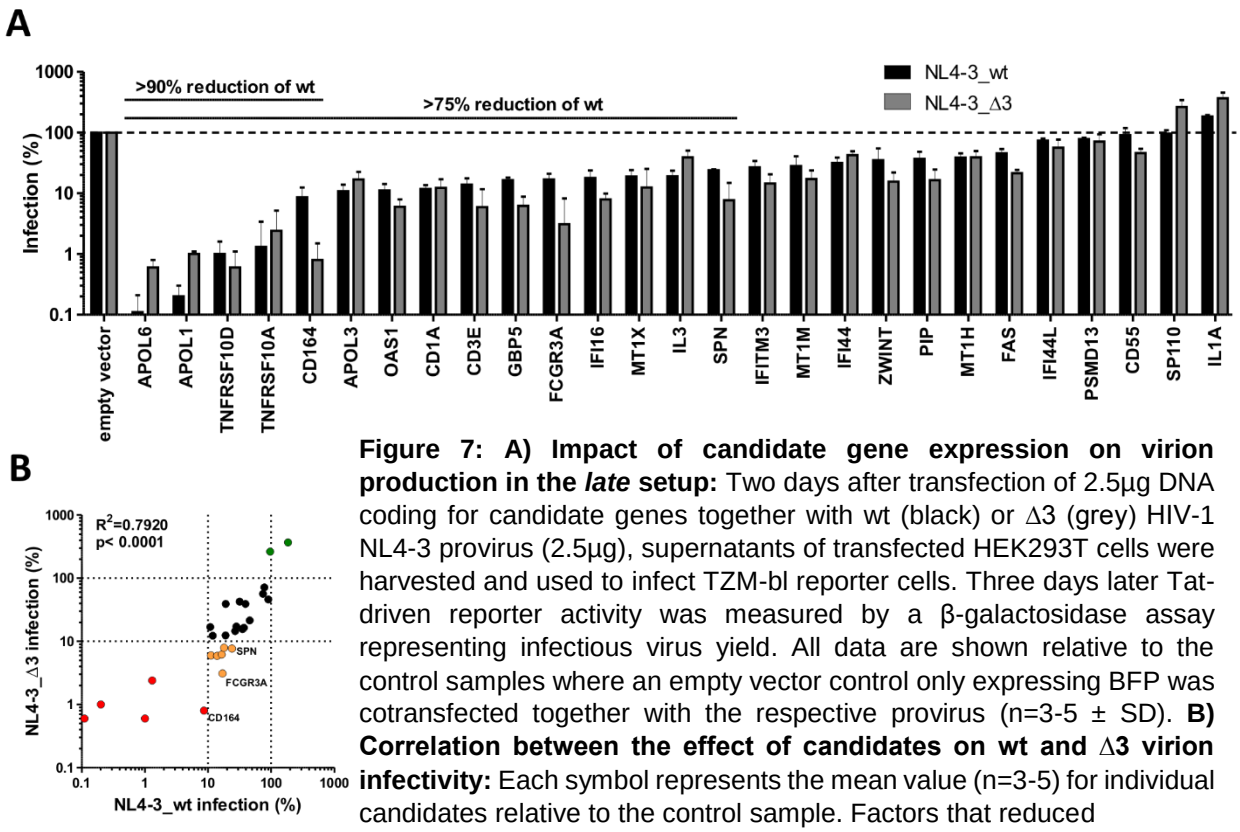
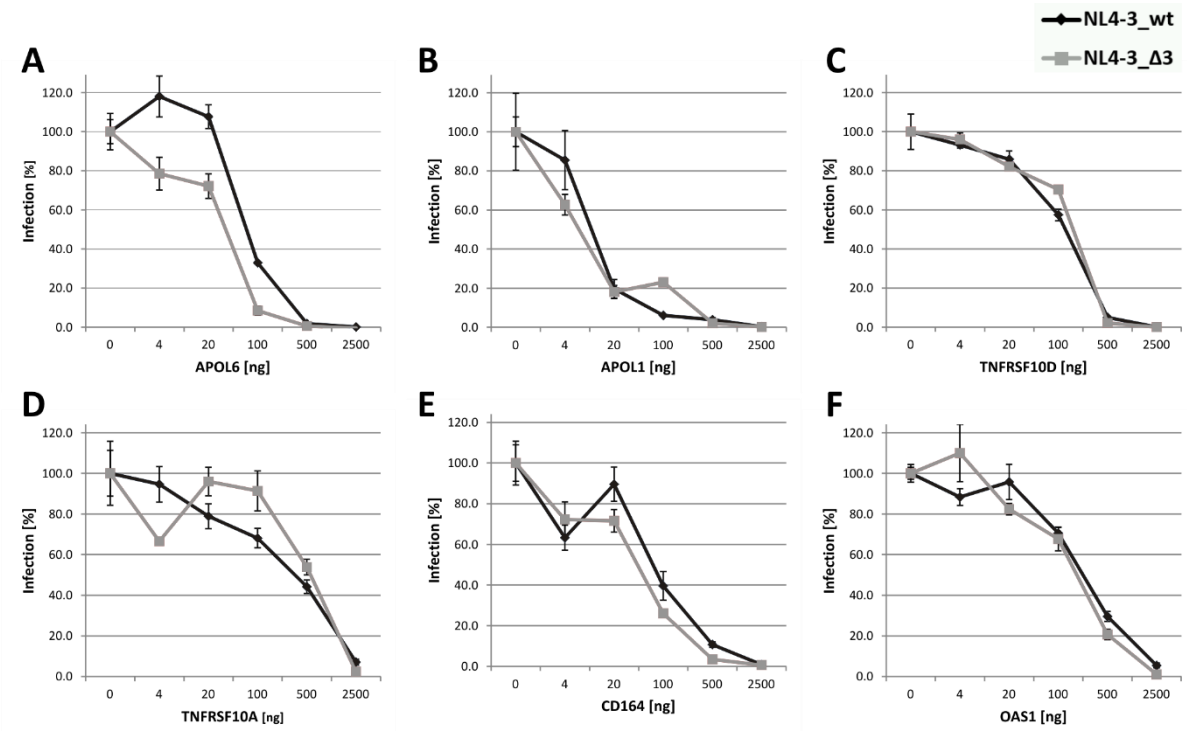


Figure 7: A) Impact of candidate gene expression on virion production in the *late* setup: Two days after transfection of 2.5µg DNA coding for candidate genes together with wt (black) or Δ3 (grey) HIV-1 NL4-3 provirus (2.5µg), supernatants of transfected HEK293T cells were harvested and used to infect TZM-bl reporter cells. Three days later Tat-driven reporter activity was measured by a β-galactosidase assay representing infectious virus yield. All data are shown relative to the control samples where an empty vector control only expressing BFP was cotransfected together with the respective provirus (n=3-5 ± SD). **B) Correlation between the effect of candidates on wt and Δ3 virion infectivity:** Each symbol represents the mean value (n=3-5) for individual candidates relative to the control sample. Factors that reduced wt HIV-1 infectivity more than 90% are shown in red, candidates that achieved this only for the Δ3 mutant are color coded in orange, and enhancers for the Δ3 construct are presented in green.

All candidate genes that suppressed the infectivity of wt HIV-1 also inhibited the Δ3 mutant (Figure 7B). Notably, the effect on Δ3 was on average more pronounced than on wt HIV-1 (p= 0.003; paired one-tailed t-test of all candidates with the exception of enhancing factors). This is reflected by the observation that six additional candidate genes (*OAS1*, *CD3E*, *GBP5*, *FCGR3A*, *IFI16* and *SPN*; shown in orange in figure 7B) also achieved a reduction of more than 90% regarding infectivity when the virus lacked functional *vpr*, *vpu* and *nef* genes. Three factors (CD164, FCGR3A and SPN) inhibited the Δ3 mutant three times more efficiently than the wt construct. In addition to IL-1A, SP110 (shown in green in figure 7B) also enhanced Δ3 virion production. The enhancing effect was about threefold for both factors.

3.3.1.2 Some candidate factors inhibit HIV-1 virion production in a dose-dependent manner

To verify antiviral as well as enhancing effects on HIV-1 infection, I next measured the infectious virus yield at different doses of selected candidate genes. To this end, HEK293T cells were transfected with wt or Δ3 HIV-1 constructs, together with increasing amounts of vector coding for individual candidates. Subsequently, the cell culture supernatants were tested on TZM-bl reporter cells for infectivity (Figure 8). The results confirmed that APOL1, APOL6, TNFRSF10A, TNFRSF10D, CD164, OAS1, CD3E, IFI16 and GBP5 inhibited wt and Δ3 HIV-1 in a dose-dependent manner thereby confirming the inhibitory effects described above. Notably, low expression levels of FAS increased both wt and Δ3 HIV-1 infection but significantly reduced infection at higher doses (Figure 8J). Finally, increasing amounts of SP110 and especially IL-1A enhanced production of infectious HIV-1 (Figure 8 K and L) which is in agreement with the data shown above.



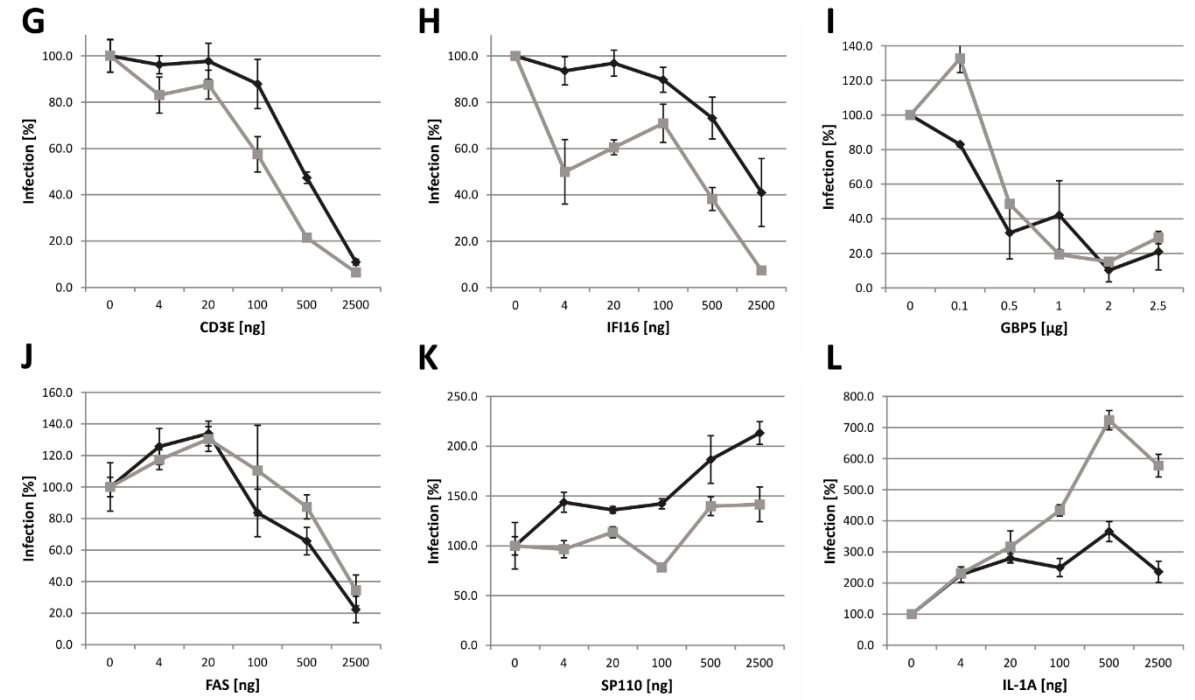


Figure 8: Dose-dependent effects of candidate genes on HIV-1 production: Two days after cotransfection of 2.5µg wt (black) or Δ3 (grey) proviral HIV-1 constructs with increasing amounts of vectors expressing indicated candidate genes, the supernatants of transfected HEK293T cells were used to infect TZM-bl reporter cells. Three days later Tat-driven β-galactosidase expression was measured as a reporter for infectious virus yield. All data are shown relative to the control samples where an empty vector control only expressing BFP was cotransfected with the respective provirus. Representative experiments with mean values (± SD) derived from triplicate infections are shown (n=1-3).

3.3.1.3 Flow cytometric analysis in the cotransfection setup

Next, I examined BFP and eGFP expression in cotransfected HEK293T cells, representing the expression of candidate genes and viral genes, respectively (Figure 9A). To monitor the effects of the candidate factors on virus production, I determined the percentage of HIV-1 producing ($eGFP^+$) cells within the BFP^+ population expressing individual candidates compared to the numbers of $eGFP^+$ in the BFP^- population (Figure 9B). On average, the frequency of HIV-1 producing (GFP^+) cells was reduced by nearly 30%. In the presence of four genes (*APOL1*, *APOL3*, *APOL6* and *TNFRSF10D*) the reduction of infected cells achieved over 50%, whereas IFI44L increased the number of HIV-1 producing cells within the BFP^+ population. As shown in figure 9D, the effects on wt and Δ3 HIV-1 reporter constructs highly correlated. This was expected in this experimental setup since the absence of the three accessory genes should not influence early viral gene expression upon transfection of

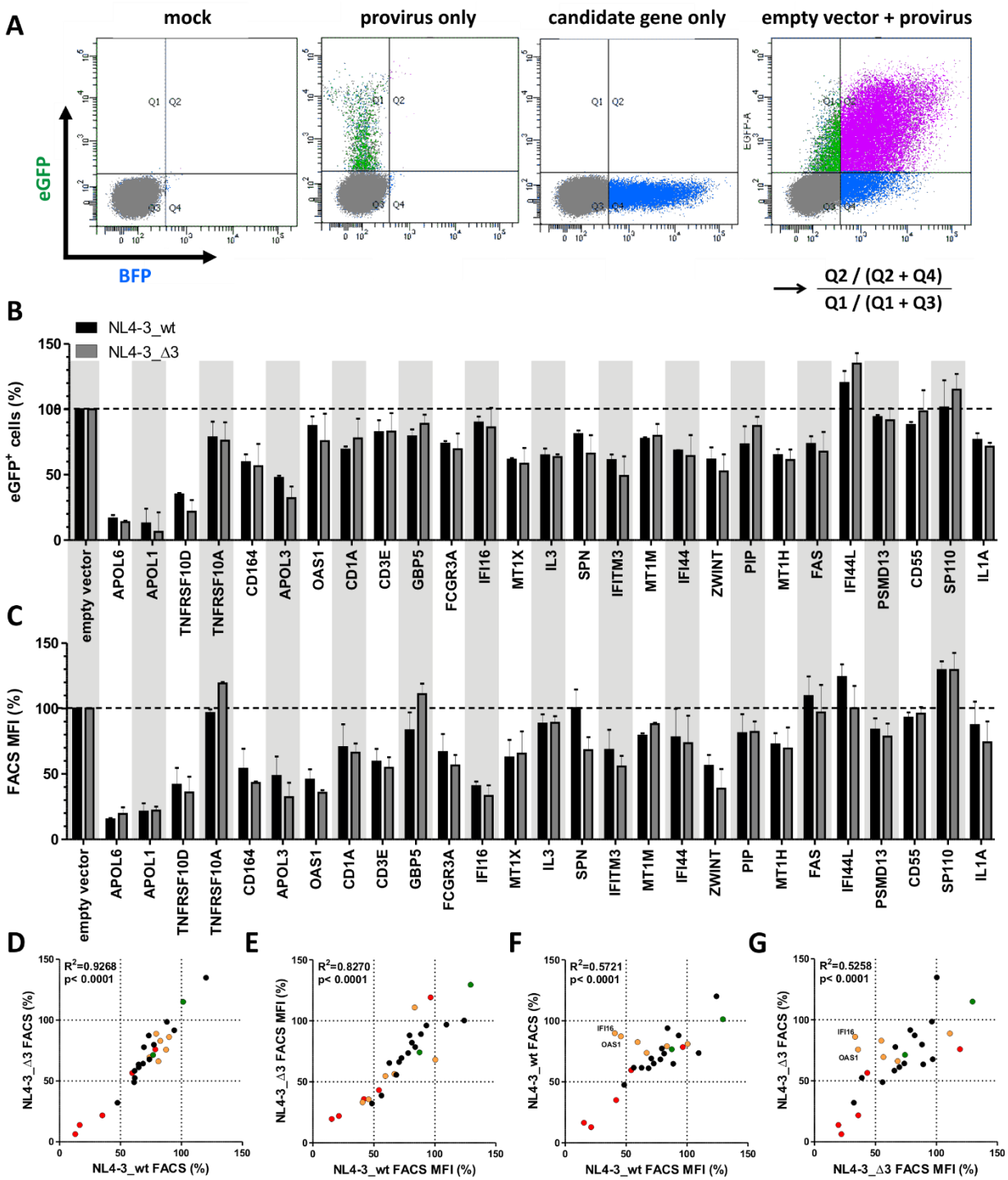


Figure 9: Flow cytometric analysis in the *late* cotransfection setup: A) Gating strategy: HEK293T cells were transfected with 2.5µg of vector coding for individual candidate genes together with 2.5µg wt (black) or Δ3 (grey) HIV-1 eGFP-reporter provirus. Two days later cells were analyzed by flow cytometry to determine, **B) percentage of HIV-1 producing cells (eGFP$^+$) in BFP$^+$ HEK293T cells**, and **C) eGFP-MFI in cells overexpressing the candidate genes.** All values are shown relative to the corresponding control sample (n=3-5 ± SD). **D) Correlation analyses between the effects on percentage of wt versus Δ3 HIV-1 producing cells coexpressing individual candidate genes,** and **E) on the MFI of eGFP within the BFP$^+$ population. F) Correlation between percentage of HIV-1 transfected cells and eGFP-MFI for the wt construct,** and **G) for the Δ3 derivate**. Each symbol represents the mean

value (n=3-5) for individual candidates relative to the control sample. The color code is based on the results achieved in the infectivity assay on TZM-bl cells (see figure 7B).

HIV-1 proviral constructs. Furthermore, I determined the mean fluorescence intensity (MFI) of eGFP within the BFP^+ cells as an indicator of viral gene expression since eGFP is expressed from the bicistronic mRNA that is also coding for the early viral Nef protein (Figures 6C and 9C). Most candidates suppressed eGFP expression. In cells transfected with the wt provirus six cellular genes (*APOL1*, *APOL3*, *APOL6*; *TNFRSF10D*, *OAS1* and *IFI16*) reduced the MFI of eGFP by more than 50% compared to the control sample, whereas two factors (IFI44L and SP110) enhanced eGFP expression. As expected, the effects on wt and Δ3 construct correlated well in this experimental setup (Figure 9E). Two additional candidates (CD164 and ZWINT) decreased the MFI of eGFP by more than half in the context of the Δ3 mutant. Unexpectedly, the enhancing effect of IFI44L was not detectable for the Δ3 mutant, whereas SP110 as well as TNFRSF10A increased the MFI of eGFP in Δ3 HIV-1 infected cells. I observed a significant correlation between the influence on percentage of $eGFP^+$ cells compared to the level of eGFP expression for both wt (Figure 9F) and Δ3 HIV-1 infected cells (Figure 9G). Interestingly, two factors (OAS1 and IFI16) reduced the MFI of eGFP by over 50%, without decreasing the percentage of $eGFP^+$ cells was detectable in the presence of these candidates, suggesting an impact on viral gene expression.

3.3.1.4 A high proportion of candidates reduces viral p24 capsid antigen production

To monitor the impact of individual candidates on late viral gene expression and virion release, a p24-ELISA was performed to determine the amount of cell-associated and cell-free viral capsid antigen in the presence of each cellular factor. As shown in figure 10A, nine candidates (indicated by '#') reduced p24 levels in wt HIV-1 transfected cells more than 75% compared to the empty vector control only expressing BFP. For four genes (*APOL1*, *APOL6*, *TNFRSF10A* and *TNFRSF10D*) the decrease in p24 levels in wt HIV-1 producing cells achieved more than 90%. In contrast, three factors (PSMD13, SP110 and IL-1A) slightly enhanced p24 capsid

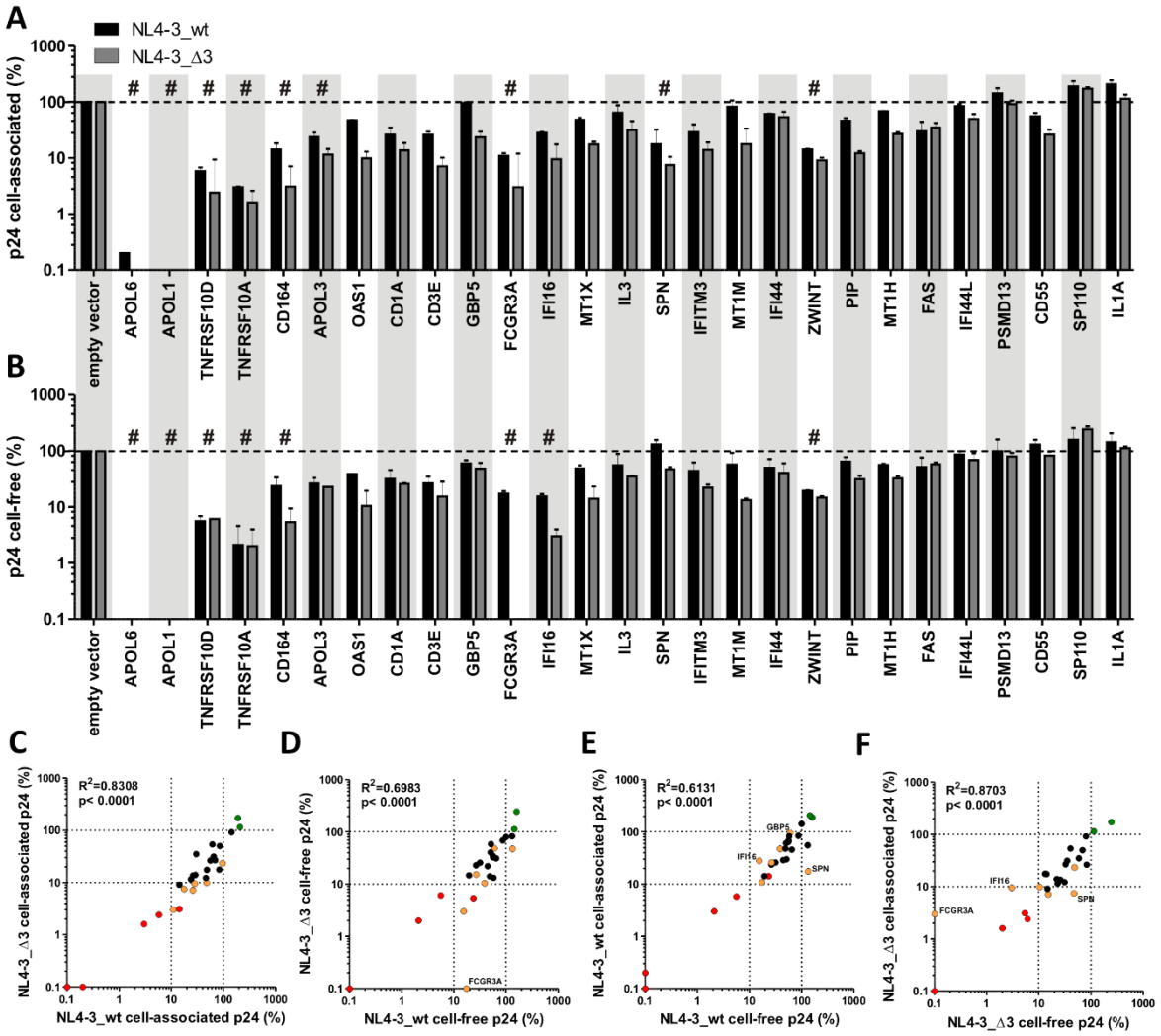


Figure 10: Impact of candidate factors on late viral gene expression and virion release in the cotranfection setup: HEK293T cells were transfected with 2.5µg of constructs expressing the indicated candidate gene together with wt (black) or Δ3 (grey) HIV-1 provirus. After two days the amount of p24 capsid protein **A) in the cells** and **B) released into the supernatant** was determined by ELISA. All data are shown relative to the control samples where an empty vector control only expressing BFP was cotransfected together with the respective provirus (n=3-5 ± SD). **Correlation analyses between the impact on p24 antigen quantity C) within cells,** and **D) in the cell culture supernatant of wt versus Δ3 HIV-1 transfected cells coexpressing individual candidate genes. Comparison of cell-free and cell-associated amounts of p24 capsid protein for E) wt HIV-1,** and **F) for cells transfected with Δ3 HIV-1 derivate.** Each symbol represents the mean value (n=3-5) for individual candidates relative to the control sample. The color code is based on the results achieved in the infectivity assay on TZM-bl cells (see figure 7B).

protein production in wt HIV-1 transfected cells. All candidate genes that reduced the quantity of p24 antigen in wt HIV-1 producing cells also decreased the level of cell-associated p24 capsid protein when the Δ3 mutant was cotransfected (Figure 10C), and this effect was in general more pronounced (p= 0.006; paired one-tailed t-test of

all candidates with the exception of enhancing factors). Seven additional candidate genes (*FCGR3A, CD164, ZWINT, SPN, CD3E, IFI16* and *OAS1*) also achieved a reduction of cell-associated p24 over 90% when the virus lacked functional *vpr*, *vpu* and *nef* genes. Surprisingly, PSMD13 did not increase the quantity of p24 antigen in Δ3 HIV-1 producing cells, whereas SP110 and IL-1A also marginally elevated the amount of cellular p24 capsid protein when the Δ3 mutant was cotransfected.

As mentioned above, I also measured the quantity of p24 antigen released into the cell culture supernatant (Figure 10B). On average, the expression of the 27 candidates reduced the amount of cell-free p24 antigen by over 46% in the context of wt HIV-1 (61.6% when enhancers were excluded). In the presence of eight cellular factors (indicated by '#' in figure 10B) the p24 levels within the supernatants were decreased by over 75%, among them again APOL1, APOL6, TNFRSF10A and TNFRSF10D, which lowered the wt HIV-1 cell-free p24 quantity by over 90%. In addition to SP110 and IL-1A, CD55 as well as SPN marginally enhanced the amount of p24 antigen released from wt HIV-1 transfected cells compared to the control. This was unexpected, especially for SPN, as the amount of cell-associated p24 antigen was strongly reduced (Figure 10E). Furthermore, some factors (e.g. IFI16 and GBP5) reduced the amount of cell-free p24 antigen more severely than the p24 protein quantity within wt HIV-1 transfected cells (Figure 10E), suggesting that these factors might also inhibit later steps of the HIV-1 replication cycle after late viral gene expression and translation. As shown in figure 10D, the effects on released p24 from wt and Δ3 HIV-1 producing cells correlated well, whereby the reduction of cell-free p24 levels was more pronounced in the context of the Δ3 derivate. Unexpectedly, in the presence of FCGR3A no p24 capsid protein was released from Δ3 HIV-1 infected cells (Figure 10F), although low levels of cell-associated p24 antigen were detectable. Taken together, a high proportion of cotransfected candidate genes reduced the production and release of p24 capsid protein. Among them were the tested members of the APOL and TNRS protein families that reduced p24 levels by over 90%, suggesting an impact on viral gene expression.

3.3.2 Transduction setup targeting *early steps* of HIV-1 replication

To monitor possible effects of candidate genes on early steps of HIV-1 replication, HEK293T cells were transduced with Vesicular Stomatitis Virus glycoprotein- (VSVg)

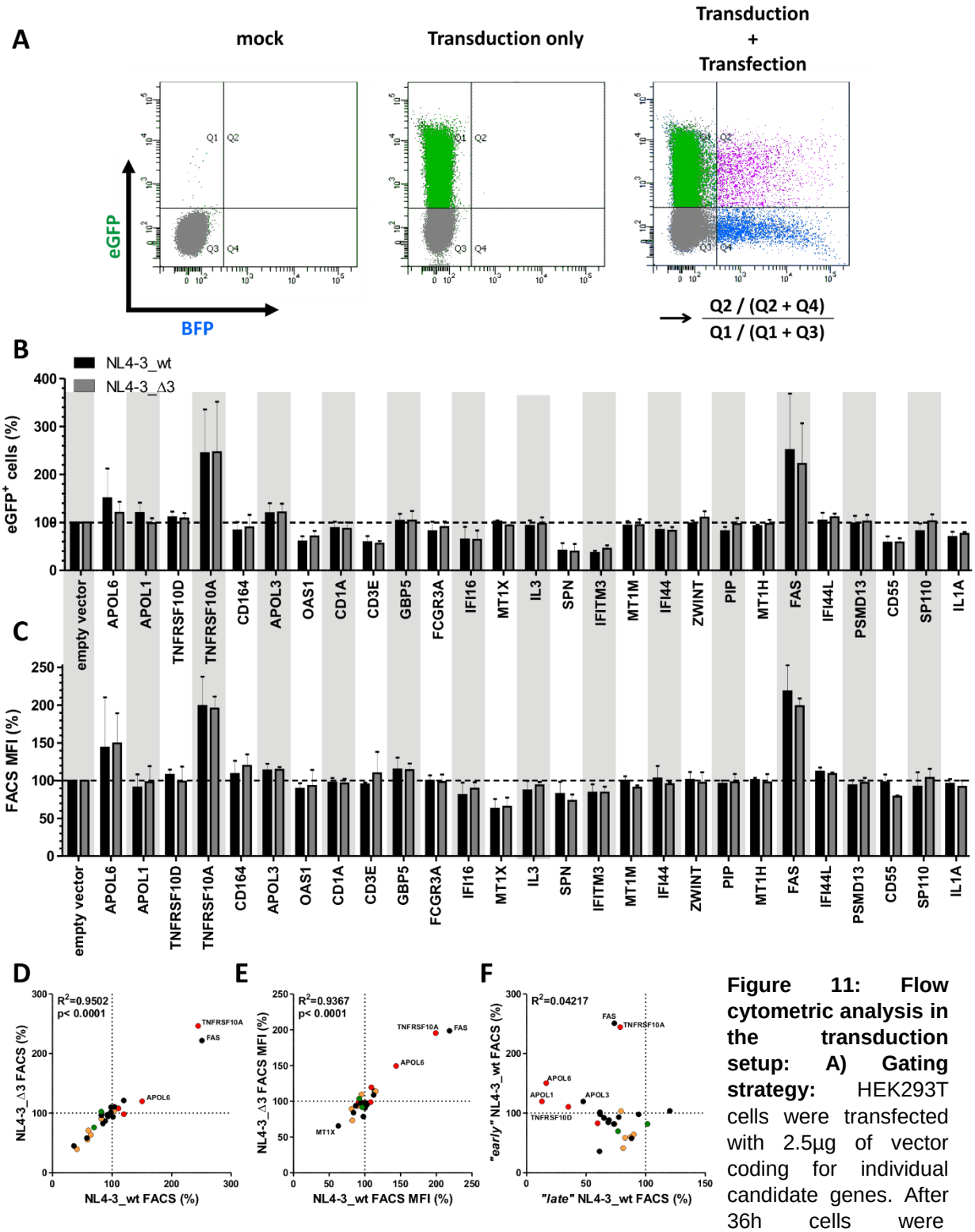


Figure 11: Flow cytometric analysis in the transduction setup: A) Gating strategy: HEK293T cells were transfected with 2.5µg of vector coding for individual candidate genes. After 36h cells were

transduced with VSVg-pseudotyped eGFP-reporter wt (black) or Δ3 (grey) HIV-1. Two days later cells were analyzed by flow cytometry to determine, **B) the percentage of HIV-1 transduced (eGFP$^+$) cells in the BFP$^+$ population compared to transduced cells in BFP$^-$ cells**, and **C) eGFP-MFI in cells overexpressing individual candidate gene.** All values are shown relative to the corresponding control sample (n=3-6 ± SD). **D) Correlation analysis between the effects on percentage of wt versus Δ3 HIV-1 transduced cells within their respective BFP$^+$ population,** and **E) on the MFI of eGFP in cells expressing individual candidate gene. F) Correlation analysis between the impact on percentage of wt HIV-1 producing (eGFP$^+$) cells in the *"late"* versus *"early"* setup.** Each symbol represents the mean value (n=3-6) for individual candidates relative to the control sample. The color code is based on the results achieved in the infectivity assay on TZM-bl cells (see figure 7B).

pseudotyped eGFP-reporter viruses (wt and Δ3 HIV-1 NL4-3) 36h after transfection with the candidate genes. In this way, I was additionally able to monitor the effects of candidate genes prior to viral integration such as uncoating or reverse transcription (Figure 6A). However, this setup had the disadvantage of altered virus entry, as HEK293T cells do not express CD4. 36h after transfection, HEK293T cells were transduced and another 48h later analyzed by flow cytometry. I determined the ratio of wt or Δ3 HIV-1 transduced cells within the BFP$^+$ population to the numbers of HIV-1 transduced cells in cells not expressing the individual candidate genes (Figure 11A). As shown in figure 11B, seven cellular factors (IFITM3, SPN, CD55, CD3E, OAS1, IFI16 and IL-1A) reduced the frequency of HIV-1 transduced cells by over 30%. Unexpectedly, besides FAS all tested members of the *apolipoprotein L* gene family, and tumor necrosis factor receptor superfamily that showed inhibitory effects in the cotransfection assays rather enhanced the quantity of HIV-1 transduced cells in the transduction setting (Figure 11F). The impact on the MFI of eGFP within the BFP$^+$ population was generally not profound (Figure 11C). Four cellular genes (*MTX1*, *IFI16*, *SPN* and *IFITM3*) reduced eGFP expression by over 15%, and APOL6, TNFRSF10A as well as FAS increased the MFI of eGFP within the BFP$^+$ population. I did not observe significant differences for any candidate gene when experiments were performed in the absence of functional *vpr*, *vpu* and *nef* genes (Figure 11D). In addition, the effects on the MFI of eGFP highly correlated for VSVg-pseudotyped wt and Δ3 HIV-1 (Figure 11E).

3.4 Impact of candidates on promoter activities

Since my results suggested that many candidate factors might inhibit transcription and/or translation, I determined the impact of candidates on diverse promoters.

3.4.1 A high proportion of candidates reduces HIV-1 LTR activity

To determine the impact of candidate genes on the HIV-1 long terminal repeat (LTR) promoter, HEK293T cells were transfected with a reporter construct expressing firefly luciferase under the control of the HIV-1 LTR promoter together with expression vectors for individual candidate genes (Figure 12A). Twelve candidates (indicated with '#' in figure 12A) inhibited LTR-dependent reporter activity by more than 75%. Amongt these, six factors (APOL1, APOL3, APOL6, IFITM3, TNFRSF10D and ZWINT) reduced luciferase signals by more than 90%. In contrast, SPN and IFI44L enhanced basal LTR-driven reporter activity by 1.6- and 8.6-fold, respectively.

In the presence of HIV-1 Tat, which enhances transcriptional initiation and elongation from the LTR promoter, inhibitory effects above 75% were observed for eight candidate genes (*APOL1*, *APOL3*, *APOL6*, *CD164*, *FAS*, *FCGR3A*, *TNFRSF10D* and *ZWINT*; Figure 12A). Interestingly, five factors (CD1A, MT1X, IL-3, MT1M and CD55) now enhanced LTR promoter activity when HIV-1 Tat protein was cotransfected, whereas IFI44L did not influence reporter activity in the presence of viral Tat. In contrast, CD164 and FAS inhibited LTR-driven reporter gene expression over 75% when HIV-1 Tat protein was present, and robust inhibition over 90% was observed for four candidate genes (*APOL1*, *APOL6*, *TNFRSF10D* and *CD164*). Furthermore, SPN did not enhance but rather reduced LTR promoter activity in the presence of Tat. Notably, also some other candidate genes, e.g. *CD3E*, *TNFRF10A*, *GBP5*, and *OAS1* that strongly reduced Δ3 HIV-1 production (Figure 7A) had only moderate inhibitory effects on HIV-1 LTR promoter activity in the presence of viral Tat protein, suggesting that they might exert their inhibitory effects on later steps than viral transcription.

3.4.2 Several candidate genes inhibit diverse viral promoters

Since a high proportion of candidate genes reduced virus production, it was expected that some candidates might exert more global effects on promoter activity rather than specifically targeting the HIV-1 LTR promoter. Thus, the experiment was repeated with additional reporter constructs controlled by the herpes simplex virus (HSV) thymidine kinase (TK) or human cytomegalovirus (HCMV) immediate early (IE) promoter. As shown in figure 12A, many candidate genes also affected expression

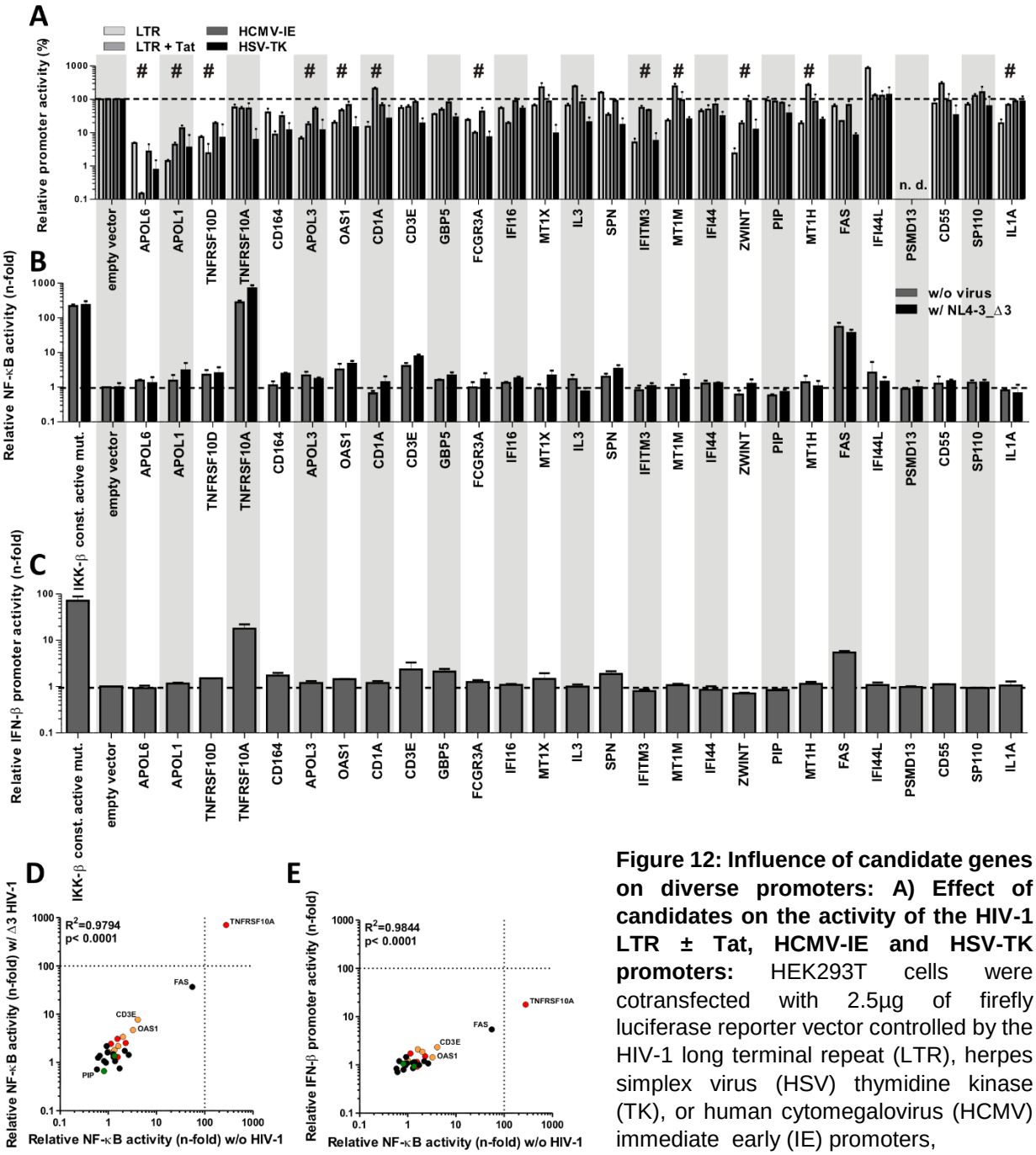


Figure 12: Influence of candidate genes on diverse promoters: A) Effect of candidates on the activity of the HIV-1 LTR ± Tat, HCMV-IE and HSV-TK promoters: HEK293T cells were cotransfected with 2.5µg of firefly luciferase reporter vector controlled by the HIV-1 long terminal repeat (LTR), herpes simplex virus (HSV) thymidine kinase (TK), or human cytomegalovirus (HCMV) immediate early (IE) promoters,

as well as 2.5µg of vectors expressing individual candidate genes. The HIV-1 LTR promoter was activated by additional cotransfection of 0.5µg of a plasmid expressing HIV-1 Tat protein if indicated. In this instance, the amount of cotransfected LTR-reporter vector and plasmids coding for candidates was reduced to 2µg. 40h post transfection, cells were lysed and firefly luciferase activity was determined. All values were normalized to the empty vector control sample not expressing any candidate gene (n=3 ± SD for HCMV-IE and HSV-TK; data for LTR ± Tat were derived from a single experiment in triplicate transfections). **B) Effect of candidates on NF-κB activity:** HEK293T cells were cotransfected with 2µg of reporter vector expressing firefly luciferase under the control of three NF-κB binding sites, a control vector expressing Gaussia luciferase controlled by a minimal promoter (0.5µg), and 1µg of vectors coding for the indicated candidate genes. The experiment was also performed in the presence of 1.5µg Δ3 HIV-1 construct. The IKK-β constitutively active mutant was used as a positive control for NF-κB activation. Two days post transfection luciferase activities were measured in triplicates (± SD). All firefly luciferase signals were normalized to the internal Gaussia luciferase control, and are shown relative to the corresponding control sample (n-fold). **C) Impact of candidates on human IFN-β core promoter activity:** HEK293T cells cotransfected with 2µg of reporter vector expressing firefly luciferase controlled by the human IFN-β core promoter together with 1µg of plasmids expressing the indicated candidate genes. All DNA amounts, time points and controls are listed in figure 12B. Luciferase activities were determined in triplicates (± SD), and are shown relative to the control sample only expressing BFP (n-fold). **D) Correlation analysis between the effects of candidates on NF-κB promoter activity in the presence and absence of Δ3 HIV-1. E) Correlation analysis between the impact of candidates on IFN-β versus NF-κB promoter activity.** Each symbol represents the mean value (n=2-3) for individual candidates relative to the control sample. The color code is based on the results achieved in the infectivity assay on TZM-bl cells (see figure 7B).

driven by these promoters, although the inhibitory effect was on average more pronounced on the HSV-TK promoter. Only APOL6 reduced the HCMV-IE promoter activity by more than 90%, whereas eight candidate genes (*APOL1*, *APOL6*, *IFITM3*, *FAS*, FCGR3A, *TNFRSF10A*, *TNFRSF10D*, and *MT1X*) decreased the HSV-TK promoter driven reporter activity by over 90%. In summary, a high proportion of candidate genes did not only inhibit the activation of the HIV-1 LTR promoter, but also reduced the reporter activity when controlled by other tested viral promoters.

3.4.3 FAS and TNFRSF10A are potent NF-κB activators

In addition, I also measured the impact of candidate genes on nuclear factor kappa-light-chain-enhancer of activated B cells (NF-κB) and the interferon-β (IFN-β) core promoter activity. Thereby, I wanted to investigate whether some of these candidate factors might act as sensors and/or activate a signaling cascade to induce an antiviral response rather having a direct and dominant effect on HIV-1. Furthermore, the NF-κB reporter was tested because LTR promoter activity depends on activated NF-κB. Thus,

candidate factors that inhibit LTR-driven transcription may do so by blocking the activation of this transcription factor. I started with a reporter construct expressing firefly luciferase under the control of three NF-κB binding sites. Thus, I indirectly determine the activation of NF-κB upon expression of individual candidate genes in the absence and presence of Δ3 HIV-1 provirus (Figure 12B). Three factors (PIP, ZWINT and CD1A) reduced basal NF-κB driven reporter activity by more than 30%, whereas OAS1 and CD3E moderately enhanced luciferase signals up to fourfold. Notably, FAS and especially TNFRSF10A potently activated NF-κB dependent gene expression. I observed similar results when the experiment was performed in the presence of Δ3 HIV provirus (Figure 12D), with the notable exception that the enhancing effect by TNFRSF10A on NF-κB activation was even more pronounced. These results correlated with the data obtained for the human IFN-β core promoter that also contains NF-κB binding sites (Figure 12C and E). However, the increase of IFN-β promoter activity was less pronounced in the presence of FAS and TNFRSF10A. Taken together, the majority of candidate genes did neither block NF-κB activation, nor activate the IFN-β core promoter. Therefore, the modulation of NF-κB activity as well as the induction of an antiviral state, especially in HEK293T cells, could be excluded as causes for the observed inhibition of HIV-1 when candidate genes were cotransfected to the provirus (Figure 9). Furthermore, the potent activation of NF-κB by FAS and especially TNFRSF10A might explain their enhancing effect on HIV-1 in the transduction assay (Figure 11).

3.5 Effects of candidate genes on late viral gene expression & protein processing

To confirm the impact of several candidates (APOL6, CD164, OAS1, CD1A, GBP5, CD3G, IFI16, SPN, FAS and IL-1A) on late viral gene products, Western blot analyses were performed to measure HIV-1 p24 capsid and gp120 Env protein levels within cells as well as released into the culture supernatants. By quantifying the signals for cellular HIV-1 Gag precursor (p55) and gp160 Env, the precursor of the mature gp120 surface glycoprotein, I was able to monitor possible effects of the above mentioned candidate genes on viral Gag and Env protein processing.

3.5.1 Western blot confirmed the impact of several candidates on late viral gene products

I transfected individual vectors expressing candidate genes together with the Δ3 HIV-1 proviral construct, and performed Western blots for late viral gene products detectable in the cell culture supernatant (Figure 13A) and within the cells (Figure 13B). Based on three to five independent experiments, I quantified the signal

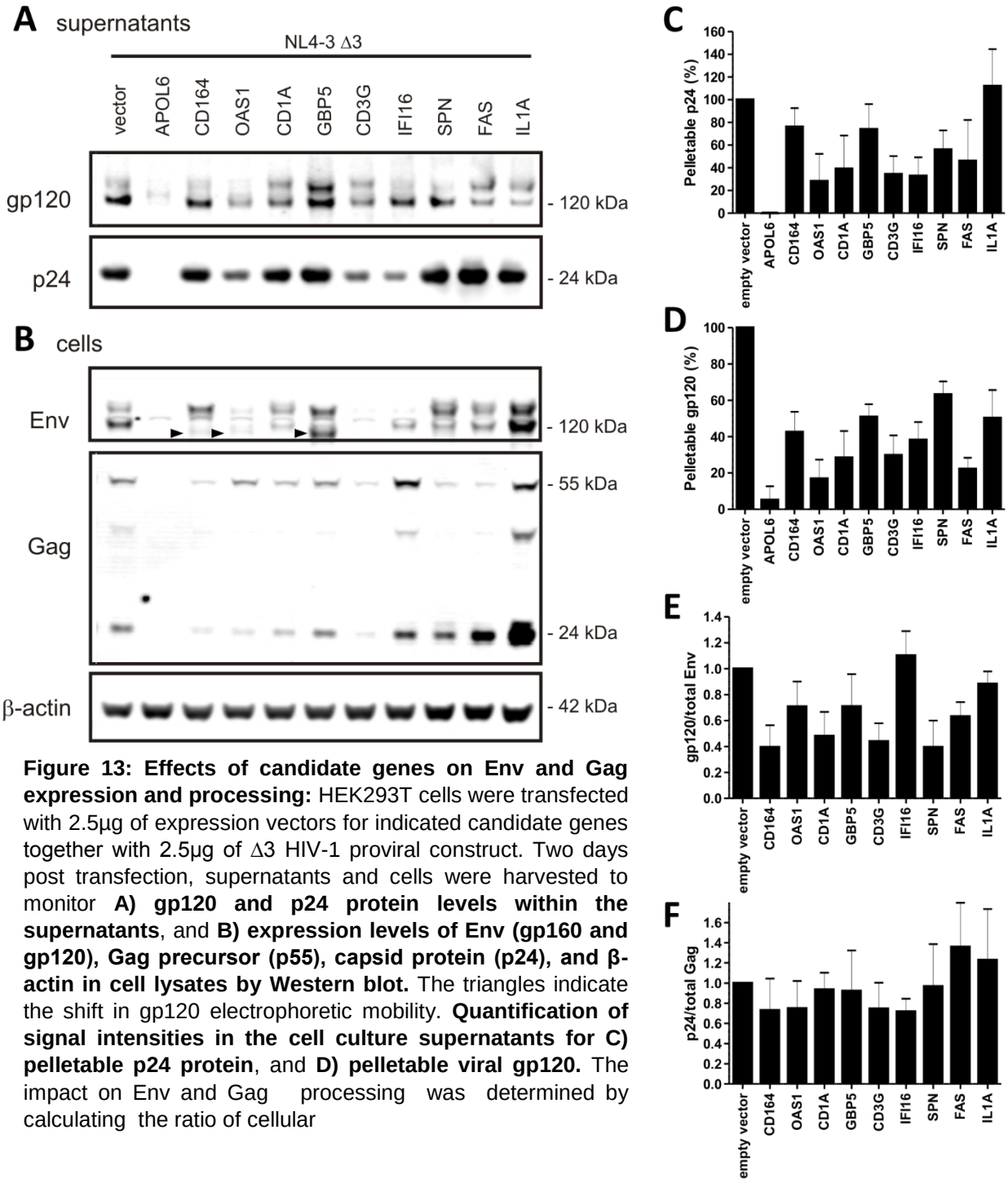


Figure 13: Effects of candidate genes on Env and Gag expression and processing: HEK293T cells were transfected with 2.5µg of expression vectors for indicated candidate genes together with 2.5µg of Δ3 HIV-1 proviral construct. Two days post transfection, supernatants and cells were harvested to monitor **A) gp120 and p24 protein levels within the supernatants**, and **B) expression levels of Env (gp160 and gp120), Gag precursor (p55), capsid protein (p24), and β-actin in cell lysates by Western blot.** The triangles indicate the shift in gp120 electrophoretic mobility. **Quantification of signal intensities in the cell culture supernatants for C) pelletable p24 protein**, and **D) pelletable viral gp120.** The impact on Env and Gag processing was determined by calculating the ratio of cellular

E) gp120 to total Env (gp120 + gp160), and **F) p24 to total Gag (p24 + p55)**. APOL6 was omitted from these analyses due to complete loss of signals. All results were obtained from three to five independent experiments (± SD), and representative Western blots are shown in A and B. The order of candidate genes is based on the results achieved in the infectivity assay on TZM-bl cells (see figure 7B).

intensities for HIV-1 p24 capsid protein released into the supernatant (Figure 13C). In line with the results obtained by p24-ELISA (Figure 10B), p24 capsid protein was not detectable within the supernatant when APOL6 was coexpressed. In the presence of four other candidate genes (*OAS1*, *CD1A*, *CD3G* and *IFI16*) the abundance of cell-free p24 capsid protein was reduced by more than 60% compared to the negative control. Unexpectedly, the amount of cell-free p24 was not as severely reduced in the presence of CD164 as seen by p24-ELISA. In agreement with previous results, GBP5, FAS and SPN moderately inhibited the release of p24 capsid protein from transfected cells, whereas IL-1A expression slightly increased it. In the same way, I also quantified the signal intensities for viral gp120 Env glycoprotein within the cell culture supernatants. As shown in figure 13D, six cellular factors (APOL6, OAS1, CD1A, CD3G, IFI16 and FAS) decreased cell-free gp120 protein levels by more than 60%. All other tested candidates also reduced the amount of gp120 glycoprotein within the supernatants to a moderate level. In summary, Western blot analyzes of pelletable late HIV-1 proteins mainly confirmed the impact of tested candidate genes on late viral gene products when cotransfected to the Δ3 provirus.

3.5.2 CD164, CD1A, CD3G and SPN affect viral Env processing

Next, I determined the processing of Gag and Env by calculating the ratio of cellular p24 to total Gag and gp120 to total Env, respectively. In the presence of four candidates (CD164, CD1A, CD3G and SPN) processing of the gp160 Env precursor protein into the mature gp120, mediated by cellular furin-like proteases, was significantly reduced suggesting that these factors may impair Env function (Figure 13E). Notably, I observed a slight but highly reproducible shift in the electrophoretic mobility of the gp120 glycoprotein in the presence of CD164, OAS1 and especially GBP5 in cell lysates but not in the released Δ3 HIV-1 virions (Figure 13B, indicated by triangles), indicating that these candidate genes may interfere with the glycosylation of viral gp120. I also found

that CD3G, IFI16, CD164 and OAS1 might affect viral Gag protein processing since their coexpression decreased the levels of cellular p24 capsid protein without reducing the amount of the p55 Gag precursor protein that is processed by the viral protease, although the effects were modest (Figure 13F). In summary, I confirmed that several candidate genes inhibited late viral gene expression, and some factors may reduce the abundance of infectious progeny virions by affecting viral Env and Gag processing, or the glycosylation of gp120.

3.6 Expression of candidate genes in HIV-1 target cells

So far, all experiments were performed in HEK293T cells. To better assess the possible *in vivo* relevance of my findings, I determined the expression of several candidate genes in primary $CD4^+$ T cells and monocyte-derived macrophages (MDMs), which constitute the main target cells of HIV-1.

3.6.1 Detection of candidate genes in primary cells by Western blot

My main objective was to determine the protein levels of various candidates in HIV-1 target cells. Therefore, I isolated $CD4^+$ T cells by negative selection, and differentiated macrophages from monocytoid progenitors using human serum. Besides untreated primary cells, $CD4^+$ T cells and MDMs were differently stimulated to monitor basal as well as inducible protein levels. Figure 14A shows examples for the detection of candidate proteins (*SP110*, *IFI16*, *GBP5* and *APOL6*) by Western blot. Activation of $CD4^+$ T cells via CD3/CD28 generally stimulated cell proliferation and thereby enhanced protein expression as reflected by increased actin levels. SP110 and IFI16 were detectable in untreated $CD4^+$ T cells, and their expression was slightly increased upon CD3/CD28 stimulation but not by IFN treatment. GBP5 was not detectable in unstimulated $CD4^+$ T cells, but induced upon CD3/CD28 stimulation and treatment with IFN-γ. APOL6 was neither detectable in untreated nor in stimulated $CD4^+$ T cells, whereas untreated MDMs expressed APOL6, and its expression was increased by IFN treatment. I observed basal SP110, IFI16, and GBP5 protein expression in untreated

MDMs. Further, their expression levels were increased in the presence of IFN-α and IFN-γ, whereby the effects on SP110 and GBP5 were more profound.

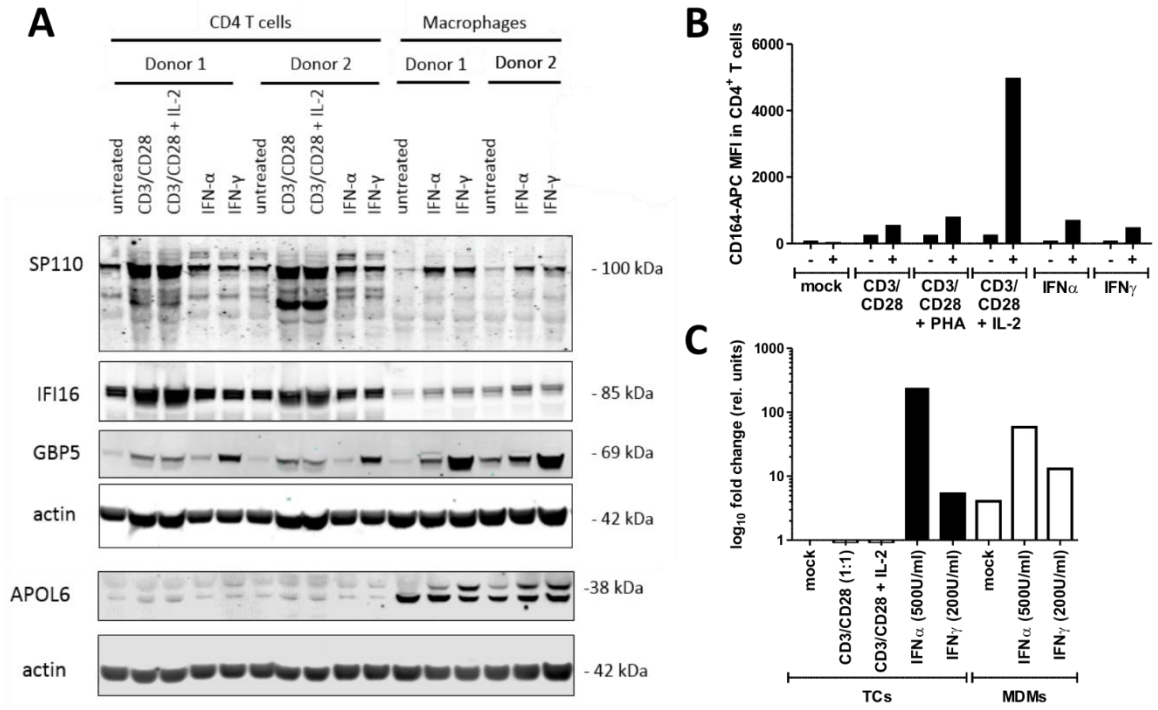


Figure 14: A) Protein expression of selected candidate genes in primary CD4⁺ T cells and monocyte-derived macrophages (MDMs): Isolated CD4⁺ T cells and MDMs were left untreated or stimulated via CD3/CD28 ± IL-2 (10ng/ml), or alternatively treated with IFN-α (500U/ml) or IFN-γ (200U/ml). Two days later, cells were lysed and analyzed for protein levels of the indicated candidates and β-actin by Western blot. **B) CD164 surface expression on CD4⁺ T cells:** CD4⁺ T cells were treated as described above, and CD164 surface expression was determined via flow cytometry (n=1). An isotype control was included to exclude unspecific antibody binding. - = unstained, + = stained (isotype values subtracted) **C) OAS1 mRNA levels after stimulation of HIV-1 target cells:** As described above, untreated and stimulated primary cells were lysed after two days. Total mRNA was harvested and used for cDNA synthesis. OAS1 and GAPDH mRNA levels were measured by quantitative PCR (n=1). All data were normalized to the corresponding GAPDH values, and are shown relative to mock treated CD4⁺ T cells (set to 1).

3.6.2 Detection of CD164 and OAS1 in primary blood cells

Since I did not detect CD164 by Western blot, I established alternative methods for its detection in HIV-1 main target cells. Flow cytometric analyses revealed that CD164 was not constitutively expressed in primary CD4⁺ T cells, but moderately induced upon IFN treatment and CD3/CD28 stimulation (Figure 14B). Interestingly, stimulation via CD3/CD28 in combination with IL-2 greatly enhanced CD164 surface expression on CD4⁺ T cells. Concerning OAS1, direct protein detection was not achieved in primary HIV-1 target cells neither by Western blotting, nor by flow cytometry. Therefore, I

decided to quantify mRNA levels by real time quantitative polymerase chain reaction (qPCR). I established a TaqMan® based assay for OAS1 and were able to detect OAS1 specific mRNA in HIV-1 target cells (Figure 14C). Moderate OAS1 mRNA levels were detectable in untreated primary $CD4^+$ T cells (cycle threshold at 28.9 within 38 total cycles), and stimulation via CD3/CD28 ± IL-2 did not alter OAS1 mRNA levels. Conversely, treatment with IFNs increased OAS1 mRNA levels in $CD4^+$ T cells. Not only IFN-α potently induced OAS1 transcription but also treatment with IFN-γ increased OAS1 mRNA level over fivefold compared to OAS1 mRNA levels in untreated $CD4^+$ T cells. MDMs showed fourfold higher OAS1 mRNA amounts compared to untreated $CD4^+$ T cells. Here again, type I and type II IFN treatment significantly enhanced OAS1 mRNA levels, although the increase was not as pronounced as seen for $CD4^+$ T cells. Taken together, the detection of candidate factors in primary blood cells presents a crucial tool for further characterization of the underlying antiviral mechanisms. Moreover, this allows additional experiments in HIV-1 target cells to better assess the possible *in vivo* relevance of candidate factors against HIV-1.

3.7 IL-1A does not increase HIV-1 infection of human primary cells

In HEK293T cells, cotransfection of a vector expressing IL-1A enhanced HIV-1 production (Figure 7A) and this effect was dose-dependent (Figure 8L). To assess the relevance of IL-1A mediated enhancement of virus production in primary HIV-1 target cells, I infected peripheral blood mononuclear cells (PBMCs) with eGFP-reporter wt or Δ3 HIV-1 in the presence of recombinant IL-1A. As shown in figure 15A, HIV-1 infection rates, as measured by FACS analysis, were not increased when recombinant IL-1A was added during infection of human PBMCs, and the supernatants, containing recombinant IL-1A, showed equal reporter signals on TZM-bl cells (Figure 15B). Next, I thought that IL-1A might exert its enhancing effect on HIV-1 infection exclusively when already present during virus production. Therefore, IL-1A was delivered *in trans* by tranfection of HEK293T cells with a vector expressing IL-1A together with wt or Δ3 HIV-1 proviral constructs. As expected, I observed

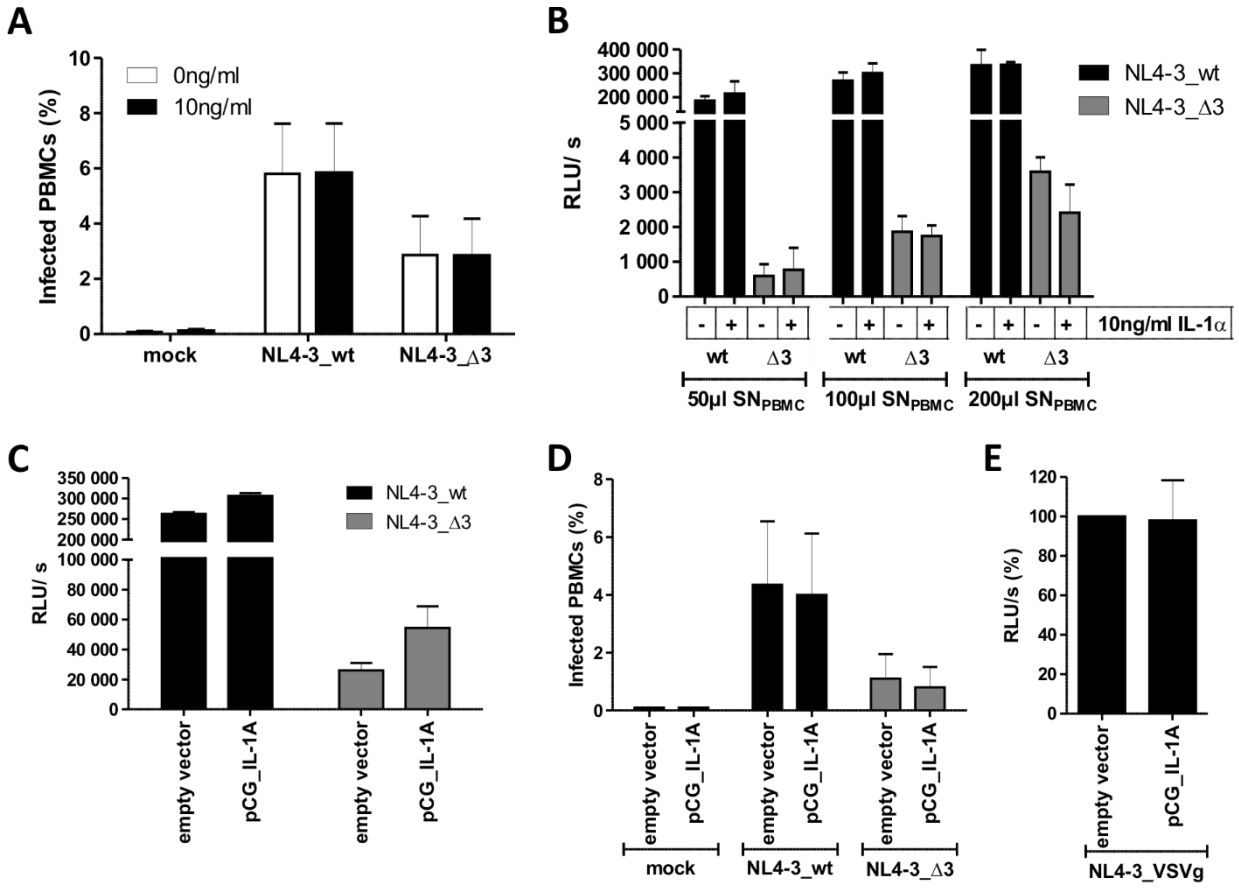


Figure 15: IL-1A does not increase HIV-1 infection in primary cells: A) Infection of human PBMCs in the presence of IL-1A: Stimulated PBMCs were incubated with recombinant IL-1A (10ng/ml) one hour prior to infection with eGFP-reporter wt or Δ3 HIV-1 with (black) and without recombinant IL-1A (white). Three days post infection, the percentage of infected cells was determined by flow cytometric analysis (n=3 ± SD), and **B)** supernatants were tested on TZM-bl reporter cells in different volumes (n=2 ± SD). **C) Virus production in the presence of IL-1A:** HEK293T cells were cotransfected with a pCG_IL-1A expression vector or a control plasmid, together with eGFP wt (black) or Δ3 (grey) HIV-1 proviral constructs in a ratio of 1:4. Two days post transfection, cell culture supernatants were harvested and tested on TZM-bl reporter cells. Reporter activity was measured in triplicates (± SD). **D) Infection of human PBMCs:** Stimulated PBMCs were infected with normalized virus stocks (5µg p24 antigen), and 3 days later, infection rates were determined by flow cytometry for wt (black) and Δ3 (grey) HIV-1 (n=3 ± SD). **E) Transduction of human MDMs in the presence of IL-1A:** According to section C), wt (black) or Δ3 (grey) HIV-1 were produced in the presence of a pCG_IL-1A expression vector. Additionally, particles were VSVg-pseudotyped (1µg) to achieve higher transduction rates in MDMs. Three days post transduction with equal amounts of HIV-1 p24 antigen, supernatants were harvested and tested on TZM-bl cells. All values are shown relative to the control sample (n=3 ± SD).

enhanced HIV-1 infection of TZM-bl cells when IL-1A was coexpressed during virion production (Figure 15C). Stimulated PBMCs were infected with either equal volumes or normalized virus stocks (5µg p24 antigen). As before, however, I did not observe an increase in HIV-1 infection rates in PBMCs when IL-1A was expressed during virion production, irrespectively, whether equal volume (data not shown) or normalized virus stocks were applied (Figure 15D). I repeated these experiments in MDMs using VSVg-

pseudotyped virions to achieve higher transduction rates. Here again, IL-1A did not increase the amount of HIV-1 transduced cells when added as recombinant cytokine (data not shwon). Indeed, as before, IL-1A enhanced virus production in HEK293T cells were cotransfected (Figure 15C), but did not enhance HIV-1 transduction rates in MDMs (data not shown). Consequently, the supernatants of transduced MDMs did not trigger enhanced reporter activity in TZM-bl cells (Figure 15E). Thus, IL-1A only increased HIV-1 production in HEK293T cells, but did not influence HIV-1 infection of human primary cells, irrespective of whether added as recombinant cytokine, or when present during virus production.

3.8 IFI16 restricts the production of infectious HIV-1

IFI16 has been shown to act as an innate immune sensor that recognizes DNA structures of several pathogenic viruses including HIV-1 resulting in the production of antiviral cytokines via the STING-TBK1-IRF3 signaling pathway [37, 98]. Only recently, it has been reported that IFI16 is responsible for the death of abortively HIV-1 infected $CD4^+$ T cells by triggering caspase-1 dependent pyroptosis by activating the inflammasome [64]. Thus, IFI16 may play a key role in $CD4^+$ T cell depletion underlying the progression to AIDS. My findings suggested that IFI16 restricts HIV-1 infection independently of its DNA sensing activity, since HEK293T cells used in this screen do not express STING. Therefore, I performed a more detailed analysis to gain insights into IFI16 function as a restriction factor for HIV-1 infection.

3.8.1 IFI16 impairs HIV-1 LTR promoter activity and Gag processing

To confirm that IFI16 inhibited HIV-1 LTR promoter activity, I repeated the experiment in the presence of a vector expressing viral Tat protein as described before (Figure 12A), and additionally by cotransfecting the Δ3 HIV-1 proviral construct. As shown in figure 16A, IFI16 impaired LTR promoter activity in a dose-dependent manner irrespective whether the promoter was activated by viral Tat protein alone or by Δ3

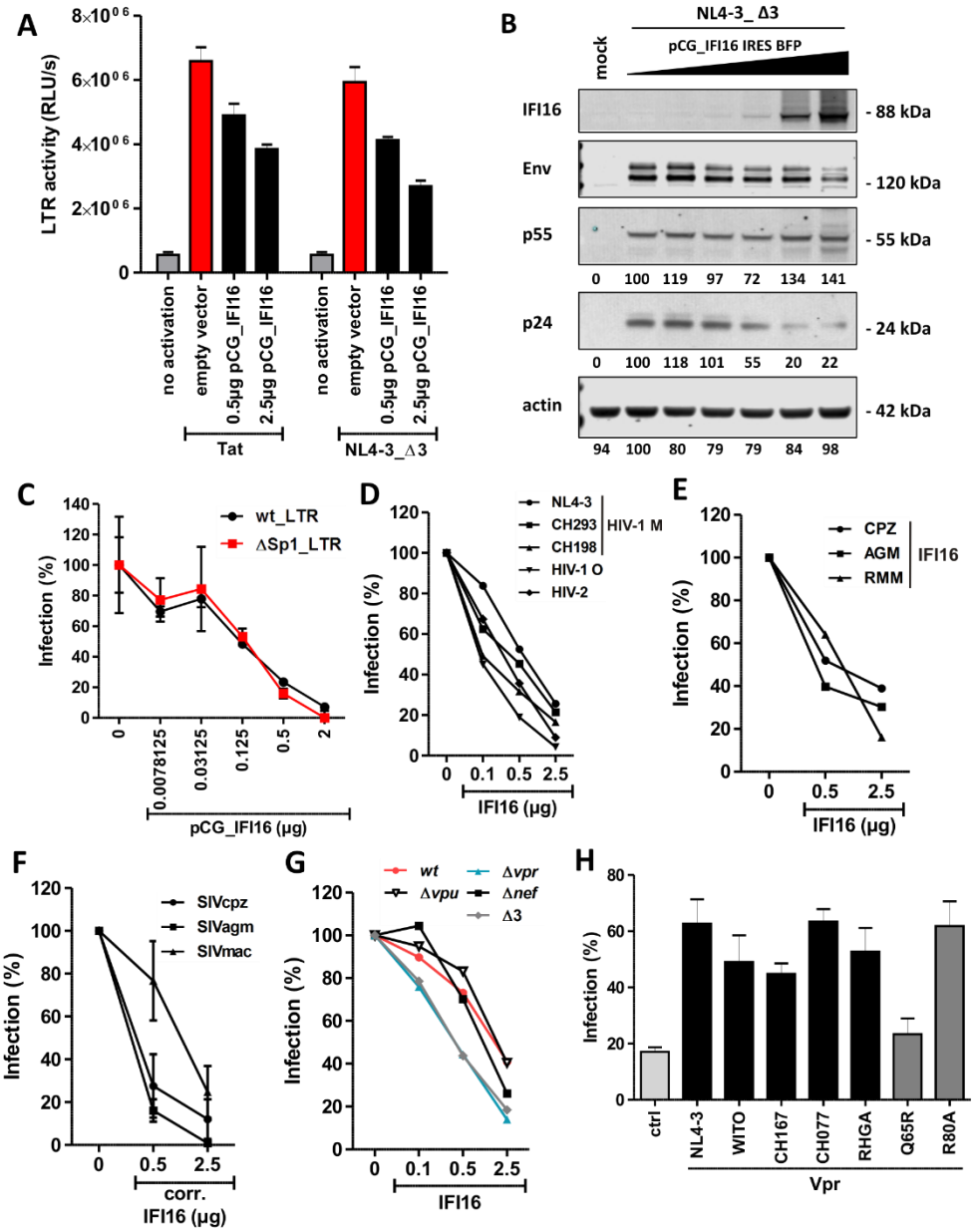


Figure 16: Antiviral mechanism of IFI16: A) IFI16 inhibits HIV-1 LTR promoter activity: HEK293T cells were transfected with 2µg of firefly luciferase reporter vector controlled by the HIV-1 LTR promoter together with 0.5 or 2µg of vector expressing IFI16. The HIV-1 LTR promoter was activated by additional cotransfection of 0.8µg of a plasmid expressing HIV-1 Tat protein (left) or Δ3 HIV-1 proviral construct (right). 40h post transfection, cells were lysed and firefly luciferase activity was determined in triplicates (n=2 ± SD). **B) IFI16 interferes with Gag precursor processing:** HEK293T cells were transfected with increasing amounts of a vector expressing IFI16 (starting with 7.8ng with stepwise fourfold increase) together with 2.5µg Δ3 HIV-1 proviral construct. Two days later, cells were lysed and analysed by Western blot for IFI16 expression as well as HIV-1 Gag and Env. β-actin served as a loading control and signal intensities were determined relative to the control sample not expressing IFI16. **C) IFI16 inhibits HIV-1 LTR promoter activity independently of Sp1 binding sites:** HEK293Ts cells were transfected with increasing amounts of a plasmid expressing IFI16 together with 3µg of Δ3 HIV-1 proviral construct with an intact LTR (black) or a promoter lacking functional Sp1 binding sites (red) in the presence of 0.8µg of a vector expressing a constitutively active mutant of IKK-β. 40h post transfection, cell culture supernatants were harvested and tested on TZM-bl indicator cells. Reporter activity was

measured in triplicates and values are shown relative to those in the absence of IFI16 (n=2 ± SD). **D) IFI16 inhibits various HIV strains:** HEK293T cells were transfected with increasing quantities of a vector expressing IFI16 together with 2.5µg of indicated HIV proviral constructs. Two days later, supernatants were harvested and tested on TZM-bl cells. Reporter activity was measured in triplicates and values are shown relative to those in the absence of IFI16 (n=2 ± SD). **E) IFI16 orthologues from different primate species inhibits HIV-1 production:** Two days after transfection of HEK293T cells with increasing amounts of a plasmid expressing IFI16 variants together with 2.5µg of wt HIV-1 proviral construct, supernatants were harvested and tested on TZM-bl cells. All data are shown relative to the control sample not expressing IFI16 (n=2 ± SD). **F) SIV strains are sensitive to IFI16 orthologues found in their respective hosts:** HEK293T cells were transfected with 2.5µg of different SIV strains together with increasing amounts of a vector expressing their corresponding IFI16 variant. Two days post transfection, supernatants were harvested and infectious yield was determined on TZM-bl reporter cells (n=3 ± SD). **G) HIV-1 Vpr might attenuate the antiviral effect(s) of IFI16:** HEK293T cells were transfected with increasing quantities of an expression vector coding for IFI16 together with wt, Δ3 or single mutant HIV-1 proviral derivates. After two days, supernatants were harvested and tested on TZM-bl indicator cells. All values are shown relative to those in the absence of IFI16 (n=3-4 ± SD). **H) HIV-1 Vpr *in trans* counteracts the inhibitory effect of IFI16:** HEK293T cells transfected with 1.25µg of a plasmid expressing IFI16 together with 2.5µg Δ3 HIV-1 proviral construct. Additionally, 1.25µg of expression vectors coding for different HIV-1 Vpr proteins were delivered to the cells. Two days post transfection, supernatants were harvested and tested on TZM-bl cells. All data are shown relative to the control sample not expressing IFI16 (n=3-4 ± SD); the Vpr mutants are NL4-3-based.

HIV-1. For HCMV it has been shown that IFI16 mediates its antiviral effect by blocking the interaction of Sp1-like transcription factors with the UL54 DNA polymerase promoter [20]. Since the HIV-1 LTR promoter also contains Sp1 transcription factor binding sites, I hypothesized that this might be the mode of action by which IFI16 reduced LTR activity. However, I did not observe a loss in IFI16-mediated suppression of LTR promoter activity in the absence of intact Sp1 binding sites when HEK293T cells were cotransfected with a Δ3 HIV-1 proviral construct with an intact LTR or a promoter lacking functional Sp1 binding sites (Figure 16C). Notably, in the absence of Sp1-binding sites, virus production was only detectable after the activation of NF-κB by constitutively active IKK-β as a Sp1-independent activator of LTR activity (data not shown). Interestingly, titration experiments revealed that IFI16 also reduced the level of viral p24 as well as gp120 antigen, and impaired the proteolytic processing of the p55 Gag precursor protein (Figures 13F and 16B). Whether this is due to an IFI16-mediated reduction of total HIV proteins, also reducing the levels of the viral protease mediating the Gag processing, or an additional, independent effect remains to be determined. In summary, IFI16 inhibited viral gene expression by suppressing HIV-1 LTR promoter activity in a Sp1-independent way, and further impaired HIV-1 Gag protein processing.

3.8.2 IFI16 inhibits different HIV strains and its antiviral effect is evolutionarily conserved

Next, I was interested if HIV strains other than group M NL4-3 are also inhibited by IFI16. As shown in figure 16D, human IFI16 was also highly active against two tested primary subtype C HIV-1 group M strains, as well as against highly diverse HIV-1 group O and HIV-2 strains. Furthermore, IFI16 orthologues from different primate species also diminished the production of HIV-1 NL4-3 (Figure 16E). Finally, primate lentiviruses infecting chimpanzees, African green monkeys and rhesus macaques were sensitive to the IFI16 orthologues from their respective host species, although the effects on SIVmac was less pronounced (Figure 16F). Altogether, IFI16 was active against different HIV strains and its antiviral activity was evolutionarily conserved.

3.8.3 The antiviral effect of IFI16 is antagonized by HIV-1 Vpr

In the initial titration experiments I observed that IFI16-mediated inhibition of the ∆3 HIV-1 mutant was more pronounced compared to wt HIV-1 (Figure 8H), suggesting a possible antagonistic role of HIV-1 Vpr, Vpu and/or Nef. Therefore, the experiment was repeated including single HIV-1 mutants bearing premature stop codons within the *nef*, *vpu* or *vpr* gene. The absence of functional viral Nef or Vpu did not influence the inhibitory effect of IFI16 on HIV-1 infection, whereas the effect on the ∆*vpr* variant was as strong as on the ∆3 HIV-1 mutant, suggesting that IFI16-mediated inhibition might be attenuated by the viral protein Vpr (Figure 16G). Indeed, cotransfection of several HIV-1 Vpr proteins with the Δ3 derivate significantly rescued the IFI16-mediated inhibitory effects on HIV-1 (Figure 16H). Interestingly, the ability of HIV-1 Vpr to counteract IFI16 was impaired by the mutation of Q65R but not R80A. Both Vpr mutants are unable to induce cell cycle arrest but the mutants differ in the numbers of known cellular interaction partners [47]. In summary, the accessory protein Vpr was able to counteract the antiviral activity of IFI16. If this antagonistic effect is directly mediated by viral Vpr or indirectly caused by interaction with other cellular factors remains to be determined.

4. Discussion

Evolutionary signatures of positive selection, altered gene expression during human immunodeficiency virus (HIV) infection, responsiveness to Interferon (IFN) treatment, and direct interaction with viral proteins are common features of known antiviral restriction factors. In the present study, I used these characteristics to identify novel cellular factors that may inhibit the replication of HIV-1. Initially, our collaborators from Lausanne performed a genome-wide screen revealing that 3.9% of coding genes show evidence of strong positive selection in primates ($d_N/d_S \geq 1$). Based on this, they examined which of these 841 genes are significantly upregulated during HIV-1 infection *in vivo*, and/or encode for factors that are known to interact with HIV-1 proteins (Figure 3). Telenti and colleagues showed that the overlap between these datasets is very limited: thirty human genes that show significant evidence for local positive selection at one or more amino acid sites were thus selected for closer examination.

With three exceptions (*PARP9*, *SGOL2* and *SPAG5*), all thirty candidate genes were amplified from human blood cells and cloned into an expression vector (Table 1). None of the candidate factors reduced the metabolic activity of transfected HEK293T cells and only APOL6 and ZWINT induced apoptosis when overexpressed (Figure 5). To determine the impact of the candidate genes on HIV-1 gene expression, virus production, release and infectivity, I established HEK293T cell-based assays. In a cotransfection setup targeting the late steps of HIV-1 replication, overexpression of a strikingly high proportion of the tested candidate genes impaired the production of infectious HIV-1 particles by more than 75%, and the inhibitory effect was even more pronounced in the absence of intact viral *vpr*, *vpu* and *nef* genes (Figure 7). In addition to CD164, two members of the *apolipoprotein L* gene family (*APOL1* and *APOL6*) as well as TNFRSF10A and TNFRSF10D strongly reduced the production of infectious virions, whereas IL-1A and SP110 enhanced HIV-1 production. Notably, *TNFRSF10A* was also identified as one of the most potent anti-HIV-1 factors among 380 type I IFN-stimulated genes in a previous study [91]. Recently, APOL1, known to confer immunity against African trypanosomes [100], has been reported to inhibit HIV-1 replication by multiple mechanisms including cellular depletion of the viral accessory protein Vif and targeting of HIV-1 Gag precursor protein for endosomal degradation [95]. Dose-

dependency studies for the most promising candidates confirmed their antiviral impact on HIV-1 production (Figure 8). Remarkably, at low expression levels FAS increased particle production but significantly reduced it at higher doses.

Flow cytometric analyses (Figure 9) and the quantification of p24 capsid (Figure 10) revealed that many candidates affect viral gene expression. Again, the most potent inhibitors belonged to the *APOL* gene family or tumor necrosis factor receptor superfamily. Notably, cotransfection of IFI16 or OAS1 affected the level of eGFP expression much more severely than the percentage of HIV-1 positive cells (Figure 9F), reflecting the reduction of viral gene expression. This is in agreement with a possible role of OAS1 in RNaseL-mediated degradation of retroviral RNA species [32]. In support of a possible role *in vivo,* it has recently been shown that HIV-1 downregulates OAS1 transcription in primary macrophages [102]. The enhancing effect of SP110 on HIV-1 could be confirmed by FACS and p24-ELISA, whereas IL-1A only showed elevated p24 capsid protein levels, indicating that IL-1A does not affect early viral gene expression to enhance HIV-1 production. Surprisingly, IL-1A reduced the frequency of $eGFP^+$ cells when already expressed before transduction, as seen in the second HEK293T cell-based assay also targeting early steps of HIV-1 replication (Figure 11). In addition to FAS, all tested members of the *APOL* gene family and TNF-receptor superfamily that showed inhibitory effects in the cotransfection assays enhanced the number of HIV-1 positive ($eGFP^+$) cells in the transduction setup. This clearly shows that the time point of expression in the context of the HIV-1 replication cycle determines their impact on HIV-1 infection. Overall, the inhibitory effects in the transduction setup were rather weak. In addition, the usage of Vesicular Stomatitis Virus glycoprotein-(VSVg) pseudotyped virions altered the usual HIV-1 entry process. I tried to overcome this issue in a third assay setup by cotransfection of HEK293T cells with expression plasmids for CD4 and CXCR4 to employ the natural HIV infection route and avoid VSVg-pseudotyping. However, low and varying transfection efficiencies did not allow the establishment of reproducible infection rates (data not shown). Further studies, e.g. with CD4-stably transfected HEK293T cell lines expressing sufficient endogenous CXCR4 levels, or well transfectable T cell lines, are required to avoid VSVg-pseudotyping and to elucidate in detail the outcome of candidate genes on early steps of HIV-1 replication.

Most known HIV-1 restriction factors are counteracted by viral accessory proteins [39, 56] like Tetherin by HIV-1 Vpu [87], or APOBEC3G by Vif [28, 58]. Interestingly, several candidate factors, e.g. CD164, GBP5, IFI16, SPN and CD3E, showed increased inhibitory effects on p24 capsid protein expression and infectious virus production in the absence of functional HIV-1 *vpr*, *vpu* and *nef* genes (Figure 7 and 10). Since overexpression of known restriction factors like Tetherin may 'overpower' their cellular antagonists, I performed titration experiments and confirmed these differences between the wt and the Δ3 viruses, although the differences were modest as even wt HIV-1 was efficiently inhibited at high doses of candidate genes (Figure 8). Notably, the Δ3 HIV-1 mutant was per se less infectious than the wt construct. However, the fact that only a small subset of tested candidates showed different inhibitory effects on wt versus mutated HIV-1 suggests that Vpr, Vpu and/or Nef protein may antagonize the inhibitory impact on HIV-1 of some candidate factors. Further studies, e.g. with HIV-1 single gene mutants or knockdown studies in human primary cells, are necessary to elucidate the antiviral mechanisms of the most potent candidate genes as well as their possible antagonisation by with HIV-1 proteins.

Many of the candidate factors affected viral gene expression and may exert broad effects on various promoters. Indeed, in-depth analysis of APOL6 revealed global, non-specific inhibitory effects on gene expression of incoming plasmids but not infection (Amalio Telenti, unpublished data), challenging the possible role of APOL proteins as specific HIV-1 restriction factors [95]. Therefore, I monitored the influence of candidate genes on diverse promoter activities (Figure 12). Many candidate factors, among them the tested members of the APOL and TNFRSF protein families, as well as IFITM3, FAS, FCGR3A, and MT1X did not exclusively inhibit HIV-1 LTR, but also reduced the activity of other viral promoters. It is noteworthy, however, that non-specific does not necessarily mean not relevant. Broad transcriptional silencing of various viral and cellular promoters could potentially represent a very effective means to control viral replication and further studies on the possible relevance of such mechanisms in innate immunity seem warranted. I also determined the impact of the candidate genes on NF-κB activation (Figure 12B), since this influence LTR activity. In addition to PIP and ZWINT, CD1A reduced basal NF-κB driven reporter activity, which might explain their moderate inhibitory effect on HIV-1 in the transduction assay (Figure 11). FAS and

especially TNFRSF10A were identified as potent activators of NF-κB dependent gene expression both in the presence and as absence of HIV-1 (Figure 12B). When already expressed before transduction, these candidates enhanced the numbers of HIV-1 transduced cells. However, I did not observe an enhancing effect on HIV-1 LTR promoter activity in the presence or absence of the viral Tat protein, and both cellular factors inhibited HIV-1 production in the cotransfection assay. One possible idea is that FAS and TNFRSF10A lead to enhanced NF-κB activation, and consequently resulting to upregulated HIV-1 LTR promoter activity. This combination might in turn lead to 'over-infection' of reporter cells at higher doses of the candidate gene (Figure 8J), and therefore result in false negative results in the cotransfection setup (Figure 7A). The effects on NF-κB activation correlated well with the data obtained for the IFN-β core promoter (Figure 12E). This was expected, since the IFN-β core promoter also contains NF-κB binding sites. Overall, the majority of candidate genes did neither block NF-κB activation, nor activate the IFN-β core promoter. Therefore, the modulation of NF-κB activity as well as the induction of an antiviral state, especially in HEK293T cells, can be excluded as causes for the observed inhibition of HIV-1 when candidate genes were cotransfected to the provirus (Figure 9). Further studies are needed to show whether candidate genes directly and dominantly influence HIV-1 replication rather than interacting with and blocking HIV-1 'dependency factors'. This is an essential precondition for the definition of candidate genes as novel anti-HIV-1 restriction factors. Especially, experiments in primary target cells are necessary to reveal the *in vivo* relevance of candidate genes on HIV-1.

Western blot analyses of the p24 capsid protein in the presence of selected candidate factors (Figure 13) showed distinct effects on the amounts of viral proteins, mostly confirming the results obtained by p24-ELISA (Figure 10). By quantification of cellular gp160 and gp120 Env protein levels, I showed that some candidate genes (*CD164*, *CD1A*, *CD3G* and *SPN*) impaired processing of the gp160 Env precursor protein to the mature gp120, and therefore may reduce virion infectivity by interfering with Env maturation. CD1A is expressed on antigen-presenting cells like Dendritic cells and particularly in the thymus [61]. This MHC-I like protein is known to interact with CD74 and presents self and non-self glycolipid antigens to Natural killer cells [93]. The physiological relevance, HIV-1 specificity and underlying mechanisms concerning the

impact on Env function require further investigations, which also applies to CD3G that is part of the T cell receptor-CD3 complex [46]. For instance, experiments in primary HIV-1 target cells with virions that are pseudotyped with different viral glycoproteins, in combination with specific gene silencing of individual candidate factor, would be very helpful to answer these questions. In support of a relevant role *in vivo*, SPN is involved in $CD4^+$ T cell proliferation and migration [15] and shows reduced expression as well as altered glycosylation in HIV-1 infected patients [50]. CD164 is known to interact with CXCR4 [13]; whether its inhibitory effect on HIV-1 is dependent on the viral co-receptor tropism remains to be determined. Notably, I observed a slight but highly reproducible shift in the electrophoretic mobility of cellular, but not cell-free HIV-1 gp120 glycoprotein in the presence of CD164, OAS1 and especially GBP5, indicating that these candidates may influence Env glycosylation. OAS1 altered not only the mobility of the gp120 but also reduced viral gene expression. In contrast, GBP5 efficiently reduced the infectivity of HIV-1 particles but had only low effects on viral gene expression and the release of progeny virions. Notably, another member of this dynamin superfamily of GTPases (GBP2) is required for the enhancement of HIV-1 infectivity by Nef [74]. My results suggest that GBP5 may reduce the abundance of infectious progeny virions by affecting HIV-1 Env function. Further experiments showed that GBP5 impairs Env function of diverse HIV-1 and -2 strains as well as Murine Leukemia Virus and Measles Virus glycoproteins, but does not reduce the infectivity of VSVg- and Ebola Virus glycoprotein-pseudotyped particles (data not shown). Furthermore, Western blot analyses suggest that some candidate genes, including *CD3G* and *IFI16*, might affect HIV-1 Gag processing, since their coexpression decreased the levels of cell-associated p24 capsid protein without reducing the amount of the p55 Gag precursor protein, although the effects were modest. Whether this is due to a reduction of total HIV proteins, also reducing the levels of the viral protease that mediates Gag processing, or an additional, independent effect remains to be determined.

I was able to detect SP110, IFI16, GBP5 and APOL6 in human T cells as well as in macrophages, the primary HIV target cells, by Western blot, and could monitor their induction upon IFN treatment (Figure 14). Although CD164 was not detectable by Western blot, I could show by flow cytometric analysis that CD164 is not constitutively expressed in $CD4^+$ T cells, but is induced by IFNs and by stimulation via CD3/CD28 in

the presence of IL-2. Furthermore, I established a quantitative real-time PCR for OAS1 to monitor basal OAS1 mRNA levels in blood cells, and confirmed type I IFN as a powerful inducer of OAS1 gene expression. In the meantime, I obtained a functional custom-made antibody (Eurogentec) allowing to detect OAS1 by Western blot. Further investigations of OAS1 and other promising candidate factors in primary HIV-1 target cells, especially in combination with knockdown studies are clearly necessary to better understand the underlying mechanisms and the relevance of individual candidate genes *in vivo*.

Two candidate genes (*SP110* and *IL-1A*) clearly enhanced the production of infectious HIV-1 in the cotransfection assay (Figure 7 and 8). In contrast to IL-1A, SP110 increased early viral gene expression (Figure 9C), whereas both cellular factors did not affect NF-κB activity (Figure 12B) nor enhance HIV-1 infectivity in the transduction assay (Figure 11). In addition, IL-1A and SP110 did not enhance LTR promoter activity, irrespective whether HIV-1 Tat protein was present or not (Figure 12A). SP110 is part of a leukocyte-specific nuclear body component that may play a role in the regulation of gene transcription, and mutations are associated with immunodeficiency [80]. It has been reported that Epstein-Barr Virus SM protein recruits SP110 to stabilize viral mRNAs and enhance lytic viral gene expression [68]. More research, e. g. *SP110* knockdown studies in primary macrophages or half-time measurements of viral mRNA species in the presence of SP110, is necessary to investigate HIV-1 specificity and to understand the underlying mechanisms involved in SP110-driven enhancement of viral gene expression. The strongest enhancing effect on HIV-1 was observed in the presence of IL-1A when cotransfected with the proviral construct. This cytokine plays a key role in inflammation and the regulation of early immune responses to infections, as well as in the maintenance of skin barrier function [21]. Increased IL-1A production has been reported in HIV-1 infected patients [11], and reduced levels of IL-1A expression has been detected in the genital mucosa of HIV-1 exposed seronegative sexworkers [49]. So far, the experiments in human primary blood cells did not reveal an enhancing effect of IL-1A on HIV-1 infection. Recombinant IL-1A altered neither the infection rates (Figure 15A), nor early viral gene expression (data not shown) in HIV-1 infected peripheral blood mononucleated cells (PBMCs), or macrophages (data not shown). In addition, infected blood cells produced similar quantities of infectious virus in the

presence and absence of recombinant IL-1A (Figure 15B). Indeed, cotransfection of IL-1A enhanced virus production in HEK293T cells (Figure 15C), but the delivery *in trans* by cotransfection during virus production did not increase particle infectivity (p24 antigen normalized virus stocks), or HIV-1 infection rates (equal volume of virus stocks) in human PBMCs (Figure 15D), or macrophages (data not shown). In addition, IFI44L enhanced the numbers of HIV-1 producing cells when cotransfected with the provirus (Figure 9), and lead to a strong enhancement of basal LTR activity in the absence of viral Tat (Figure 12A). However, IFI44L did not influence late viral gene expression (Figure 10), or LTR activity in the presence of Tat (Figure 12A). The identification of cellular factors with enhancing properties on HIV-1 infection is important especially in the context of reactivation of latent HIV-1 infected resting memory $CD4^+$ T cells [84], and thus SP110, IL-1A and IFI44L clearly warrant further investigation.

The IFN-inducible protein 16 (IFI16) has been shown to be an immune sensor for viral DNA species [37, 98]. Recently, it has been demonstrated that IFI16 triggers caspase-1 activation and pyroptosis in HIV-1 abortive infected $CD4^+$ T cells [64], and restricts human cytomegalovirus replication via Sp1 [20]. In addition to its DNA sensing function, I showed that IFI16 also inhibits HIV-1 and other primate lentiviruses (Figure 16D) by impairing HIV-1 LTR promoter activity in a Sp1-independent manner (Figure 16A and C), and the proteolytic processing of the Gag precursor (Figure 16B). Whether the latter is due to an IFI16-mediated reduction of total HIV proteins, including the viral protease mediating the Gag processing or an additional, independent effect is so far unclear. Notably, cotransfection of IFI16 inhibited the production of infectious HIV-1 in HEK293T cells that lack endogenous STING expression, which is crucial for the induction of IFI16-mediated innate immune sensing [37]. Furthermore, I did not detect any type I IFN production upon transfection of HEK293T cells with any tested candidate gene (data not shown). Notably, IFI16 reduced HIV-1 infection in macrophages and differentiated THP-1 cells in single round infection assays, whereas other factors involved in viral immune sensing like cGAS, STING and Ddx41 required multiple rounds of replication and IFN induction to exert their antiviral effect [37]. These results are strong evidence that IFI16 restricts HIV-1 independently of its immune sensing function. Moreover, I showed that IFI16-mediated antiviral activity is evolutionarily conserved (Figure 16E and F) and can be attenuated by HIV-1 Vpr. Notably, it has been reported

that the herpes simplex virus protein ICP0 antagonizes IFI16 by targeting it for proteosomal degradation [71]. Delivery of several HIV-1 Vpr proteins *in trans* via cotransfection of expression constructs rescued the production of infectious HIV-1 from HEK293T cells more efficiently than *in cis* when expressed only from the provirus (Figure 16 G and H). Vpr is a late viral gene product, and thus may be expressed too late to antagonize IFI16 in the latter experimental setting. The ability of Vpr to counteract IFI16 was conserved between primary HIV-1 strains and disrupted by a single mutation of Q65R but not R80A, both leading in a loss of G2/M cell cycle arrest (Figure 16H). These preliminary findings suggest that the interaction of IFI16 with VPRBP and SLX, which is impaired by Q65R but not by R80A [47], may be critical for its ability to antagonize IFI16. If this antagonistic effect is directly mediated by viral Vpr or indirectly caused by interaction with other cellular factors remains to be determined. Ongoing studies aim at further defining the antiviral mechanism of IFI16 and to separate its antiviral activity from its sensing function by site-directed mutations. Furthermore, as Vpr is incorporated into HIV-1 particles, I am currently investigating whether virion-associated Vpr is able to counteract IFI16, and whether knockdown of IFI16 in primary $CD4^+$ T cells increases HIV-1 infection.

In conclusion, the number of cellular genes sharing the characteristics of known host restriction factors is very limited. However, a strikingly high proportion of these candidate factors inhibits HIV-1 production in cotransfection assays. Notably, all tested members of the apolipoprotein L and TNFR superfamilies that showed inhibitory effects in the cotransfection assays rather enhanced HIV-1 production when already expressed before transduction, reflecting the importance of the time point of expression during HIV-1 replication. Many identified candidates may exert broad unspecific effects but several cellular genes that impair HIV-1 infectivity by interfering with Env function were also identified. The underlying mechanisms as well as the relevance *in vivo* need to be determined in human primary cells and further characterization of these factors will improve our understanding of cellular defense mechanisms against invading pathogens. Further approaches are clearly necessary to demonstrate whether candidate genes directly and dominantly interfere with HIV-1 replication, e.g. via knock down studies in primary cells, and coimmunoprecipitation of candidate factors with HIV-1 proteins.

My finding that the immune sensor IFI16 inhibits HIV-1 by impairing HIV-1 LTR promoter activity and Gag processing, adds to the growing evidence that cellular defense factors may frequently have the capability for both immune sensing and direct inhibition. Furthermore, I showed that this sensor of retroviral DNA species and mediator of $CD4^+$ T cell depletion is counteracted by the HIV-1 Vpr protein. Additional experiments in primary HIV-1 target cells are required to understand the underlying mechanisms and the relevance of these effects for HIV replication *in vivo*.

5. Summary

APOBEC3G, Trim5α, Tetherin and SAMHD1 are host cell encoded proteins that interfere with multiple steps of human immunodeficiency virus (HIV) replication to inhibit viral spread. These antiretroviral restriction factors are commonly under positive selection, upregulated during HIV-1 infection, inducible by Interferons (IFNs), and frequently interacting with viral proteins. Here, I combined evolutionary genomics, transcriptomics, and protein interaction data to identify thirty cellular genes sharing these characteristic features of known restriction factors. With three exceptions, all thirty genes that showed significant evidence of positive selection at one or more amino acid sites were amplified from human cDNA and cloned into expression vectors for functional characterization.

To investigate their ability to inhibit HIV-1, I established HEK293T cell-based assays targeting early and/or late steps of HIV-1 replication. Cotransfection of a strikingly high proportion of candidate genes with HIV-1 proviruses impaired the production of infectious HIV-1 without affecting cell viability. Among them were members of the APOL and TNFR superfamilies, as well as CD164 that suppressed HIV-1 production by more than 90%. In the absence of the accessory viral proteins Vpr, Vpu and Nef, which are known to antagonize antiviral factors, additional candidate factors such as GBP5, IFI16, SPN and CD3E, achieved more than 90% reduction. Notably, this screening approach also led to the identification of two genes (*IL-1A* and *SP110*) that enhanced HIV-1 production.

Titration experiments for several factors confirmed their impact on HIV-1 and flow cytometric analyses, p24 capsid ELISA and Western blot revealed that many candidate genes influenced HIV-1 gene transcription and/or translation. To clarify specificity, I determined the impact of candidate factors on the activity of various promoters. Many factors exerted inhibitory effects on viral promoters not limited to the HIV-1 long terminal repeat (LTR). Furthermore, FAS and especially TNFRSF10A were identified as potent activators of NF-κB, thereby also activating the human IFN-β core promoter.

Western blot analyses demonstrated that CD164, CD1A, CD3G and SPN impaired processing of the gp160 Env precursor protein to the mature gp120, and therefore may reduce virion infectivity by interfering with Env function. Notably, I observed a slight but

highly reproducible shift in the electrophoretic mobility of cellular, but not cell-free HIV-1 gp120 glycoprotein in the presence of CD164, OAS1 and especially GBP5, indicating that these candidates may influence the glycosylation of the Env protein.

To initially analyze the *in vivo* relevance, I was able to detect APOL6, GBP5, IFI16 and SP110 by Western blotting, flow cytometry (CD164), or OAS1 by quantitative real-time PCR in primary $CD4^+$ T cells as well as macrophages, the natural target cells of HIV-1. Notably, their expression was induced upon stimulation via CD3/CD28 or IFNs.

In-depth analyses of the immune sensor IFI16 showed that this protein also restricts HIV-1 and other primate lentiviruses, independently of its DNA sensing activity, by impairing HIV-1 LTR promoter activity in a Sp1-independent manner, and the proteolytic processing of the Gag precursor. Its antiviral activity is evolutionarily conserved, and counteracted by the HIV-1 Vpr protein. Interestingly, the ability of Vpr to attenuate IFI16 restriction was conserved between primary HIV-1 strains and disrupted by a single mutation of Q65R but not R80A.

In summary, my results show that the number of human genes sharing the characteristics of known restriction factors is very limited and are a first step towards clarifying how many of them display specific antiretroviral activity. The underlying mechanisms and the relevance of these potential restriction factors to control HIV-1 replication *in vivo* need further studies. Further characterization of these factors especially in primary blood cells in combination with knockdown experiments will improve our understanding of cellular defense mechanisms against invading pathogens.

References

[1] Ambrose, Z. and Aiken, C. 2014. HIV-1 uncoating: connection to nuclear entry and regulation by host proteins. *Virology* 454-455, 371–379.

[2] Au-Yeung, N., Mandhana, R., and Horvath, C. M. 2013. Transcriptional regulation by STAT1 and STAT2 in the interferon JAK-STAT pathway. *jak-stat* 2, e23931.

[3] Barré-Sinoussi, F., Chermann, J. C., Rey, F., Nugeyre, M. T., Chamaret, S., Gruest, J., Dauguet, C., Axler-Blin, C., Vézinet-Brun, F., Rouzioux, C., Rozenbaum, W., and Montagnier, L. 1983. Isolation of a T-lymphotropic retrovirus from a patient at risk for acquired immune deficiency syndrome (AIDS). *Science* 220, 868–871.

[4] Bibollet-Ruche, F., Heigele, A., Keele, B. F., Easlick, J. L., Decker, J. M., Takehisa, J., Learn, G., Sharp, P. M., Hahn, B. H., and Kirchhoff, F. 2012. Efficient SIVcpz replication in human lymphoid tissue requires viral matrix protein adaptation. *J. Clin. Invest.* 122, 1644–1652.

[5] Bogerd, H. P. and Cullen, B. R. 2008. Single-stranded RNA facilitates nucleocapsid: APOBEC3G complex formation. *RNA* 14, 1228–1236.

[6] Bosque, A. and Planelles, V. 2009. Induction of HIV-1 latency and reactivation in primary memory CD4+ T cells. *Blood* 113, 58–65.

[7] Breuer, K., Foroushani, A. K., Laird, M. R., Chen, C., Sribnaia, A., Lo, R., Winsor, G. L., Hancock, Robert E W, Brinkman, Fiona S L, and Lynn, D. J. 2013. InnateDB: systems biology of innate immunity and beyond--recent updates and continuing curation. *Nucleic Acids Res.* 41, D1228-33.

[8] Dalgleish, A. G., Beverley, P. C., Clapham, P. R., Crawford, D. H., Greaves, M. F., and Weiss RA. 1984. The CD4 (T4) antigen is an essential component of the receptor for the AIDS retrovirus. *Nature* 312, 763–767.

[9] Daugherty, M. D. and Malik, H. S. 2012. Rules of Engagement: Molecular Insights from Host-Virus Arms Races. *Annu. Rev. Genet.* 46, 677–700.

[10] Department of Health and Human Services AIDSinfo. 2014. Panel on Antiretroviral Guidelines for Adults and Adolescents. Guidelines for the use of antiretroviral agents in HIV-1-infected adults and adolescents. http://aidsinfo.nih.gov/contentfiles/lvguidelines/AdultandAdolescentGL.pdf.

[11] Dinarello, C. A. 1996. Biologic basis for interleukin-1 in disease. *Blood* 87, 2095–2147.

[12] Endres, C. L., Bergquam, E. P., Axthelm, M. K., and Wong, S. W. 1995. Suppression of simian immunodeficiency virus replication by human immunodeficiency virus type 1 trans-dominant negative rev mutants. *Journal of Virology* 69, 5164–5166.

[13] Forde, S., Tye, B. J., Newey, S. E., Roubelakis, M., Smythe, J., McGuckin, C. P., Pettengell, R., and Watt, S. M. 2007. Endolyn (CD164) modulates the CXCL12-mediated migration of umbilical cord blood CD133+ cells. *Blood* 109, 1825–1833.

[14] Fu, W., Sanders-Beer, B. E., Katz, K. S., Maglott, D. R., Pruitt, K. D., and Ptak, R. G. 2009. Human immunodeficiency virus type 1, human protein interaction database at NCBI. *Nucleic Acids Res.* 37, D417-22.

[15] Gallego, M. D., Aguado, E., Kindelán, J. M., Peña, J., Santamaría, M., and Molina, I. J. 2001. Altered expression of CD43-hexasaccharide isoform on peripheral T lymphocytes from HIV-infected individuals. *AIDS* 15, 477–481.

[16] Gallo, R. C., Sarin, P. S., Gelmann, E. P., Robert-Guroff, M., Richardson, E., Kalyanaraman, V. S., Mann, D., Sidhu, G. D., Stahl, R. E., Zolla-Pazner, S., Leibowitch, J., and Popovic, M. 1983. Isolation of human T-cell leukemia virus in acquired immune deficiency syndrome (AIDS). *Science* 220, 865–867.

[17] Gao, F., Yue, L., Robertson, D. L., Hill, S. C., Hui, H., Biggar, R. J., Neequaye, A. E., Whelan, T. M., Ho, D. D., and Shaw, G. M. 1994. Genetic diversity of human immunodeficiency virus type 2: evidence for distinct sequence subtypes with differences in virus biology. *Journal of Virology* 68, 7433–7447.

[18] Gao, W. Y., Cara, A., Gallo, R. C., and Lori, F. 1993. Low levels of deoxynucleotides in peripheral blood lymphocytes: a strategy to inhibit human immunodeficiency virus type 1 replication. *Proc Natl Acad Sci U S A.* 90, 8925–8928.

[19] García, M. A., Gil, J., Ventoso, I., Guerra, S., Domingo, E., Rivas, C., and Esteban, M. 2006. Impact of protein kinase PKR in cell biology: from antiviral to antiproliferative action. *Microbiol. Mol. Biol. Rev.* 70, 1032–1060.

[20] Gariano, G. R., Dell'Oste, V., Bronzini, M., Gatti, D., Luganini, A., Andrea, M. de, Gribaudo, G., Gariglio, M., and Landolfo, S. 2012. The intracellular DNA sensor IFI16 gene acts as restriction factor for human cytomegalovirus replication. *PLoS Pathog.* 8, e1002498.

[21] Garlanda, C., Dinarello, C. A., and Mantovani, A. 2013. The interleukin-1 family: back to the future. *Immunity* 39, 1003–1018.

[22] Gnanadurai, C. W., Pandrea, I., Parrish, N. F., Kraus, M. H., Learn, G. H., Salazar, M. G., Sauermann, U., Topfer, K., Gautam, R., Munch, J., Stahl-Hennig, C., Apetrei, C., Hahn, B. H., and Kirchhoff, F. 2010. Genetic Identity and Biological Phenotype of a Transmitted/Founder Virus Representative of Nonpathogenic Simian Immunodeficiency Virus Infection in African Green Monkeys. *Journal of Virology* 84, 12245–12254.

[23] Goldstone, D. C., Ennis-Adeniran, V., Hedden, J. J., Groom, Harriet C T, Rice, G. I., Christodoulou, E., Walker, P. A., Kelly, G., Haire, L. F., Yap, M. W., de Carvalho, Luiz Pedro S, Stoye, J. P., Crow, Y. J., Taylor, I. A., and Webb, M. 2011. HIV-1 restriction factor SAMHD1 is a deoxynucleoside triphosphate triphosphohydrolase. *Nature* 480, 379–382.

[24] Goujon, C., Moncorgé, O., Bauby, H., Doyle, T., Ward, C. C., Schaller, T., Hué, S., Barclay, W. S., Schulz, R., and Malim, M. H. 2013. Human MX2 is an interferon-induced post-entry inhibitor of HIV-1 infection. *Nature* 502, 559–562.

[25] Graham, F. L., Smiley, J., Russell, W. C., and Nairn, R. 1977. Characteristics of a Human Cell Line Transformed by DNA from Human Adenovirus Type 5. *Journal of General Virology* 36, 59–72.

[26] Haller, O. 2013. Dynamins Are Forever: MxB Inhibits HIV-1. *Cell Host & Microbe* 14, 371–373.

[27] Haller, O., Kochs, G., and Weber, F. 2007. Interferon, Mx, and viral countermeasures. *Cytokine & Growth Factor Reviews* 18, 425–433.

[28] Harris, R. S., Bishop, K. N., Sheehy, A. M., Craig, H. M., Petersen-Mahrt, S. K., Watt, I. N., Neuberger, M. S., and Malim, M. H. 2003. DNA Deamination Mediates Innate Immunity to Retroviral Infection. *Cell* 113, 803–809.

[29] Harris, R. S., Hultquist, J. F., and Evans, D. T. 2012. The Restriction Factors of Human Immunodeficiency Virus. *Journal of Biological Chemistry* 287, 40875–40883.

[30] Hatziioannou, T., Princiotta, M., Piatak, M., Yuan, F., Zhang, F., Lifson, J. D., and Bieniasz, P. D. 2006. Generation of Simian-Tropic HIV-1 by Restriction Factor Evasion. *Science* 314, 95.

[31] Hotter, D., Kirchhoff, F., and Sauter, D. 2013. HIV-1 Vpu does not degrade interferon regulatory factor 3. *J. Virol.* 87, 7160–7165.

[32] Hovanessian, A. G. 2007. On the discovery of interferon-inducible, double-stranded RNA activated enzymes: the 2'-5'oligoadenylate synthetases and the protein kinase PKR. *Cytokine Growth Factor Rev.* 18, 351–361.

[33] Hovanessian, A. G. and Justesen, J. 2007. The human 2'-5'oligoadenylate synthetase family: unique interferon-inducible enzymes catalyzing 2'-5' instead of 3'-5' phosphodiester bond formation. *Biochimie* 89, 779–788.

[34] Hrecka, K., Hao, C., Gierszewska, M., Swanson, S. K., Kesik-Brodacka, M., Srivastava, S., Florens, L., Washburn, M. P., and Skowronski, J. 2011. Vpx relieves inhibition of HIV-1 infection of macrophages mediated by the SAMHD1 protein. *Nature* 474, 658–661.

[35] Isaacs, A. and Lindenmann, J. 1957. Virus interference. I. The interferon. *Proc. R. Soc. Lond., B, Biol. Sci.* 147, 258–267.

[36] Jäger, S., Cimermancic, P., Gulbahce, N., Johnson, J. R., McGovern, K. E., Clarke, S. C., Shales, M., Mercenne, G., Pache, L., Li, K., Hernandez, H., Jang, G. M., Roth, S. L., Akiva, E., Marlett, J., Stephens, M., D'Orso, I., Fernandes, J., Fahey, M., Mahon, C., O'Donoghue, A. J., Todorovic, A., Morris, J. H., Maltby, D. A., Alber, T., Cagney, G., Bushman, F. D., Young, J. A., Chanda, S. K., Sundquist, W. I., Kortemme, T., Hernandez, R. D., Craik, C. S., Burlingame, A., Sali, A., Frankel, A. D., and Krogan, N. J. 2011. Global landscape of HIV–human protein complexes. *Nature* 481, 365–370.

[37] Jakobsen, M. R., Bak, R. O., Andersen, A., Berg, R. K., Jensen, S. B., Tengchuan, J., Jin, T., Laustsen, A., Hansen, K., Ostergaard, L., Fitzgerald, K. A., Xiao, T. S., Mikkelsen, J. G., Mogensen, T. H., and Paludan, S. R. 2013. IFI16 senses DNA forms of the lentiviral replication cycle and controls HIV-1 replication. *Proc. Natl. Acad. Sci. U.S.A.* 110, E4571-80.

[38] Kane, M., Yadav, S. S., Bitzegeio, J., Kutluay, S. B., Zang, T., Wilson, S. J., Schoggins, J. W., Rice, C. M., Yamashita, M., Hatziioannou, T., and Bieniasz, P. D. 2013. MX2 is an interferon-induced inhibitor of HIV-1 infection. *Nature* 502, 563–566.

[39] Kirchhoff, F. 2010. Immune Evasion and Counteraction of Restriction Factors by HIV-1 and Other Primate Lentiviruses. *Cell Host & Microbe* 8, 55–67.

[40] Klein, F., Mouquet, H., Dosenovic, P., Scheid, J. F., Scharf, L., and Nussenzweig, M. C. 2013. Antibodies in HIV-1 Vaccine Development and Therapy. *Science* 341, 1199–1204.

[41] Koch, P., Lampe, M., Godinez, W. J., Müller, B., Rohr, K., Kräusslich, H.-G., and Lehmann, M. J. 2009. Visualizing fusion of pseudotyped HIV-1 particles in real time by live cell microscopy. *Retrovirology* 6, 1–14.

[42] König, R., Zhou, Y., Elleder, D., Diamond, T. L., Bonamy, G. M., Irelan, J. T., Chiang, C.-y., Tu, B. P., De Jesus, Paul D., Lilley, C. E., Seidel, S., Opaluch, A. M., Caldwell, J. S., Weitzman, M. D., Kuhen, K. L., Bandyopadhyay, S., Ideker, T., Orth, A. P., Miraglia, L. J., Bushman, F. D., Young, J. A., and Chanda, S. K. 2008. Global Analysis of Host-Pathogen Interactions that Regulate Early-Stage HIV-1 Replication. *Cell* 135, 49–60.

[43] Kosakovsky Pond, Sergei L and Frost, Simon D W. 2005. Not so different after all: a comparison of methods for detecting amino acid sites under selection. *Mol. Biol. Evol.* 22, 1208–1222.

[44] Kosiol, C., Vinař, T., da Fonseca, Rute R., Hubisz, M. J., Bustamante, C. D., Nielsen, R., Siepel, A., and Schierup, M. H. 2008. Patterns of Positive Selection in Six Mammalian Genomes. *PLoS Genetics* 4, e1000144.

[45] Kreitman, M. 2000. Methods to detect selection in populations with applications to the human. *Annu Rev Genomics Hum Genet* 1, 539–559.

[46] Kuhns, M. S. and Badgandi, H. B. 2012. Piecing together the family portrait of TCR-CD3 complexes. *Immunol. Rev.* 250, 120–143.

[47] Laguette, N., Brégnard, C., Hue, P., Basbous, J., Yatim, A., Larroque, M., Kirchhoff, F., Constantinou, A., Sobhian, B., and Benkirane, M. 2014. Premature activation of the SLX4 complex by Vpr promotes G2/M arrest and escape from innate immune sensing. *Cell* 156, 134–145.

[48] Laguette, N., Sobhian, B., Casartelli, N., Ringeard, M., Chable-Bessia, C., Ségéral, E., Yatim, A., Emiliani, S., Schwartz, O., and Benkirane, M. 2011. SAMHD1 is the dendritic- and myeloid-cell-specific HIV-1 restriction factor counteracted by Vpx. *Nature* 474, 654–657.

[49] Lajoie, J., Juno, J., Burgener, A., Rahman, S., Mogk, K., Wachihi, C., Mwanjewe, J., Plummer, F. A., Kimani, J., Ball, T. B., and Fowke, K. R. 2012. A distinct cytokine and chemokine profile at the genital mucosa is associated with HIV-1 protection among HIV-exposed seronegative commercial sex workers. *Mucosal Immunol* 5, 277–287.

[50] Lefebvre, J. C., Giordanengo, V., Limouse, M., Doglio, A., Cucchiarini, M., Monpoux, F., Mariani, R., and Peyron, J. F. 1994. Altered glycosylation of leukosialin, CD43, in HIV-1-infected cells of the CEM line. *J Exp Med* 180, 1609–1617.

[51] Li, Q., Smith, A. J., Schacker, T. W., Carlis, J. V., Duan, L., Reilly, C. S., and Haase, A. T. 2009. Microarray analysis of lymphatic tissue reveals stage-specific, gene expression signatures in HIV-1 infection. *J. Immunol.* 183, 1975–1982.

[52] Lim, E. S., Fregoso, O. I., McCoy, C. O., Matsen, F. A., Malik, H. S., and Emerman, M. 2012. The Ability of Primate Lentiviruses to Degrade the Monocyte Restriction

Factor SAMHD1 Preceded the Birth of the Viral Accessory Protein Vpx. *Cell Host & Microbe* 11, 194–204.

[53] Liu, L., Oliveira, N. M. M., Cheney, K. M., Pade, C., Dreja, H., Bergin, A.-M. H., Borgdorff, V., Beach, D. H., Bishop, C. L., Dittmar, M. T., and McKnight, Á. 2011. A whole genome screen for HIV restriction factors. *Retrovirology* 8, 94.

[54] Liu, Z., Pan, Q., Ding, S., Qian, J., Xu, F., Zhou, J., Cen, S., Guo, F., and Liang, C. 2013. The Interferon-Inducible MxB Protein Inhibits HIV-1 Infection. *Cell Host & Microbe* 14, 398–410.

[55] Lodermeyer, V., Suhr, K., Schrott, N., Kolbe, C., Stürzel, C. M., Krnavek, D., Münch, J., Dietz, C., Waldmann, T., Kirchhoff, F., and Goffinet, C. 2013. 90K, an interferon-stimulated gene product, reduces the infectivity of HIV-1. *Retrovirology* 10, 1–22.

[56] Malim, M. H. and Bieniasz, P. D. 2012. HIV Restriction Factors and Mechanisms of Evasion. *Cold Spring Harbor Perspectives in Medicine* 2, a006940.

[57] Mandal, D., Exline, C. M., Feng, Z., and Stoltzfus, C. M. 2009. Regulation of vif mRNA Splicing by Human Immunodeficiency Virus Type 1 Requires 5' Splice Site D2 and an Exonic Splicing Enhancer To Counteract Cellular Restriction Factor APOBEC3G. *Journal of Virology* 83, 6067–6078.

[58] Mangeat, B., Turelli, P., Caron, G., Friedli, M., Perrin, L., and Trono, D. 2003. Broad antiretroviral defence by human APOBEC3G through lethal editing of nascent reverse transcripts. *Nature* 424, 99–103.

[59] Massingham, T. and Goldman, N. 2005. Detecting amino acid sites under positive selection and purifying selection. *Genetics* 169, 1753–1762.

[60] Matreyek, K. and Engelman, A. 2013. Viral and Cellular Requirements for the Nuclear Entry of Retroviral Preintegration Nucleoprotein Complexes. *Viruses* 5, 2483–2511.

[61] Melián, A., Beckman, E. M., Porcelli, S. A., and Brenner, M. B. 1996. Antigen presentation by CD1 and MHC-encoded class I-like molecules. *Curr. Opin. Immunol.* 8, 82–88.

[62] Meng, B. and Lever, A. M. L. 2013. Wrapping up the bad news - HIV assembly and release. *Retrovirology* 10, 1–12.

[63] Miyauchi, K., Kim, Y., Latinovic, O., Morozov, V., and Melikyan, G. B. 2009. HIV Enters Cells via Endocytosis and Dynamin-Dependent Fusion with Endosomes. *Cell* 137, 433–444.

[64] Monroe, K. M., Yang, Z., Johnson, J. R., Geng, X., Doitsh, G., Krogan, N. J., and Greene, W. C. 2014. IFI16 DNA sensor is required for death of lymphoid CD4 T cells abortively infected with HIV. *Science* 343, 428–432.

[65] Mugal, C. F., Wolf, J. B. W., and Kaj, I. 2014. Why time matters: codon evolution and the temporal dynamics of dN/dS. *Mol. Biol. Evol.* 31, 212–231.

[66] National Institute of Allergy and Infectious Diseases. 24/06/2014. HIV replication cycle.
http://www.niaid.nih.gov/topics/hivaids/understanding/biology/pages/hivreplicationcycle.aspx.

[67] Neil, S. J. D., Zang, T., and Bieniasz, P. D. 2008. Tetherin inhibits retrovirus release and is antagonized by HIV-1 Vpu. *Nature* 451, 425–430.

[68] Nicewonger, J., Suck, G., Bloch, D., and Swaminathan, S. 2004. Epstein-Barr virus (EBV) SM protein induces and recruits cellular Sp110b to stabilize mRNAs and enhance EBV lytic gene expression. *J. Virol.* 78, 9412–9422.

[69] Nielsen, R. 2005. Molecular Signatures of Natural Selection. *Annu. Rev. Genet.* 39, 197–218.

[70] Nielsen, R., Hellmann, I., Hubisz, M., Bustamante, C., and Clark, A. G. 2007. Recent and ongoing selection in the human genome. *Nat Rev Genet* 8, 857–868.

[71] Orzalli, M. H., DeLuca, N. A., and Knipe, D. M. 2012. Nuclear IFI16 induction of IRF-3 signaling during herpesviral infection and degradation of IFI16 by the viral ICP0 protein. *Proc. Natl. Acad. Sci. U.S.A.* 109, E3008-17.

[72] Parrish, N. F., Gao, F., Li, H., Giorgi, E. E., Barbian, H. J., Parrish, E. H., Zajic, L., Iyer, S. S., Decker, J. M., Kumar, A., Hora, B., Berg, A., Cai, F., Hopper, J., Denny, T. N., Ding, H., Ochsenbauer, C., Kappes, J. C., Galimidi, R. P., West, A. P., Bjorkman, P. J., Wilen, C. B., Doms, R. W., O'Brien, M., Bhardwaj, N., Borrow, P., Haynes, B. F., Muldoon, M., Theiler, J. P., Korber, B., Shaw, G. M., and Hahn, B. H. 2013. Phenotypic properties of transmitted founder HIV-1. *Proc. Natl. Acad. Sci. U.S.A.* 110, 6626–6633.

[73] Pinney, J. W., Dickerson, J. E., Fu, W., Sanders-Beer, B. E., Ptak, R. G., and Robertson, D. L. 2009. HIV-host interactions: a map of viral perturbation of the host system. *AIDS* 23, 549–554.

[74] Pizzato, M., Helander, A., Popova, E., Calistri, A., Zamborlini, A., Palù, G., and Göttlinger, H. G. 2007. Dynamin 2 is required for the enhancement of HIV-1 infectivity by Nef. *Proc. Natl. Acad. Sci. U.S.A.* 104, 6812–6817.

[75] Platt, E. J., Bilska, M., Kozak, S. L., Kabat, D., and Montefiori, D. C. 2009. Evidence that ecotropic murine leukemia virus contamination in TZM-bl cells does not affect the outcome of neutralizing antibody assays with human immunodeficiency virus type 1. *J. Virol.* 83, 8289–8292.

[76] Powell, R. D., Holland, P. J., Hollis, T., and Perrino, F. W. 2011. Aicardi-Goutieres syndrome gene and HIV-1 restriction factor SAMHD1 is a dGTP-regulated deoxynucleotide triphosphohydrolase. *J. Biol. Chem.* 286, 43596–43600.

[77] Ptak, R. G., Fu, W., Sanders-Beer, B. E., Dickerson, J. E., Pinney, J. W., Robertson, D. L., Rozanov, M. N., Katz, K. S., Maglott, D. R., Pruitt, K. D., and Dieffenbach, C. W. 2008. Cataloguing the HIV type 1 human protein interaction network. *AIDS Res. Hum. Retroviruses* 24, 1497–1502.

[78] Rajan, D., Wildum, S., Rücker, E., Schindler, M., and Kirchhoff, F. 2006. Effect of R77Q, R77A and R80A changes in Vpr on HIV-1 replication and CD4 T cell depletion in human lymphoid tissue ex vivo. *AIDS* 20, 831–836.

[79] Rauch, I., Müller, M., and Decker, T. 2013. The regulation of inflammation by interferons and their STATs. *jak-stat* 2, e23820.

[80] Roscioli, T., Cliffe, S. T., Bloch, D. B., Bell, C. G., Mullan, G., Taylor, P. J., Sarris, M., Wang, J., Donald, J. A., Kirk, E. P., Ziegler, J. B., Salzer, U., McDonald, G. B., Wong, M., Lindeman, R., and Buckley, M. F. 2006. Mutations in the gene encoding

the PML nuclear body protein Sp110 are associated with immunodeficiency and hepatic veno-occlusive disease. *Nat. Genet.* 38, 620–622.

[81] Rotger, M., Dalmau, J., Rauch, A., McLaren, P., Bosinger, S. E., Martinez, R., Sandler, N. G., Roque, A., Liebner, J., Battegay, M., Bernasconi, E., Descombes, P., Erkizia, I., Fellay, J., Hirschel, B., Miró, J. M., Palou, E., Hoffmann, M., Massanella, M., Blanco, J., Woods, M., Günthard, H. F., Bakker, P. de, Douek, D. C., Silvestri, G., Martinez-Picado, J., and Telenti, A. 2011. Comparative transcriptomics of extreme phenotypes of human HIV-1 infection and SIV infection in sooty mangabey and rhesus macaque. *J. Clin. Invest.* 121, 2391–2400.

[82] Rotger, M., Dang, K. K., Fellay, J., Heinzen, E. L., Feng, S., Descombes, P., Shianna, K. V., Ge, D., Günthard, H. F., Goldstein, D. B., Telenti, A., and Emerman, M. 2010. Genome-Wide mRNA Expression Correlates of Viral Control in CD4+ T-Cells from HIV-1-Infected Individuals. *PLoS Pathog* 6, e1000781.

[83] Rotheram-Borus, M. J., Swendeman, D., and Chovnick, G. 2009. The Past, Present, and Future of HIV Prevention: Integrating Behavioral, Biomedical, and Structural Intervention Strategies for the Next Generation of HIV Prevention. *Annu. Rev. Clin. Psychol.* 5, 143–167.

[84] Ruelas, D. S. and Greene, W. C. 2013. An integrated overview of HIV-1 latency. *Cell* 155, 519–529.

[85] Rusinova, I., Forster, S., Yu, S., Kannan, A., Masse, M., Cumming, H., Chapman, R., and Hertzog, P. J. 2013. Interferome v2.0: an updated database of annotated interferon-regulated genes. *Nucleic Acids Res.* 41, D1040-6.

[86] Samarajiwa, S. A., Forster, S., Auchettl, K., and Hertzog, P. J. 2009. INTERFEROME: the database of interferon regulated genes. *Nucleic Acids Research* 37, D852.

[87] Sauter, D., Schindler, M., Specht, A., Landford, W. N., Münch, J., Kim, K.-A., Votteler, J., Schubert, U., Bibollet-Ruche, F., Keele, B. F., Takehisa, J., Ogando, Y., Ochsenbauer, C., Kappes, J. C., Ayouba, A., Peeters, M., Learn, G. H., Shaw, G., Sharp, P. M., Bieniasz, P., Hahn, B. H., Hatziioannou, T., and Kirchhoff, F. 2009. Tetherin-driven adaptation of Vpu and Nef function and the evolution of pandemic and nonpandemic HIV-1 strains. *Cell Host Microbe* 6, 409–421.

[88] Schindler, M., Münch, J., Kutsch, O., Li, H., Santiago, M. L., Bibollet-Ruche, F., Müller-Trutwin, M. C., Novembre, F. J., Peeters, M., Courgnaud, V., Bailes, E., Roques, P., Sodora, D. L., Silvestri, G., Sharp, P. M., Hahn, B. H., and Kirchhoff, F. 2006. Nef-mediated suppression of T cell activation was lost in a lentiviral lineage that gave rise to HIV-1. *Cell* 125, 1055–1067.

[89] Schmittgen, T. D. and Livak, K. J. 2008. Analyzing real-time PCR data by the comparative CT method. *Nat Protoc* 3, 1101–1108.

[90] Schneider, A., Souvorov, A., Sabath, N., Landan, G., Gonnet, G. H., and Graur, D. 2009. Estimates of positive Darwinian selection are inflated by errors in sequencing, annotation, and alignment. *Genome Biol Evol* 1, 114–118.

[91] Schoggins, J. W., Wilson, S. J., Panis, M., Murphy, M. Y., Jones, C. T., Bieniasz, P., and Rice, C. M. 2011. A diverse range of gene products are effectors of the type I interferon antiviral response. *Nature* 472, 481–485.

[92] Sheehy, A. M., Gaddis, N. C., Choi, J. D., and Malim, M. H. 2002. Isolation of a human gene that inhibits HIV-1 infection and is suppressed by the viral Vif protein. *Nature* 418, 646–650.

[93] Sloma, I., Zilber, M.-T., Vasselon, T., Setterblad, N., Cavallari, M., Mori, L., Libero, G. de, Charron, D., Mooney, N., and Gelin, C. 2008. Regulation of CD1a Surface Expression and Antigen Presentation by Invariant Chain and Lipid Rafts. *The Journal of Immunology* 180, 980–987.

[94] Stremlau, M., Owens, C. M., Perron, M. J., Kiessling, M., Autissier, P., and Sodroski, J. 2004. The cytoplasmic body component TRIM5alpha restricts HIV-1 infection in Old World monkeys. *Nature* 427, 848–853.

[95] Taylor, H. E., Khatua, A. K., and Popik, W. 2014. The innate immune factor apolipoprotein L1 restricts HIV-1 infection. *J. Virol.* 88, 592–603.

[96] Tebit, D. M., Zekeng, L., Kaptué, L., Gürtler, L., Fackler, O. T., Keppler, O. T., Herchenröder, O., and Kräusslich, H.-G. 2004. Construction and characterization of an HIV-1 group O infectious molecular clone and analysis of vpr- and nef-negative derivatives. *Virology* 326, 329–339.

[97] UNAIDS. 2013 report on the global AIDS epidemic. http://www.unaids.org/en/resources/campaigns/globalreport2013/globalreport/.

[98] Unterholzner, L., Keating, S. E., Baran, M., Horan, K. A., Jensen, S. B., Sharma, S., Sirois, C. M., Jin, T., Latz, E., Xiao, T. S., Fitzgerald, K. A., Paludan, S. R., and Bowie, A. G. 2010. IFI16 is an innate immune sensor for intracellular DNA. *Nat. Immunol.* 11, 997–1004.

[99] van Damme, N., Goff, D., Katsura, C., Jorgenson, R. L., Mitchell, R., Johnson, M. C., Stephens, E. B., and Guatelli, J. 2008. The Interferon-Induced Protein BST-2 Restricts HIV-1 Release and Is Downregulated from the Cell Surface by the Viral Vpu Protein. *Cell Host & Microbe* 3, 245–252.

[100] Vanhamme, L., Paturiaux-Hanocq, F., Poelvoorde, P., Nolan, D. P., Lins, L., Van Den Abbeele, Jan, Pays, A., Tebabi, P., van Xong, H., Jacquet, A., Moguilevsky, N., Dieu, M., Kane, J. P., Baetselier, P. de, Brasseur, R., and Pays, E. 2003. Apolipoprotein L-I is the trypanosome lytic factor of human serum. *Nature* 422, 83–87.

[101] Vilella, A. J., Severin, J., Ureta-Vidal, A., Heng, L., Durbin, R., and Birney, E. 2009. EnsemblCompara GeneTrees: Complete, duplication-aware phylogenetic trees in vertebrates. *Genome Res.* 19, 327–335.

[102] Wie, S.-H., Du, P., Luong, T. Q., Rought, S. E., Beliakova-Bethell, N., Lozach, J., Corbeil, J., Kornbluth, R. S., Richman, D. D., and Woelk, C. H. 2013. HIV downregulates interferon-stimulated genes in primary macrophages. *J. Interferon Cytokine Res.* 33, 90–95.

[103] Wildum, S., Schindler, M., Münch, J., and Kirchhoff, F. 2006. Contribution of Vpu, Env, and Nef to CD4 down-modulation and resistance of human immunodeficiency virus type 1-infected T cells to superinfection. *J. Virol.* 80, 8047–8059.

[104] Wyatt, R. 1998. The HIV-1 Envelope Glycoproteins: Fusogens, Antigens, and Immunogens. *Science* 280, 1884–1888.

[105] Yang, Z. 2005. The power of phylogenetic comparison in revealing protein function. *Proc. Natl. Acad. Sci. U.S.A.* 102, 3179–3180.

[106] Yang, Z. 2007. PAML 4: phylogenetic analysis by maximum likelihood. *Mol. Biol. Evol.* 24, 1586–1591.

[107] Yang, Z. and Rannala, B. 2012. Molecular phylogenetics: principles and practice. *Nat Rev Genet* 13, 303–314.

[108] Zhang, C., Silva, S. de, Wang, J.-H., and Wu, L. 2012. Co-evolution of primate SAMHD1 and lentivirus Vpx leads to the loss of the vpx gene in HIV-1 ancestor. *PLoS ONE* 7, e37477.

[109] Zhou, H., Xu, M., Huang, Q., Gates, A. T., Zhang, X. D., Castle, J. C., Stec, E., Ferrer, M., Strulovici, B., Hazuda, D. J., and Espeseth, A. S. 2008. Genome-Scale RNAi Screen for Host Factors Required for HIV Replication. *Cell Host & Microbe* 4, 495–504.

Danksagung und Lebenslauf aus datenschutzrechtlichen Gründen entfernt.
